Constraining Nuclear Models and Equation of State with Parity-violating Asymmetry of ^{208}Pb and ^{48}Ca

Tianqi Zhao

Collaborators: Zidu Lin, Andrew Steiner, Bharat Kumar, Madappa Prakash

INT-22R-2A June 27, 2023

N3AS Network for Neutrinos, Nuclear Astrophysics, and Symmetries
PHYSICS FRONTIER CENTER

NSF

1804

OHIO UNIVERSITY

DEPARTMENT OF ENERGY · UNITED STATES OF AMERICA

Symmetry energy $E_{SYM}(u = n_B/n_s, x = n_p/n_B)$

Neutron star matter ≈ Pure neutron matter = Symmetric nuclear matter + Symmetry energy

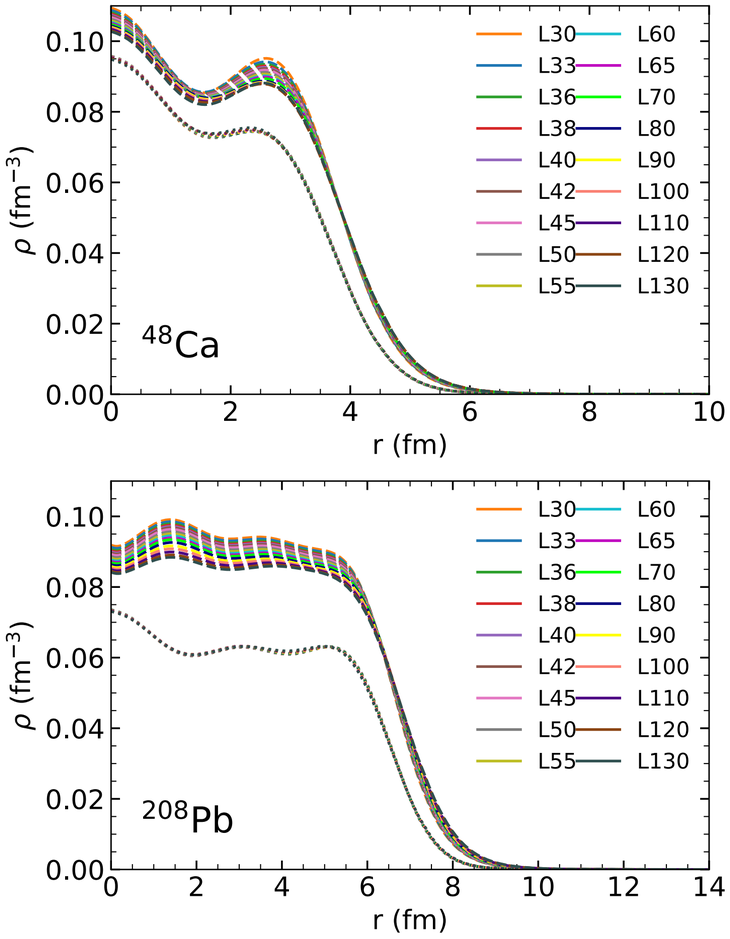

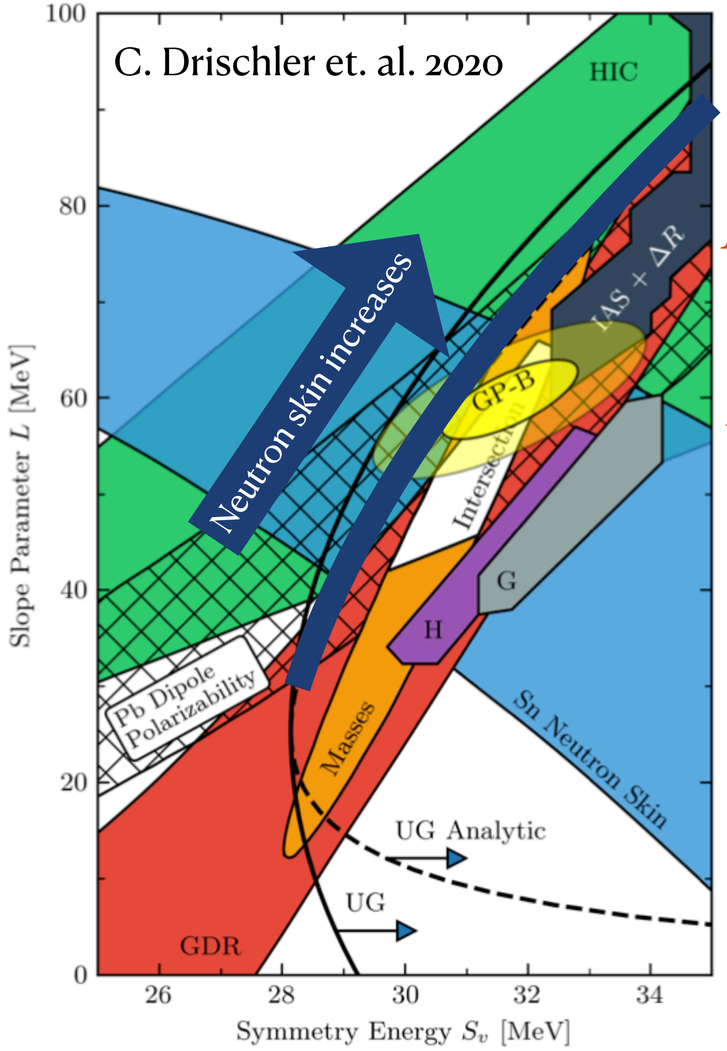

$$E(n_B, x) \approx$$

$$E_{SNM}(u) + E_{SYM}(u)\,(1-2x)^2 + \ldots$$

$$BE + \frac{K}{18}(u-1)^2 + \ldots$$

$$S_v + \frac{L}{3}(u-1) + \frac{K_{SYM}}{18}(u-1)^2 + \ldots$$

Neutron Skin $\Delta R = R_n - R_p$ is "**perpendicular**" to others

$$L = 30 - 90 \text{ MeV}$$
$$\Delta R_{^{208}Pb} = 0.11 - 0.25 \text{ fm}$$

Flowchart of Applying PREX and CREX Data

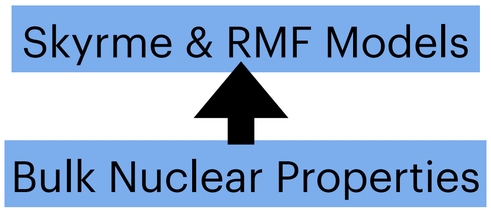

Prior in Bayesian Analysis

	CREX	PREX
(N,Z)	(28,20) Ca	(126,82) Pb
q (fm-1)	0.8733	0.3977
Fch, Rch(fm)	0.1581, 3.481	0.409, 5.503
Apv	2668±106(stat) ±40(syst)	550±16(stat) ±8(syst)
Fw	0.1304±0.0052(stat) ±0.002(syst)	0.368±0.013(exp) ±0.001(theo)
Fch-Fw	0.0277±0.0052(stat) ±0.002(syst)	0.041±0.013(exp) ±0.001(theo)
Rw	3.64±0.026(exp) ±0.023(theo)	5.8±0.075(tot)
Rw-Rch	0.159±0.026(exp) ±0.023(theo)	0.297±0.075(tot)
Rn-Rp	0.121±0.026(exp) ±0.024(theo)	0.283±0.071(tot)
	CREX 2022	PREX I 2012 PREX II 2021

	Scalar	Vector
Isoscalar	σ	$\gamma^\mu \omega_\mu$
Isovector	$\vec{\tau}\,\vec{\delta}$	$\gamma^\mu \vec{\tau}\,\vec{\rho}_\mu$

FSU-type RMF model

$$\mathscr{L} = \mathscr{L}_0 + \bar{\psi}\left(g_\sigma\sigma - g_\omega\gamma^\mu\omega_\mu - \frac{g_\rho}{2}\gamma^\mu\boldsymbol{\tau}\boldsymbol{\rho}_\mu\right)\psi - \frac{\kappa}{3!}(g_\sigma\sigma)^3 - \frac{\lambda}{4!}(g_\sigma\sigma)^4 + \frac{\zeta}{4!}(g_\omega^2\omega^\mu\omega_\mu)^2 + \Lambda_{\omega\rho}(g_\rho^2\boldsymbol{\rho}^\mu\boldsymbol{\rho}_\mu)(g_\omega^2\omega^\mu\omega_\mu)$$

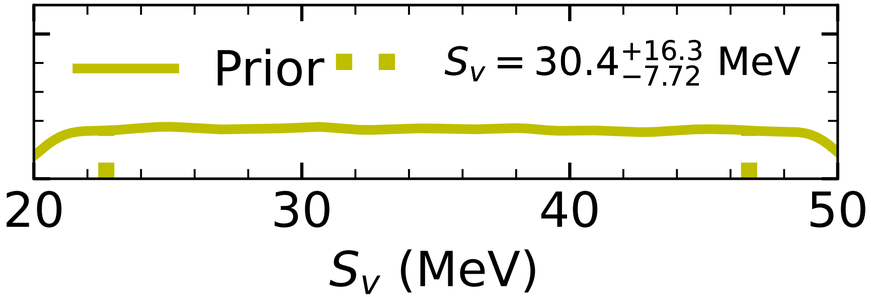

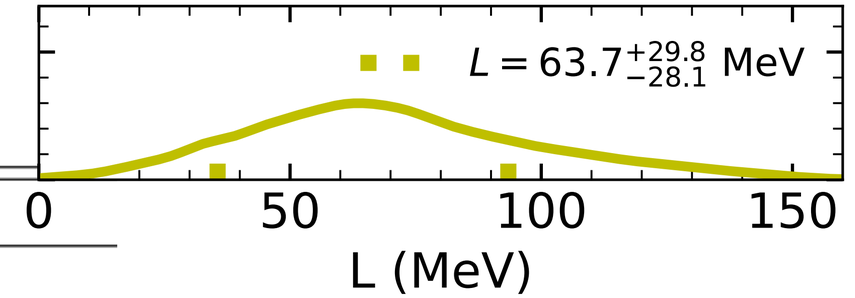

W. Chen et. al. 2014 A. Steiner et. al. 2005

	NL3	FSU	FSU2
m_σ	508.194	491.5	497.479
m_ω	782.501	782.5	782.5
m_ρ	763	763	763
g_σ^2	104.3871	112.1996	108.0943
g_ω^2	165.5854	204.5469	183.7893
g_ρ^2	79.6	138.4701	80.4656
κ	3.8599	1.4203	3.0029
λ	-0.015905	0.023762	-0.000533
ζ	0	0.06	0.0256
Λ	0	0.03	0.000823

	prior
m_σ (MeV)	[450,550]
m_ω (MeV)	782.5
m_ρ (MeV)	763
n_s (MeV)	[0.14,0.165]
BE (MeV)	[-15.5,-16.5]
M^* (MeV)	[0.5,0.8]$\times$ 939
K (MeV)	[210,250]
S_V (MeV)	[20,50]
L (MeV)	$[L_{min}, L(\Lambda = 0)]$
ζ_ω	[0,0.03]

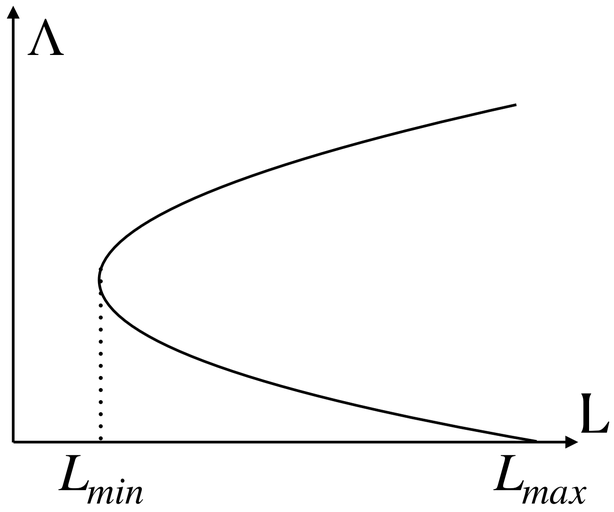

Flowchart of Applying PREX and CREX Data

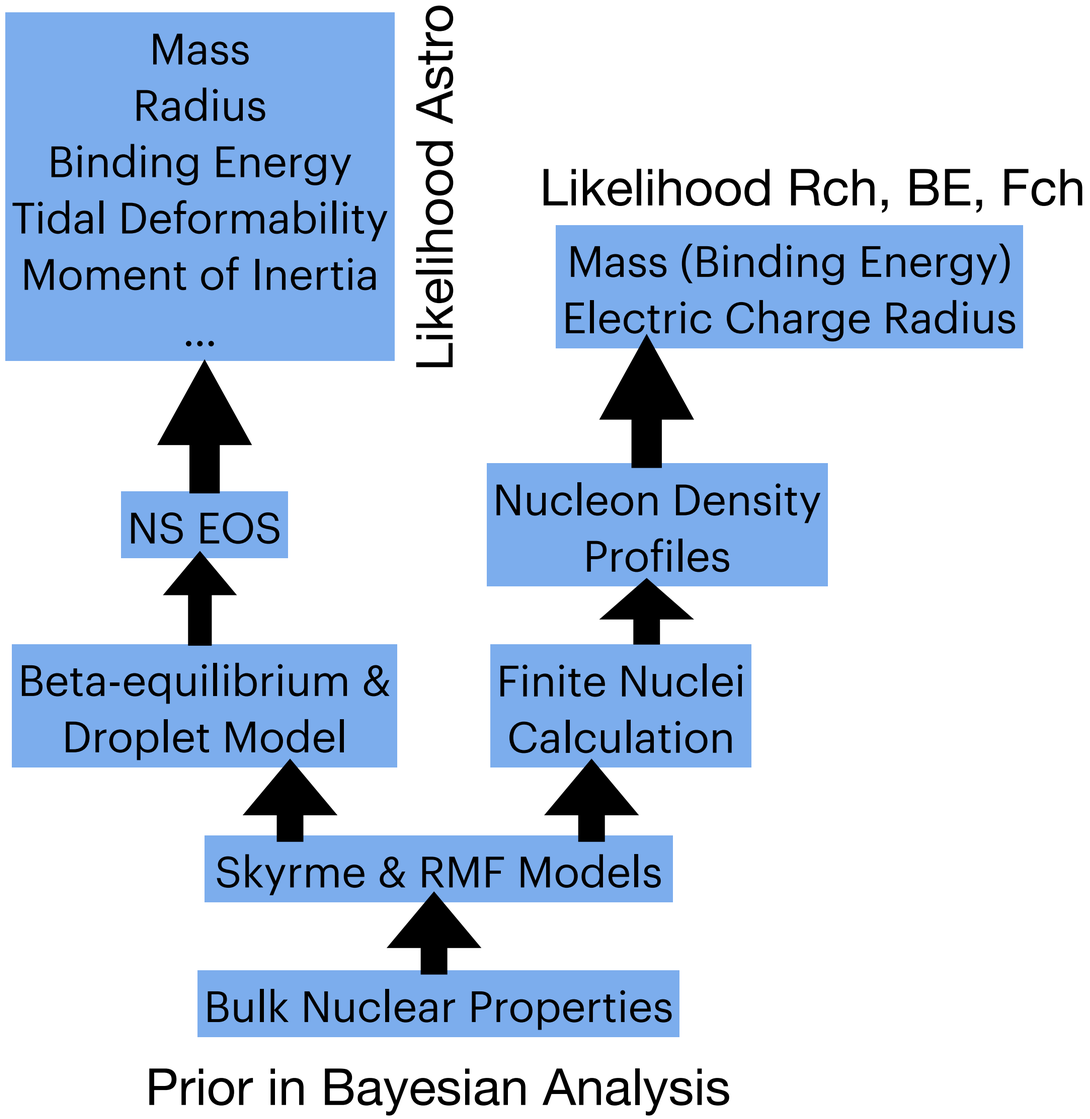

	CREX	PREX
(N,Z)	(28,20) Ca	(126,82) Pb
q (fm-1)	0.8733	0.3977
Fch, Rch(fm)	0.1581, 3.481	0.409, 5.503
Apv	2668±106(stat) ±40(syst)	550±16(stat) ±8(syst)
Fw	0.1304±0.0052(stat) ±0.002(syst)	0.368±0.013(exp) ±0.001(theo)
Fch-Fw	0.0277±0.0052(stat) ±0.002(syst)	0.041±0.013(exp) ±0.001(theo)
Rw	3.64±0.026(exp) ±0.023(theo)	5.8±0.075(tot)
Rw-Rch	0.159±0.026(exp) ±0.023(theo)	0.297±0.075(tot)
Rn-Rp	0.121±0.026(exp) ±0.024(theo)	0.283±0.071(tot)
	CREX 2022	PREX I 2012 PREX II 2021

Finite nuclei with MFT

- Nucleon densities of ${}^{A}_{Z}X$:
  (1) Guess the initial 4 density profiles.
  (2) Solve Klein-Gorden Eq for 4 mesons fields.
  (3) Construct local 4 single-particle potentials.
  (4) Solve Dirac Eq for lowest Z (N) proton (neutron) levels.
  (5) Compute ground state 4 density profiles.
  (6) Repeat (2) To (5) until converge.

	value	σ_i
$R_{ch}^{^{48}Ca}$	3.48	0.0696
$R_{ch}^{^{90}Zr}$	4.27	0.0854
$R_{ch}^{^{208}Pb}$	5.5	0.11
$\mathrm{BE}^{^{48}Ca}$	8.67	0.1734
$\mathrm{BE}^{^{90}Zr}$	8.71	0.1742
$\mathrm{BE}^{^{208}Pb}$	7.87	0.1574
$F_{ch}^{^{48}Ca}$	0.1581	0.001
$F_{ch}^{^{208}Pb}$	0.409	0.001

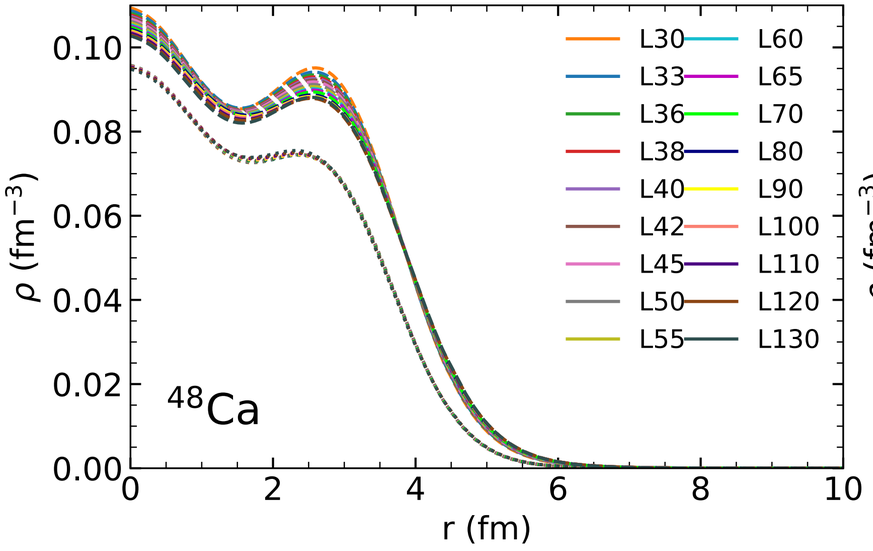

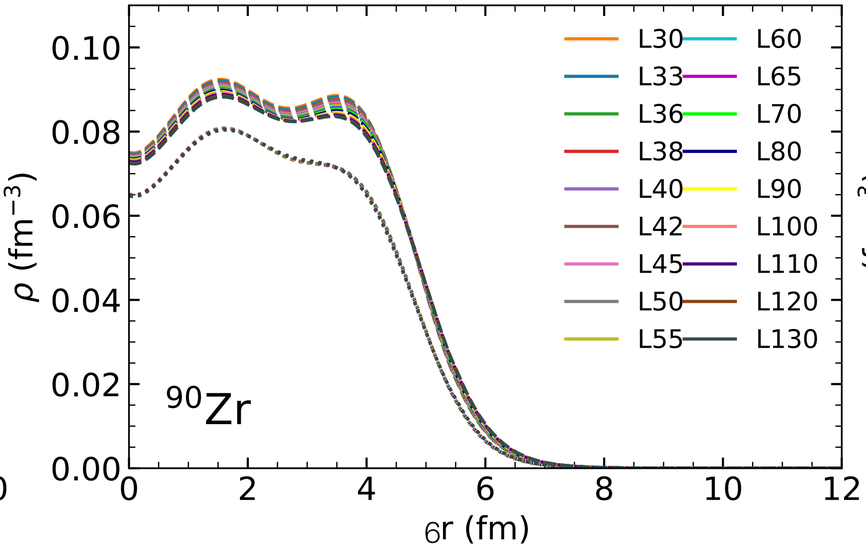

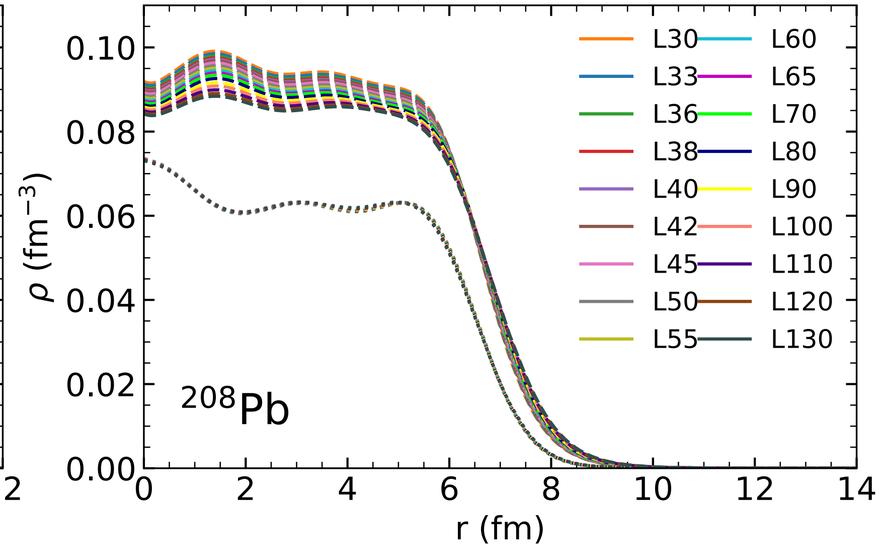

Flowchart of Applying PREX and CREX Data

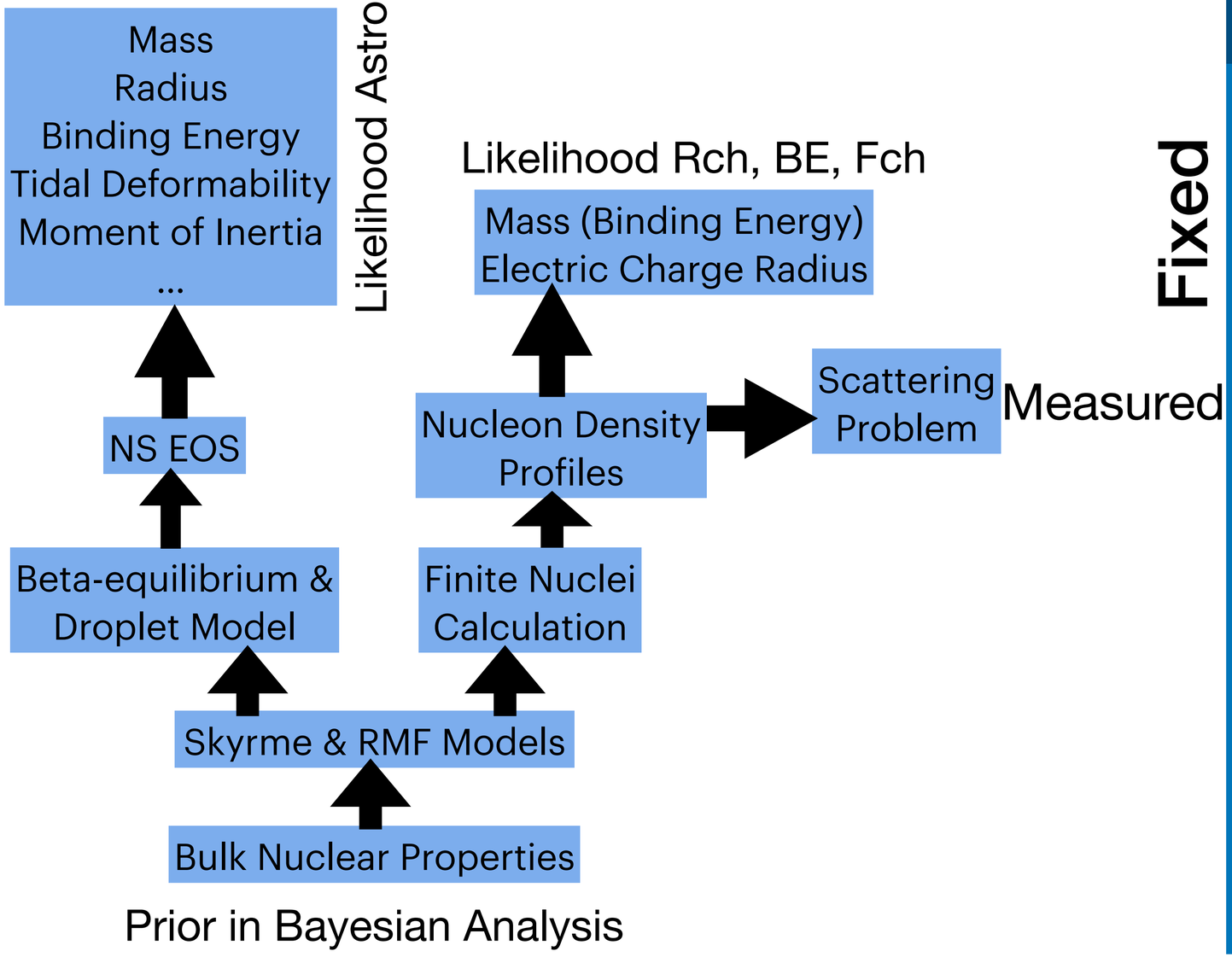

Fixed

	CREX	PREX
(N,Z)	(28,20) Ca	(126,82) Pb
q (fm-1)	0.8733	0.3977
Fch, Rch(fm)	0.1581, 3.481	0.409, 5.503
Apv	2668±106(stat) ±40(syst)	550±16(stat) ±8(syst)
Fw	0.1304±0.0052(stat) ±0.002(syst)	0.368±0.013(exp) ±0.001(theo)
Fch-Fw	0.0277±0.0052(stat) ±0.002(syst)	0.041±0.013(exp) ±0.001(theo)
Rw	3.64±0.026(exp) ±0.023(theo)	5.8±0.075(tot)
Rw-Rch	0.159±0.026(exp) ±0.023(theo)	0.297±0.075(tot)
Rn-Rp	0.121±0.026(exp) ±0.024(theo)	0.283±0.071(tot)
	CREX 2022	PREX I 2012 PREX II 2021

Parity violating asymmetry A_{PV}

The observable in PREX and CREX

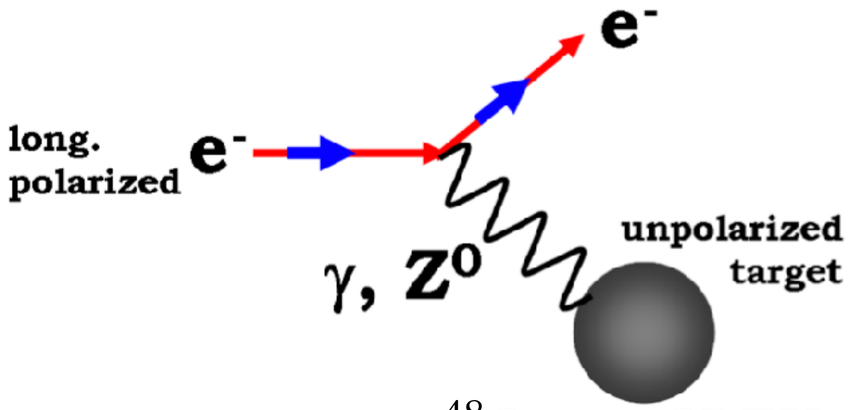

^{48}Ca – CREX

^{208}Pb – PREX

- Parity violating asymmetry: $A_{PV} = \dfrac{\sigma_R - \sigma_L}{\sigma_R + \sigma_L}$

  where σ_R, σ_L are cross-sections of the scattering problen

$$\left[\alpha \mathbf{p} + V_{L,R}(r)\right] \Psi_{L,R} = E\psi_{L,R}, \text{ where } V_{L,R}(r) = V(r) \pm A(r),$$

$$V(r) = \int d^3\mathbf{r}' \frac{\rho_E(\mathbf{r})}{|\,\mathbf{r}' - \mathbf{r}\,|}, \quad A(r) = \frac{G_F}{2^{3/2}} \rho_W(r)$$

where electric distribution ρ_E is approximately proton distribution,

and weak charge distribution ρ_W is approximately neutron distribution.

Flowchart of Applying PREX and CREX Data

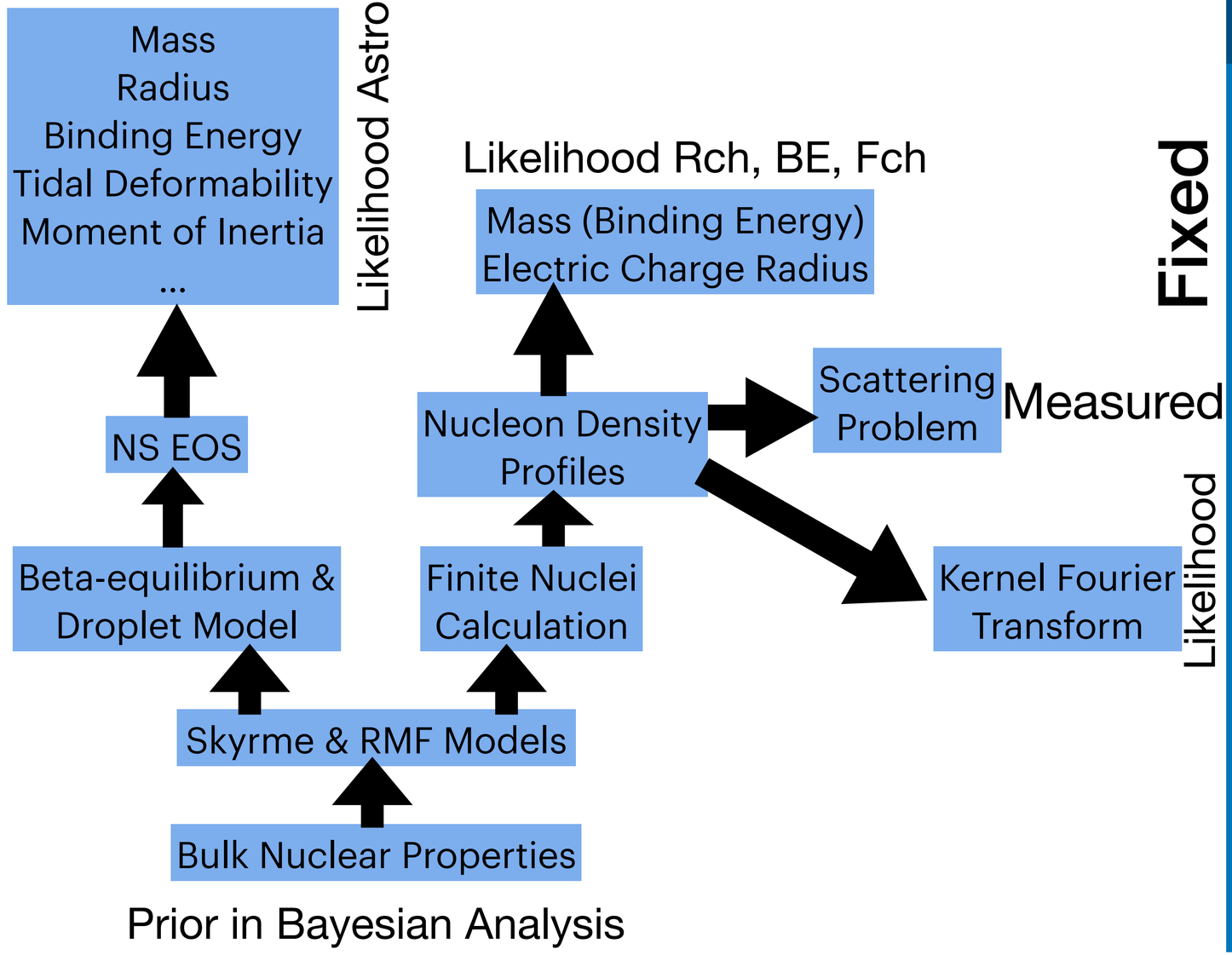

	CREX	PREX
(N,Z)	(28,20) Ca	(126,82) Pb
q (fm-1)	0.8733	0.3977
Fch, Rch(fm)	0.1581, 3.481	0.409, 5.503
Apv	2668±106(stat) ±40(syst)	550±16(stat) ±8(syst)
Fw	0.1304±0.0052(stat) ±0.002(syst)	0.368±0.013(exp) ±0.001(theo)
Fch-Fw	0.0277±0.0052(stat) ±0.002(syst)	0.041±0.013(exp) ±0.001(theo)
Rw	3.64±0.026(exp) ±0.023(theo)	5.8±0.075(tot)
Rw-Rch	0.159±0.026(exp) ±0.023(theo)	0.297±0.075(tot)
Rn-Rp	0.121±0.026(exp) ±0.024(theo)	0.283±0.071(tot)
	CREX 2022	PREX I 2012 PREX II 2021

Electric Charge Distribution

Well measured!!!

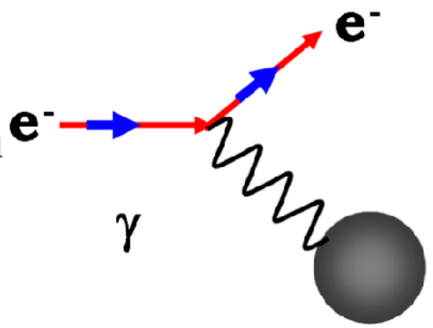

$$\frac{d\sigma}{d\Omega} = \left[\frac{d\sigma}{d\Omega}\right]_{Mott} |F(\mathbf{q})|^2 \qquad F(q) = \frac{\int j_0(qr)\rho(r)d^3r}{\int \rho(r)d^3r}$$

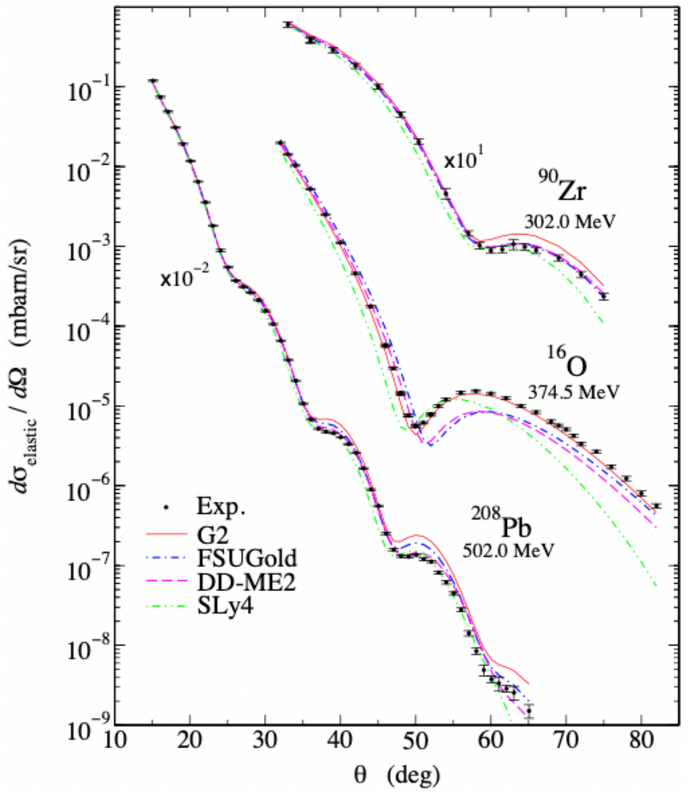

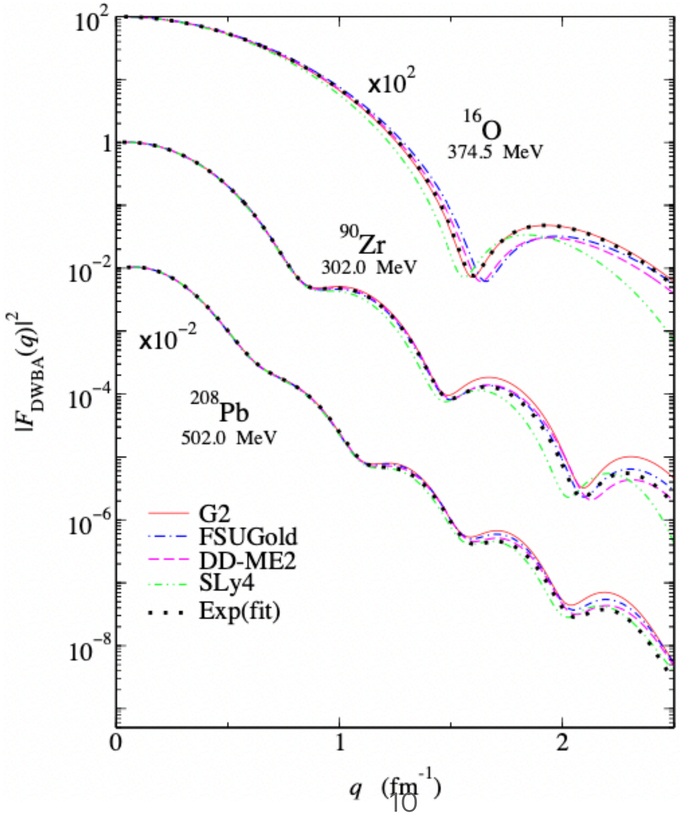

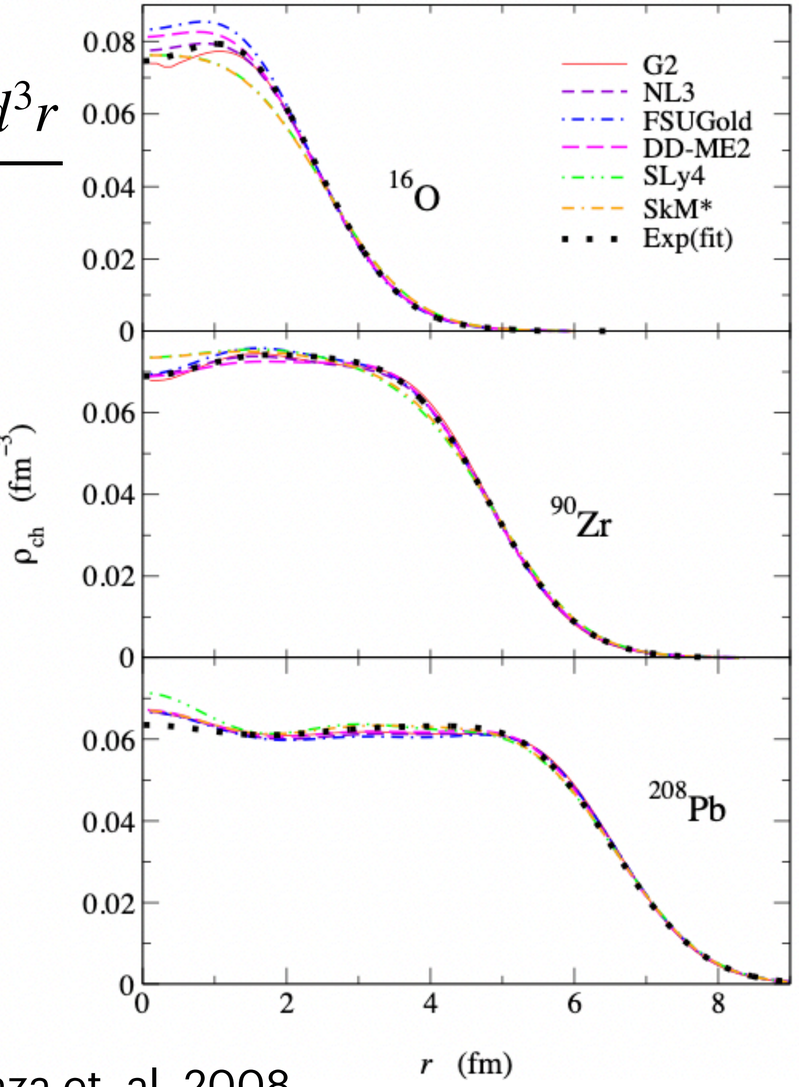

Moca-Maza et. al. 2008

Weak Charge Distribution

Extremely hard!!!

Jefferson Lab
Krishna Kumar 2018
Tao Ye 2021
Robert Radloff 2022

- $$F(\mathbf{q}) = \frac{1}{Q}\int e^{i\mathbf{q}\cdot\mathbf{r}}\rho(\mathbf{r})d^3r$$
$$= \frac{1}{Q}\int\left(1 + i\mathbf{q}\cdot\mathbf{r} - \frac{1}{2}(\mathbf{q}\cdot\mathbf{r})^2 + \ldots\right)\rho(\mathbf{r})d^3r$$
$$= 1 - \frac{1}{6}q^2 < r^2 > + \ldots \quad \text{(spherical symmetry)}$$

$$\lim_{q<<\sqrt{<r^2>}} < r^2 > = \frac{6[1 - F(q)]}{q^2}$$

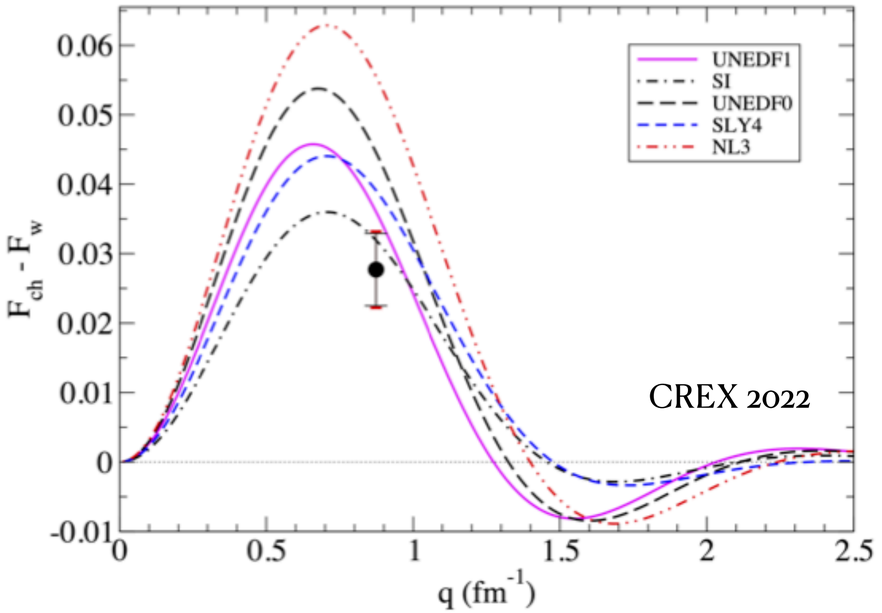

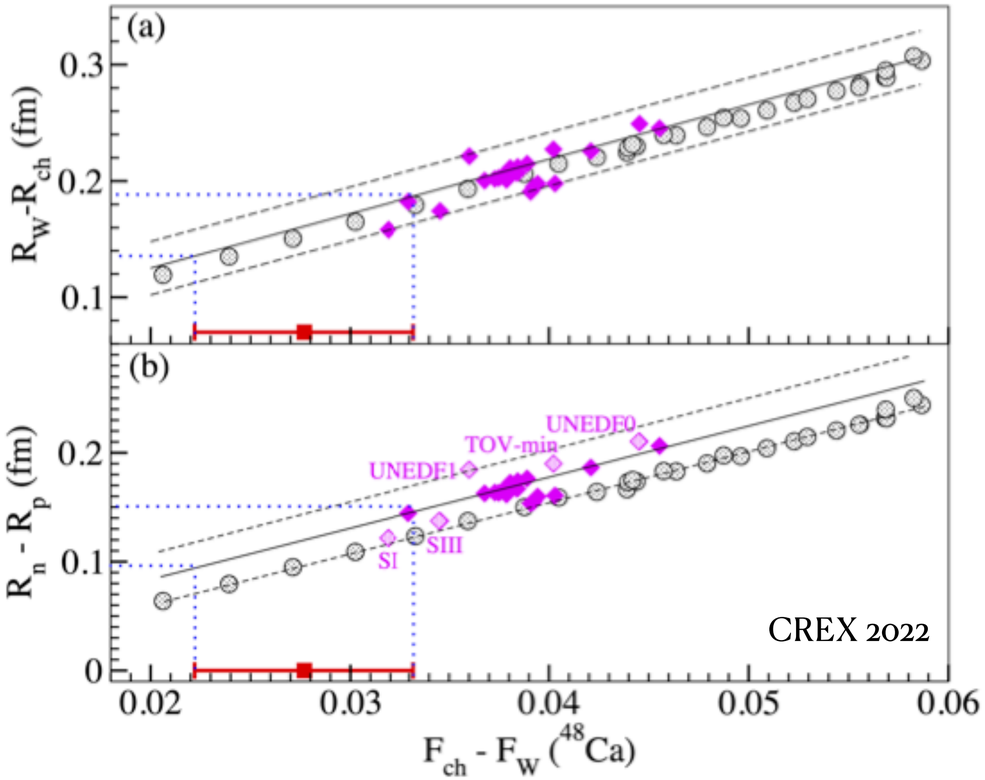

Flowchart of Applying PREX and CREX Data

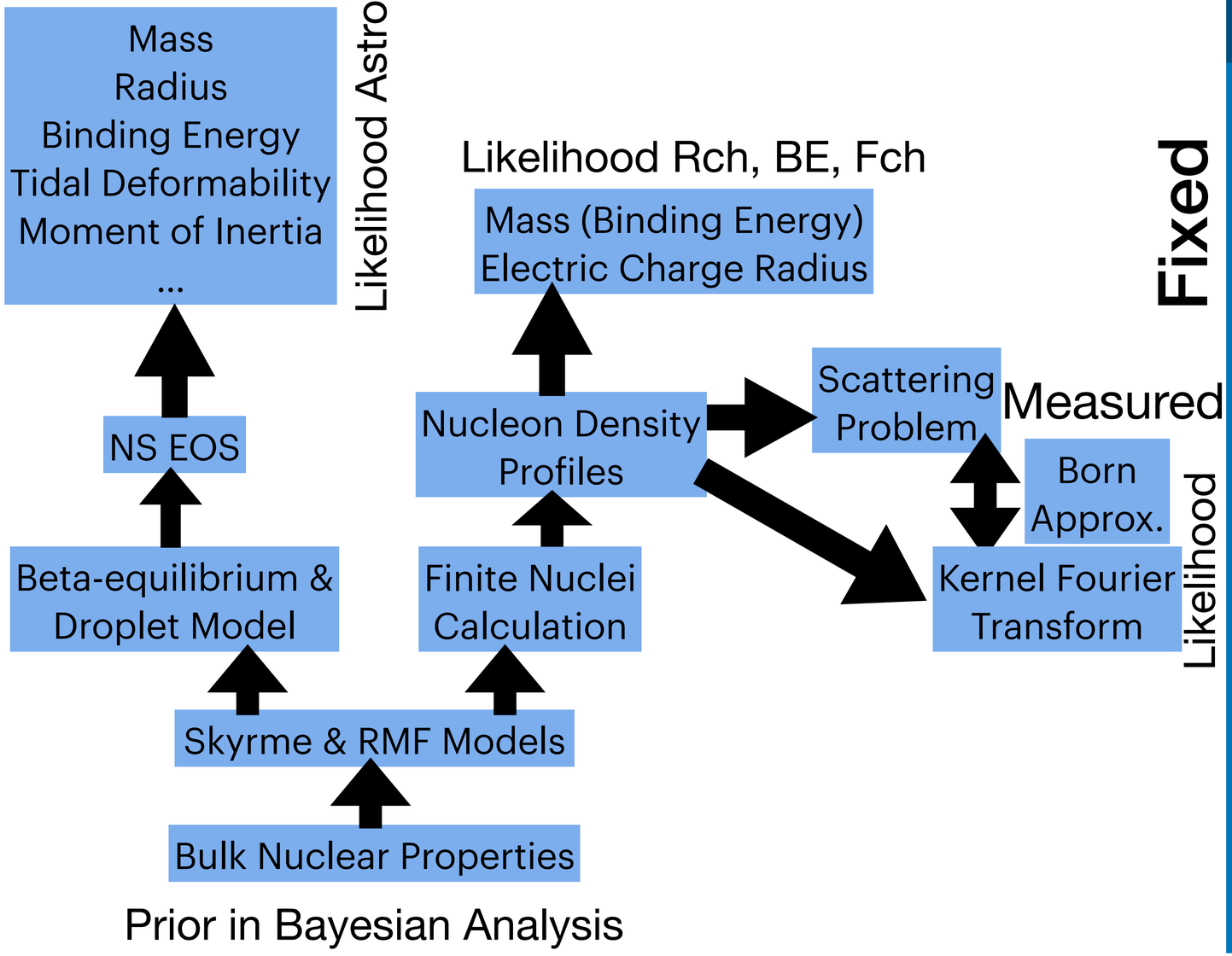

	CREX	PREX
(N,Z)	(28,20) Ca	(126,82) Pb
q (fm-1)	0.8733	0.3977
Fch, Rch(fm)	0.1581, 3.481	0.409, 5.503
Apv	2668±106(stat) ±40(syst)	550±16(stat) ±8(syst)
Fw	0.1304±0.0052(stat) ±0.002(syst)	0.368±0.013(exp) ±0.001(theo)
Fch-Fw	0.0277±0.0052(stat) ±0.002(syst)	0.041±0.013(exp) ±0.001(theo)
Rw	3.64±0.026(exp) ±0.023(theo)	5.8±0.075(tot)
Rw-Rch	0.159±0.026(exp) ±0.023(theo)	0.297±0.075(tot)
Rn-Rp	0.121±0.026(exp) ±0.024(theo)	0.283±0.071(tot)
	CREX 2022	PREX I 2012 PREX II 2021

Born approximation

- Axial weak potential, $A(r) = \dfrac{G_F}{2^{3/2}}\rho_W(r)$
- Scattering amplitude:
  $$\int < \psi_{in} \,|\, A(r) \,|\, \psi_{out} > d^3r = \frac{G_F}{2^{3/2}} \int e^{i\mathbf{q}\cdot\mathbf{r}} \rho_W(\mathbf{r}) d^3r = \frac{G_F Q_W}{2^{3/2} q^2} F_W(q)$$
- $$A_{PV} = \frac{\sigma_R - \sigma_L}{\sigma_R + \sigma_L} \approx \frac{G_F q^2 \,|\, Q_W \,|}{4\sqrt{2}\pi\alpha Z} \frac{F_W(q)}{F_E(q)} \propto \frac{(F_E + F_W)^2 - (F_E - F_W)^2}{(F_E + F_W)^2 + (F_E - F_W)^2}$$
  where $F(q) = \dfrac{\int j_0(qr)\rho(r)d^3r}{\int \rho(r) d^3r}$, and $j_0(qr) = \dfrac{\sin(qr)}{qr}$ is spherical Bessel function

Flowchart of Applying PREX and CREX Data

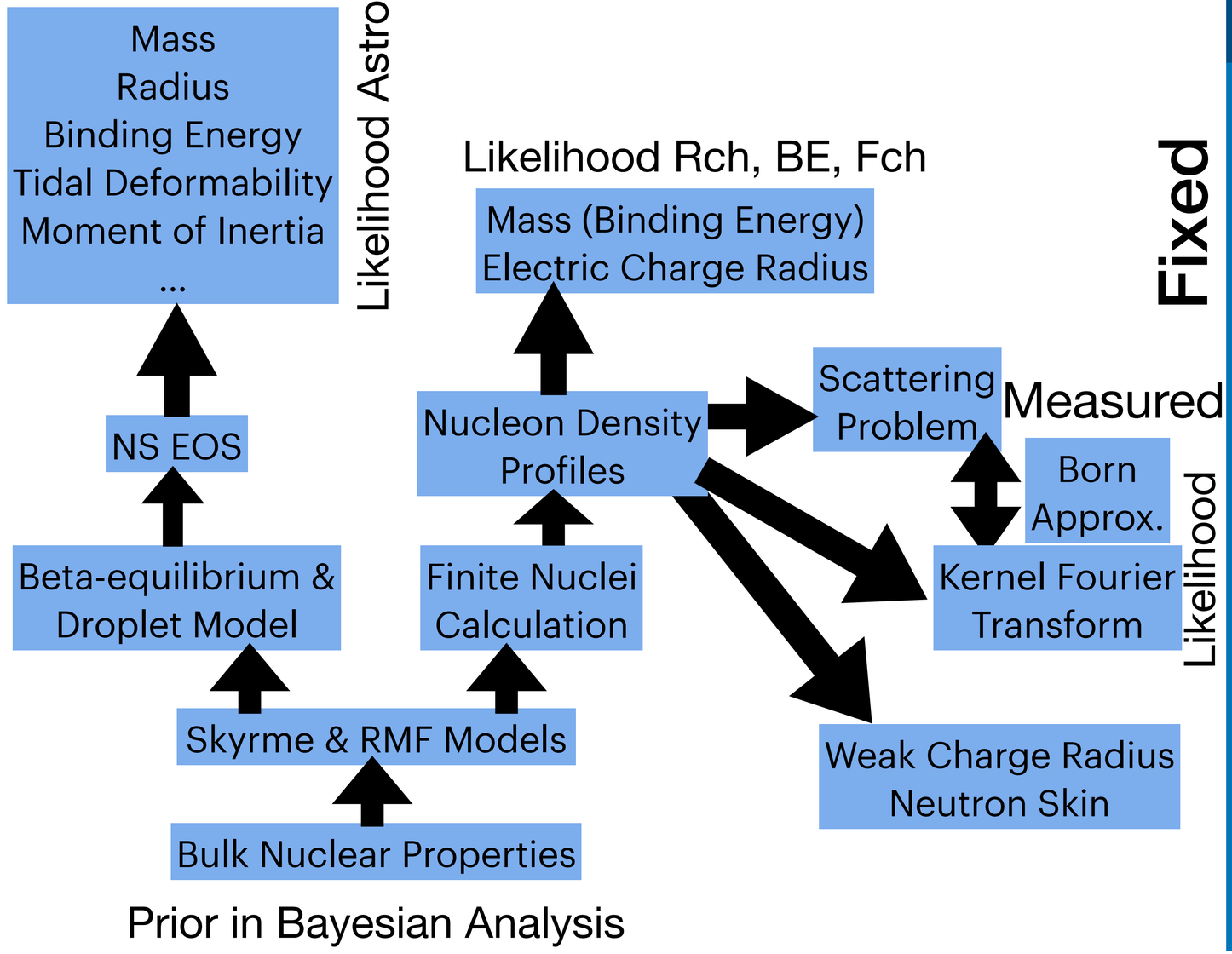

	CREX	PREX
(N,Z)	(28,20) Ca	(126,82) Pb
q (fm-1)	0.8733	0.3977
Fch, Rch(fm)	0.1581, 3.481	0.409, 5.503
Apv	2668±106(stat) ±40(syst)	550±16(stat) ±8(syst)
Fw	0.1304±0.0052(stat) ±0.002(syst)	0.368±0.013(exp) ±0.001(theo)
Fch-Fw	0.0277±0.0052(stat) ±0.002(syst)	0.041±0.013(exp) ±0.001(theo)
Rw	3.64±0.026(exp) ±0.023(theo)	5.8±0.075(tot)
Rw-Rch	0.159±0.026(exp) ±0.023(theo)	0.297±0.075(tot)
Rn-Rp	0.121±0.026(exp) ±0.024(theo)	0.283±0.071(tot)
	CREX 2022	PREX I 2012 PREX II 2021

Tension between PREX and CREX

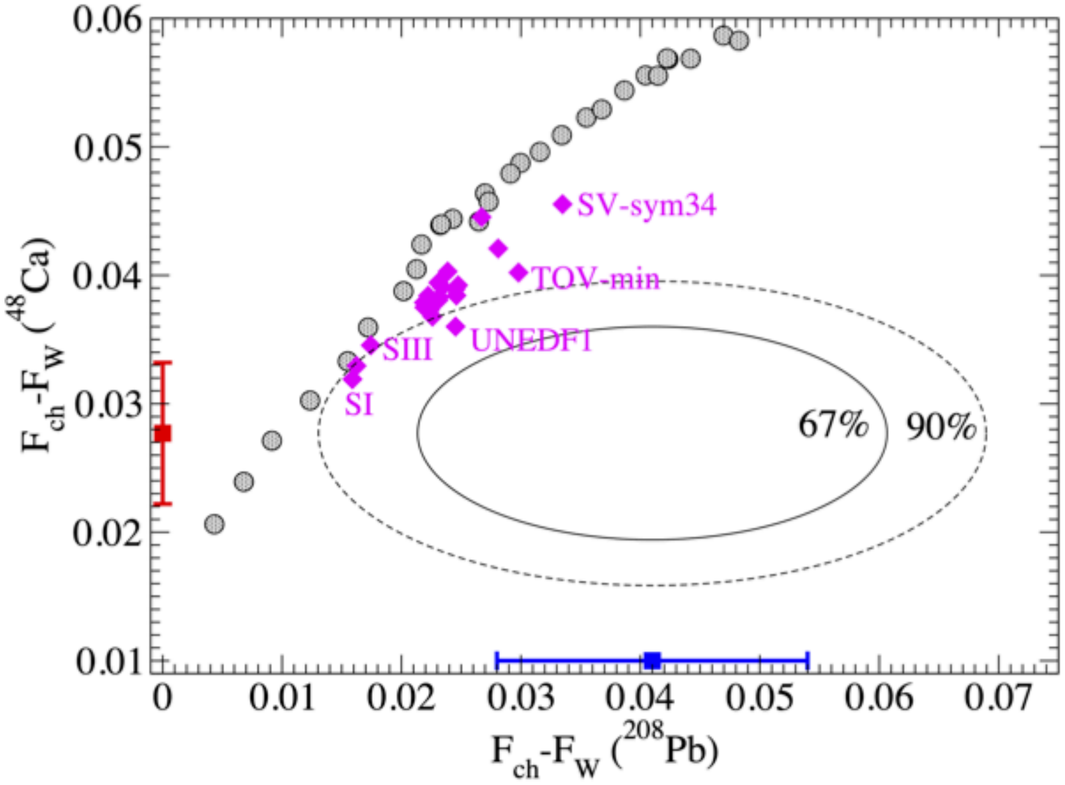

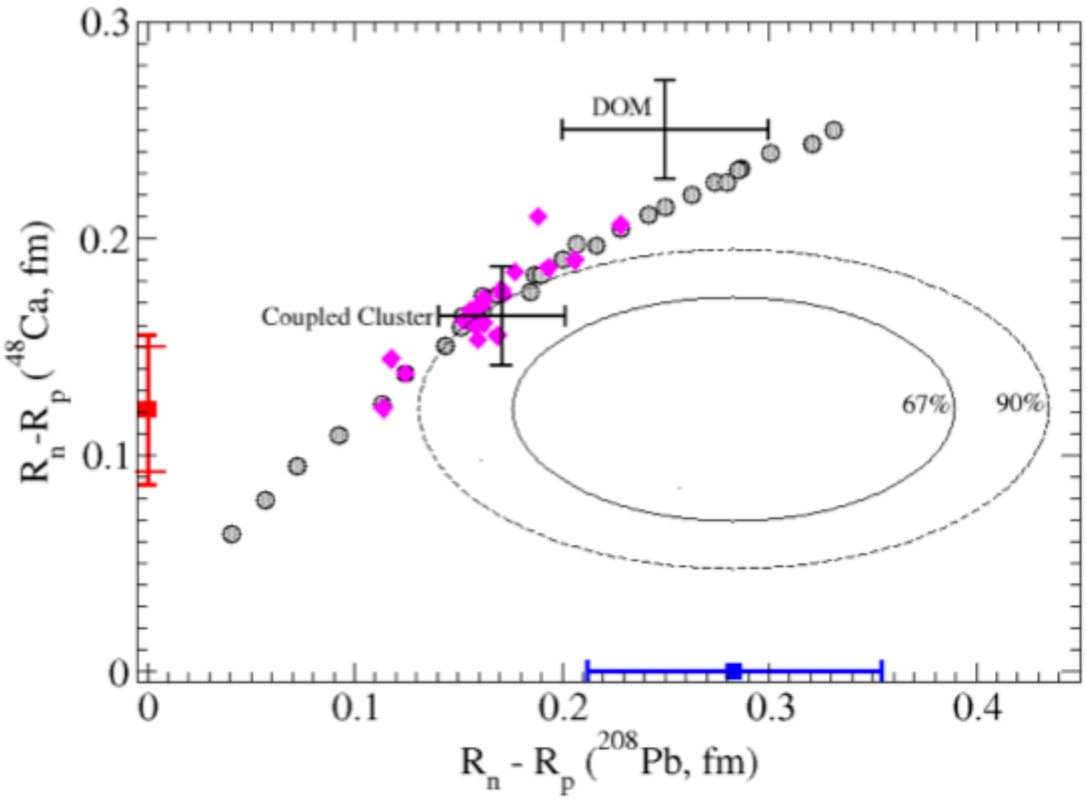

Figures from CREX 2022

How Much Tension?

RMF models

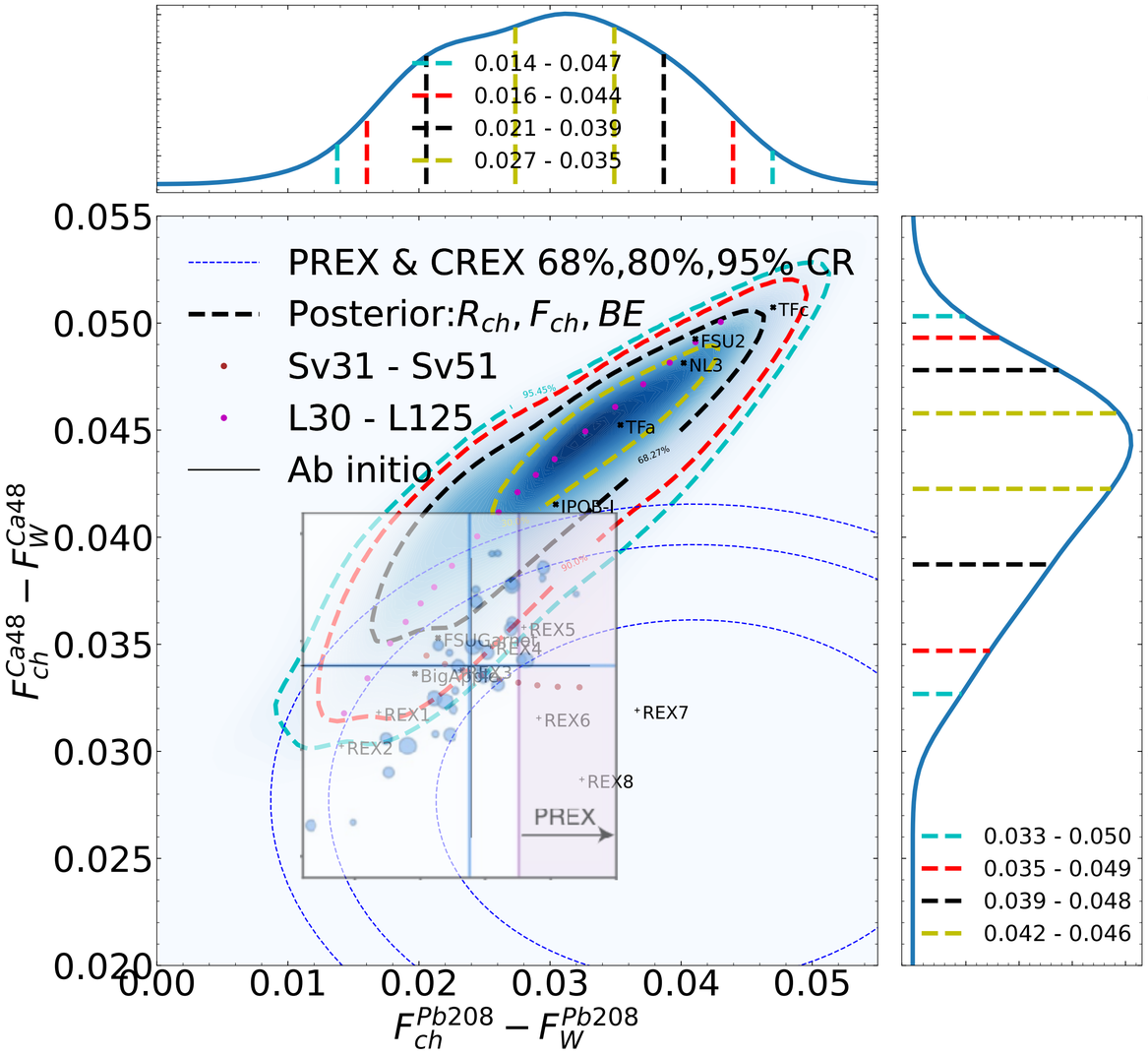

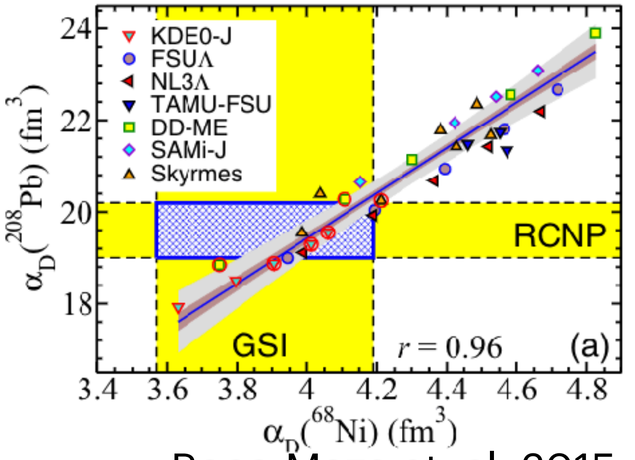

Roca-Maza et. al. 2015

- Confidence discrepancy:

$$P(\Delta\vec{x}) = \int P_{data}(\vec{x}) P_{posterior}(\vec{x} + \Delta\vec{x}) d^n\vec{x}$$

$$P_{disagree} = \int_{P(\Delta\vec{x}) > P(0)} P(\Delta\vec{x}) d^n\Delta\vec{x}$$

Sigma Tension	Rch, BE, Fch	+PREX
Rch, BE, Fch	1.98 (95.2%)	2.12 (96.6%)
+CREX	1.59 (88.8%)	1.52 (87.2%)

- Consistent with Ab-initio calculation:

$$z = M(\theta) + \varepsilon_{\mathrm{exp}} + \varepsilon_{\mathrm{em}} + \varepsilon_{\mathrm{method}} + \varepsilon_{\mathrm{model}},$$

IMSRG, MBPT and CC calculation of 48Ca and 208Pb.
Hu et. al. 2022

How Much Tension?

Skyrme models

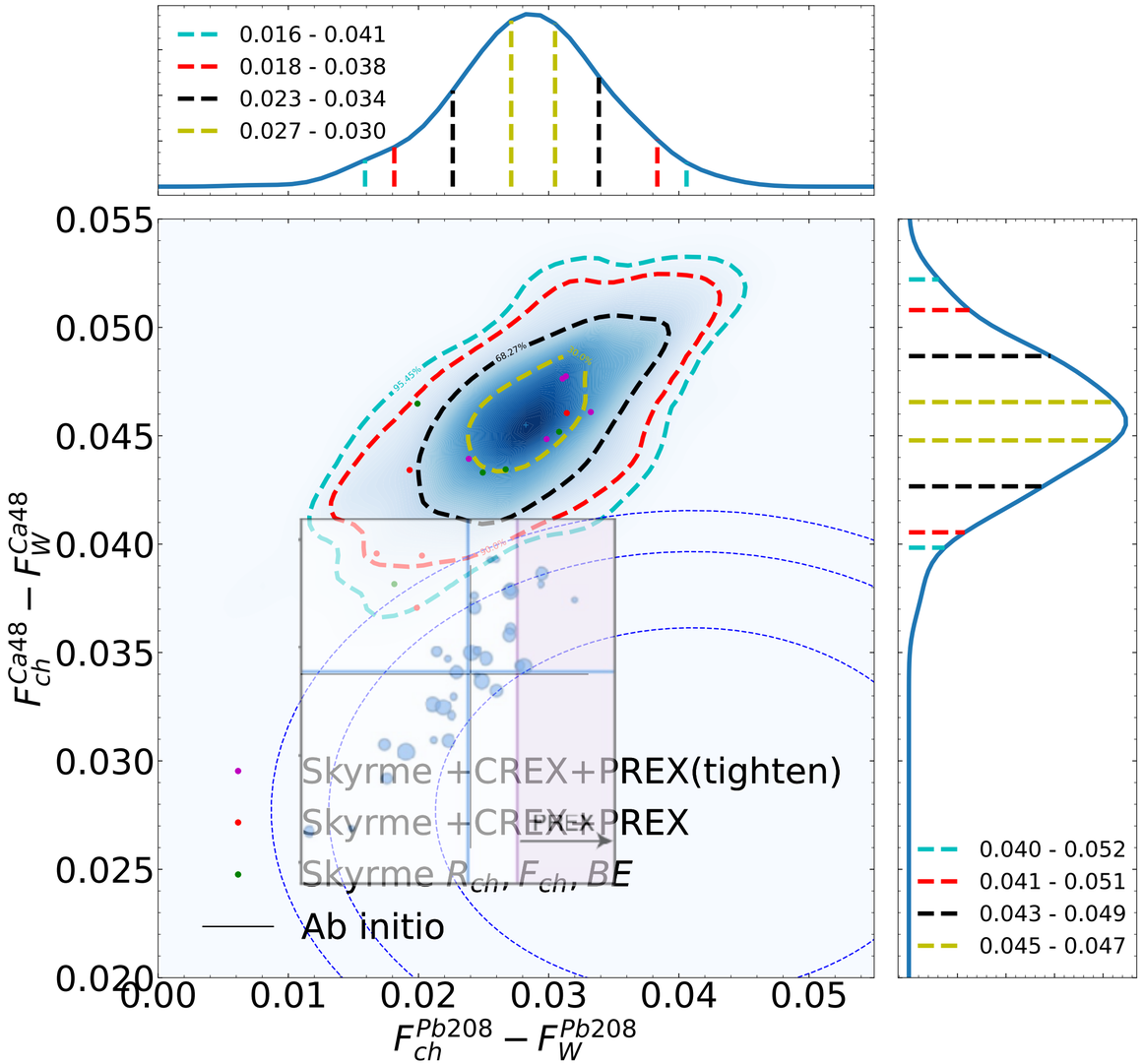

- Confidence discrepancy:

$$P(\Delta\vec{x}) = \int P_{data}(\vec{x})P_{posterior}(\vec{x}+\Delta\vec{x})d^n\vec{x}$$

$$P_{disagree} = \int_{P(\Delta\vec{x})>P(0)} P(\Delta\vec{x})d^n\Delta\vec{x}$$

Sigma Tension	Rch, BE, Fch	+PREX
Rch, BE, Fch	2.59(99.0%)	2.72(99.3%)
+CREX	2.34(98.1%)	2.44(98.5%)

- Consistent with Ab-initio calculation:

$$z = M(\theta) + \varepsilon_{\text{exp}} + \varepsilon_{\text{em}} + \varepsilon_{\text{method}} + \varepsilon_{\text{model}},$$

IMSRG, MBPT and CC calculation of 48Ca and 208Pb.
Hu et. al. 2022

Attempts to Solve the Tension

Density dependence of symmetry energy: ‘bulk’ density variation ‘localized’ density variation

- L30-L130 are traditional
- Sv31-Sv51 are unusual

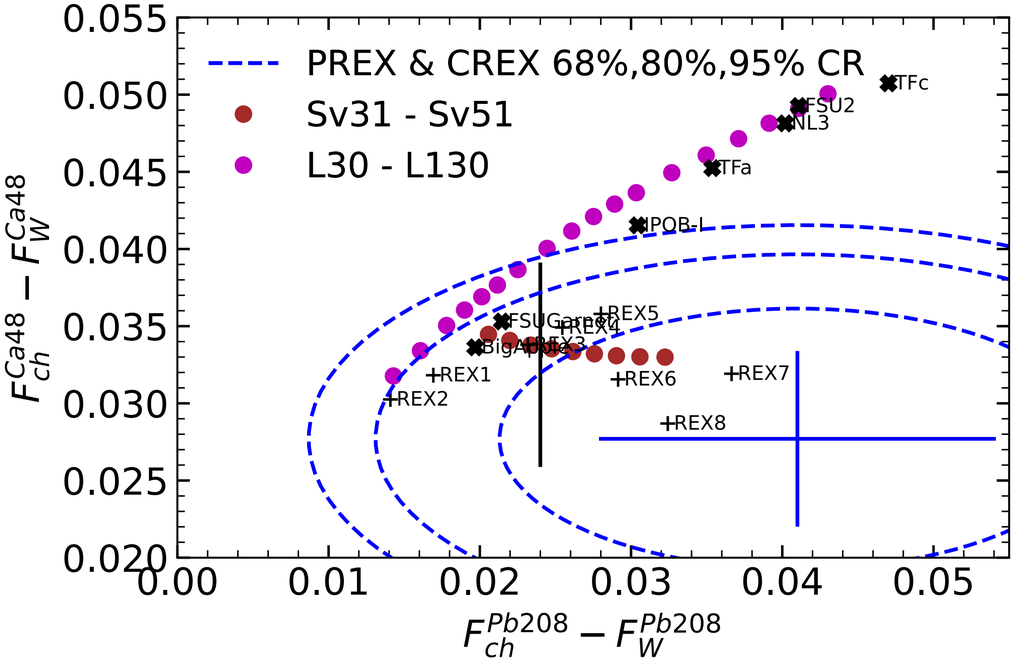

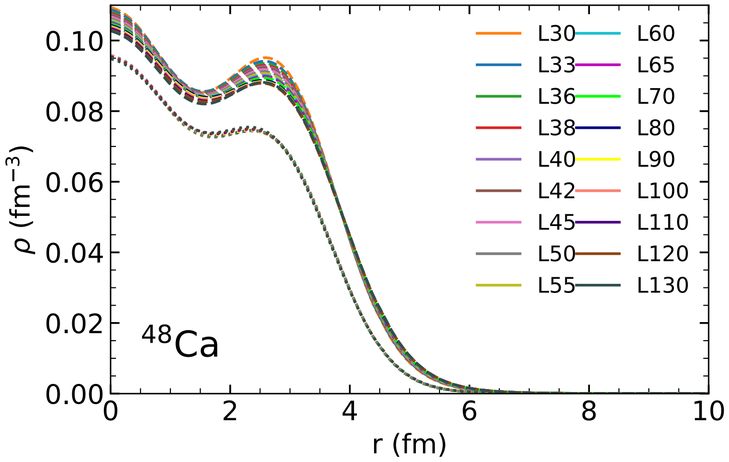

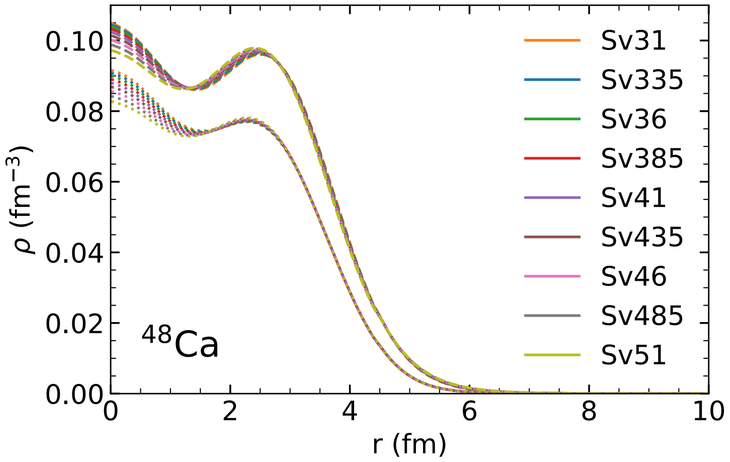

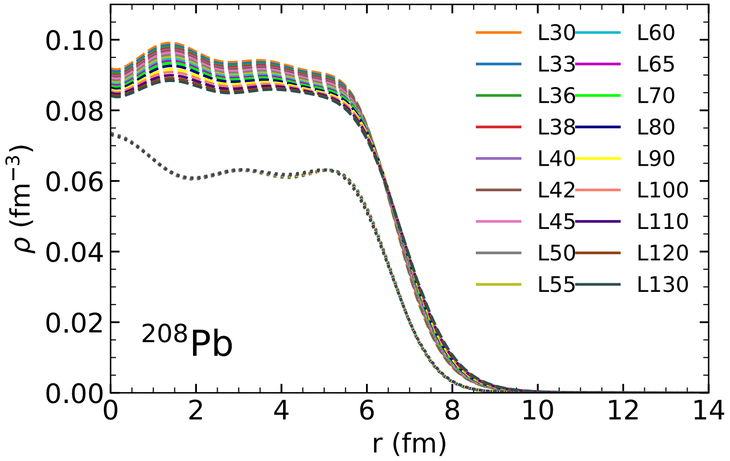

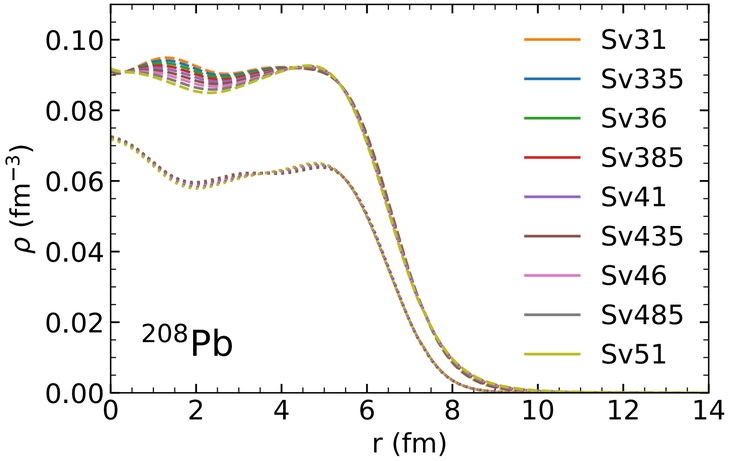

Can CREX Measure Neutron skin?

- RMS radius: $< r^2 > = \frac{1}{Q}\int r^2 \rho(\mathbf{r}) d^3r$
- Form Factor: $F(\mathbf{q}) = \frac{1}{Q}\int e^{i\mathbf{q}\cdot\mathbf{r}} \rho(\mathbf{r}) d^3r = 1 - \frac{1}{6}q^2 < r^2 > + \ldots$
- $\lim_{q<<1/\sqrt{< r^2 >}} < r^2 > = \frac{6[1 - F(q)]}{q^2}$

208Pb	1	-0.8	0.19
48Ca	1	-1.56	0.73

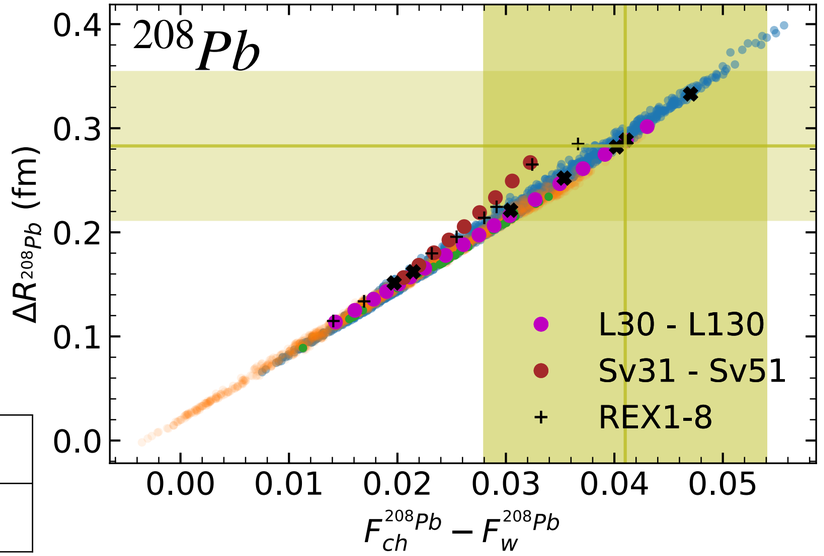

- Form factor to radius mapping is much less accurate for CREX:
  1. Momentum transfer q is a bit too large for CREX.
  2. MFT uncertainty increase for lighter nuclei.
- Better use form factor to constrain nuclear model.

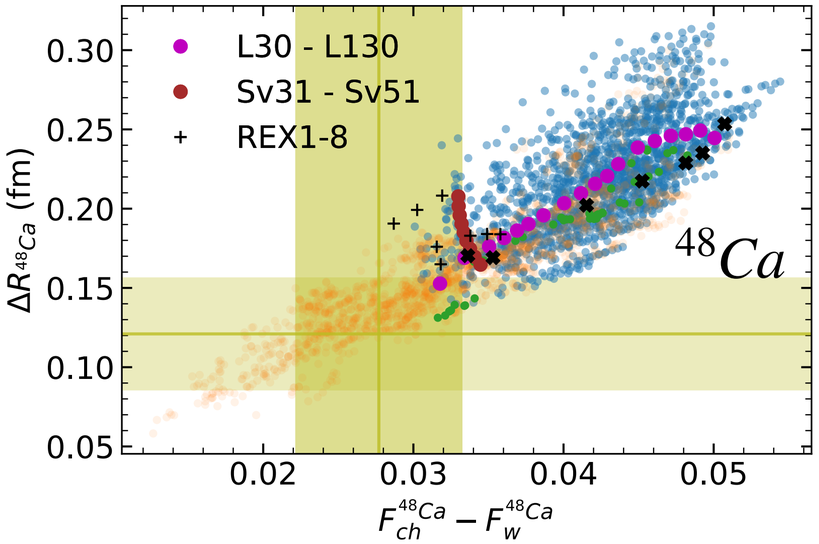

Sensitivity to Symmetry Energy Slope L

- ^{48}Ca form factor is sensitive
- ^{48}Ca skin is not sensitive

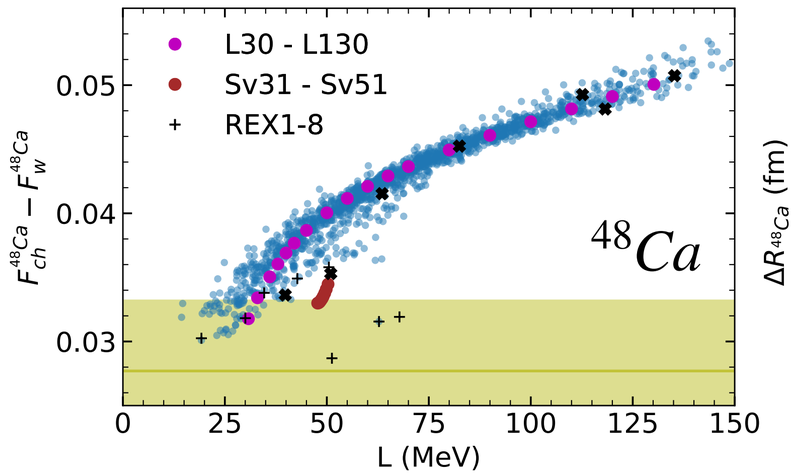

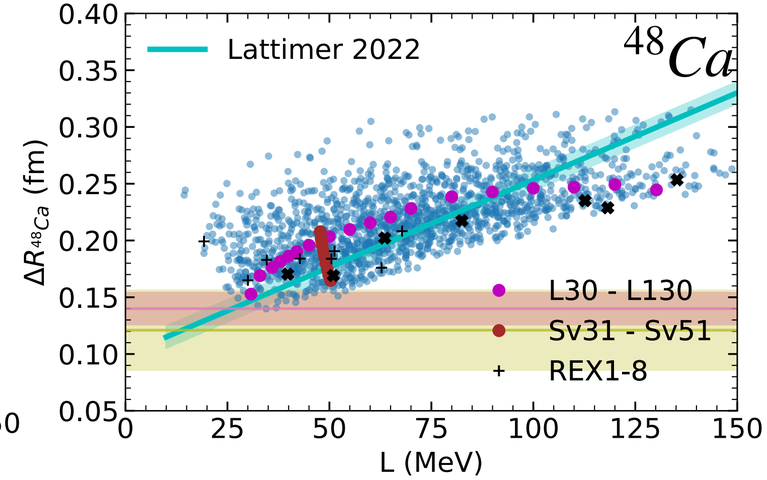

Neutron skin = 0.12-0.15 fm
Hagen et. al. 2016
Neutron skin = 0.141-0.187 fm
Hu et. al. 2022
Neutron skin = 0.126-0.154 fm
From other experiment

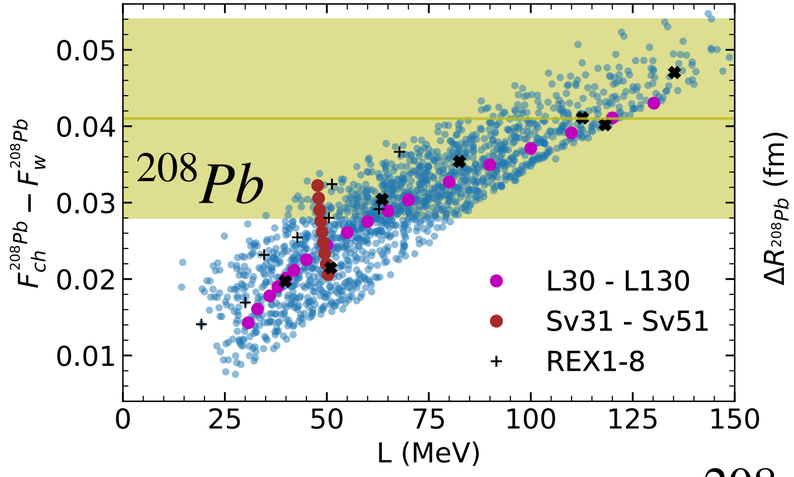

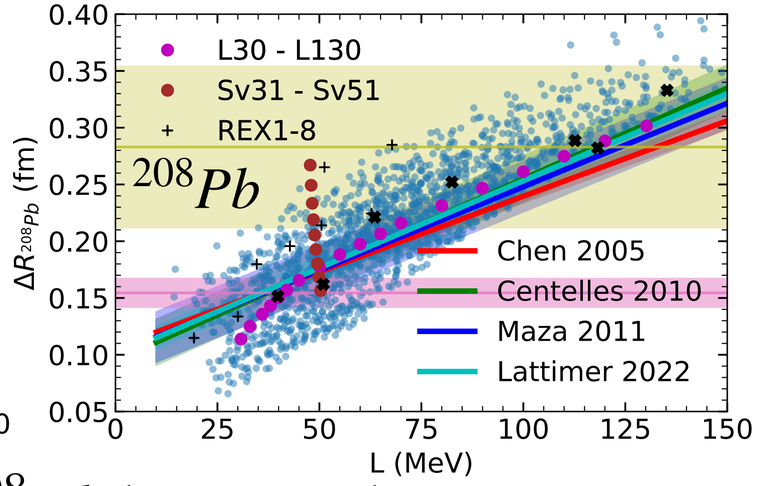

Neutron skin = 0.139-0.20 fm
Hu et. al. 2022
Neutron skin = 0.142-0.167 fm
From other experiment

- Skin and form factor of ^{208}Pb have similar sensitivity

Pearson Correlation

$$\mathrm{cov}[\mathrm{X}, \mathrm{p}(\mathrm{n_B}), \mathrm{P}] = \sum_{\mathrm{i}} \mathrm{P_i} \frac{(\mathrm{X_i} - \bar{\mathrm{X}})(\mathrm{p_i} - \bar{\mathrm{p}})}{\sigma_{\mathrm{X}} \sigma_{\mathrm{p}}}$$

Observable — Likelihood

Pressure at given density

$$S(X, n_1) = \frac{r_X}{\sqrt{2\pi}\sigma_X} \exp[-\frac{(n_1 - \mu_X)^2}{2\sigma_X^2}]$$

[fm]	Fch-Fw	Skin	Fch-Fw	Skin
μ_X	0.147	0.0932	0.121	0.113
σ_X	6E-04	7E-04	0.0522	0.0616
r_X	0.00214	0.00197	0.00250	0.00268

$$\mathrm{cov}[\mathrm{X}, \mathrm{p}(\mathrm{n_2})] = \int \mathrm{cov}[\mathrm{p}(\mathrm{n_1}), \mathrm{p}(\mathrm{n_2})] \mathrm{S}(\mathrm{X}, \mathrm{n_1}) \mathrm{dn_1}$$

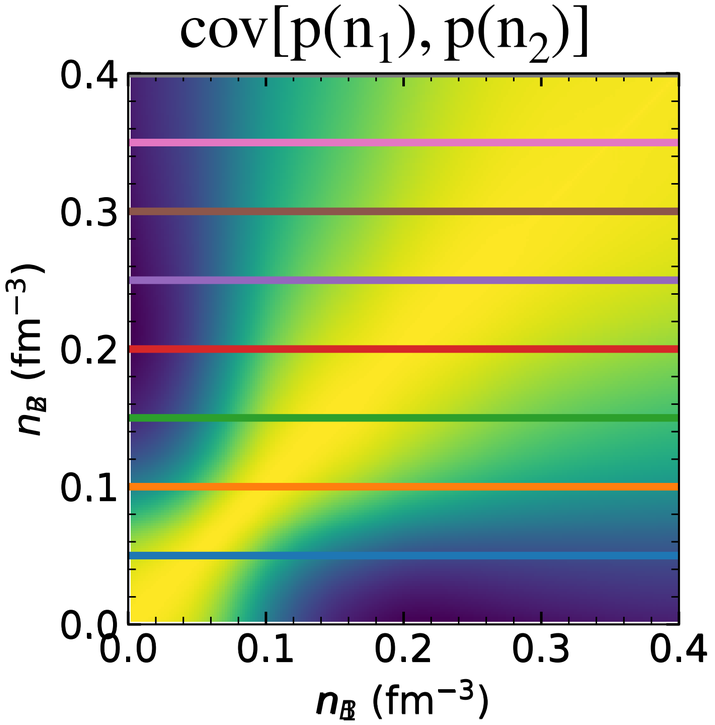

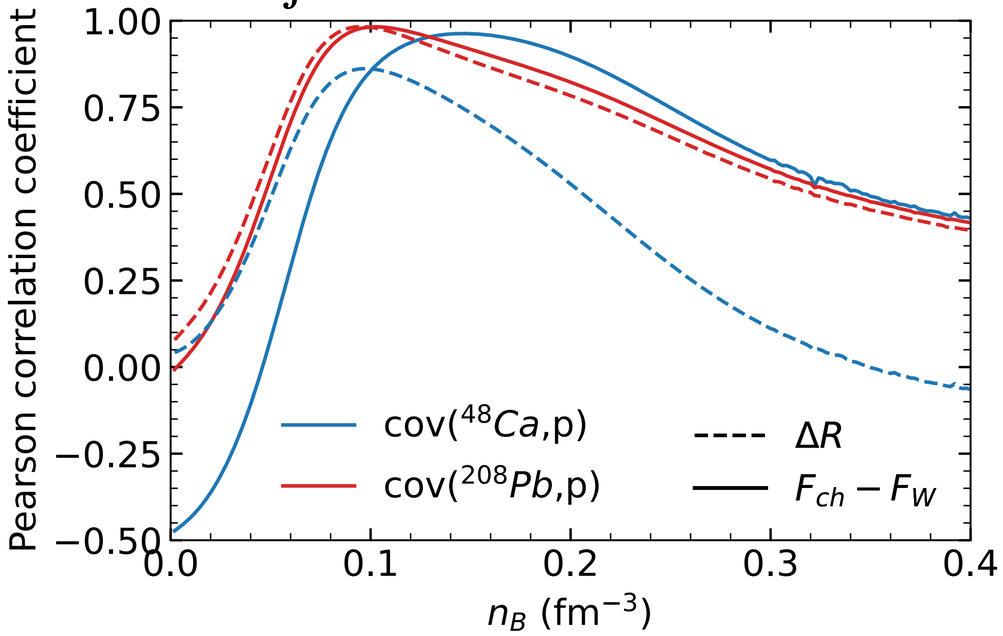

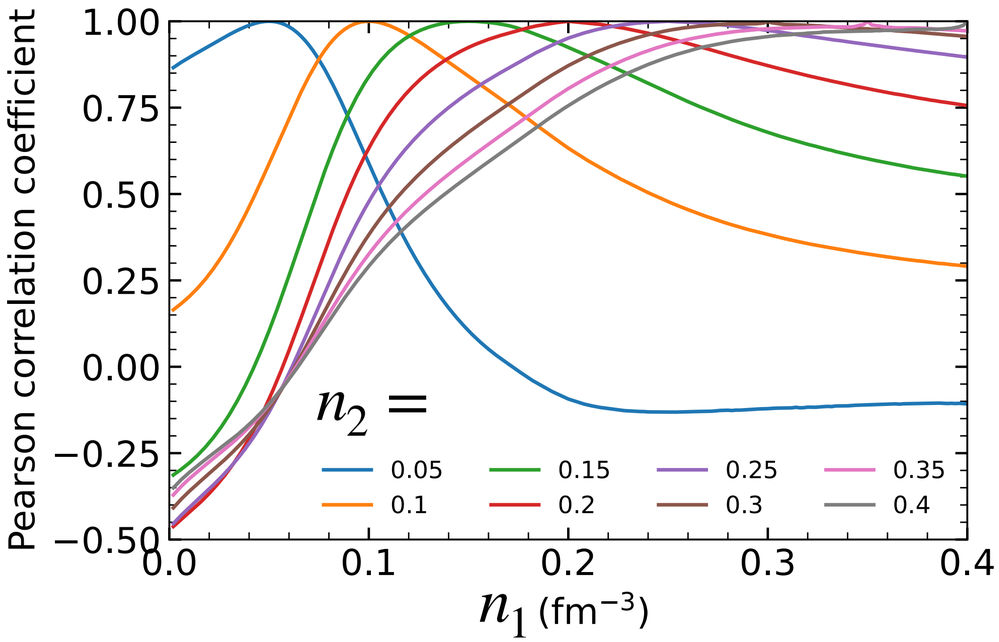

Bayesian Analysis

Posterior of Sv and L

- The weak form factor of PREX+CREX:

$$S_V = 33.2^{+5.7}_{-7.33}\text{MeV}, L = 41.8^{+15.5}_{-16.7}\text{MeV}$$

- Dipole polarizability of ^{208}Pb:

$$L = \left[6.11 \pm 0.316\right] S_v - \left[146 \pm 1\right] \text{ MeV}$$

$$S_V = 30.6^{+3.12}_{-2.79} \text{ MeV}$$

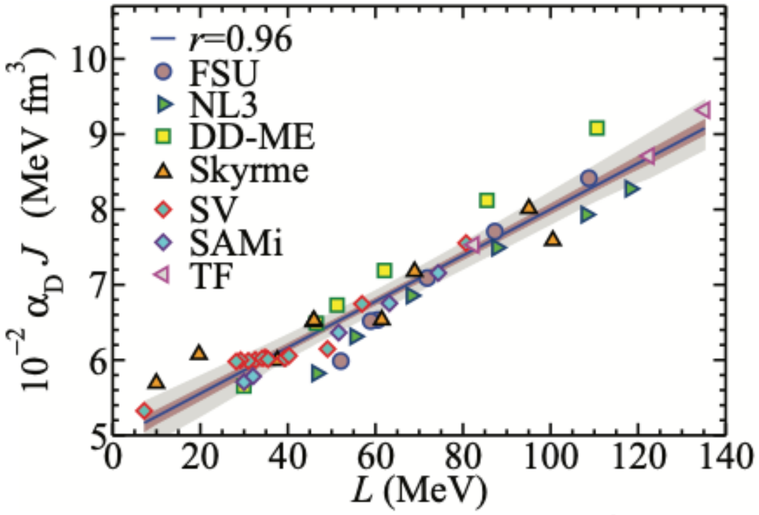

Moca-Maza et. al. 2013

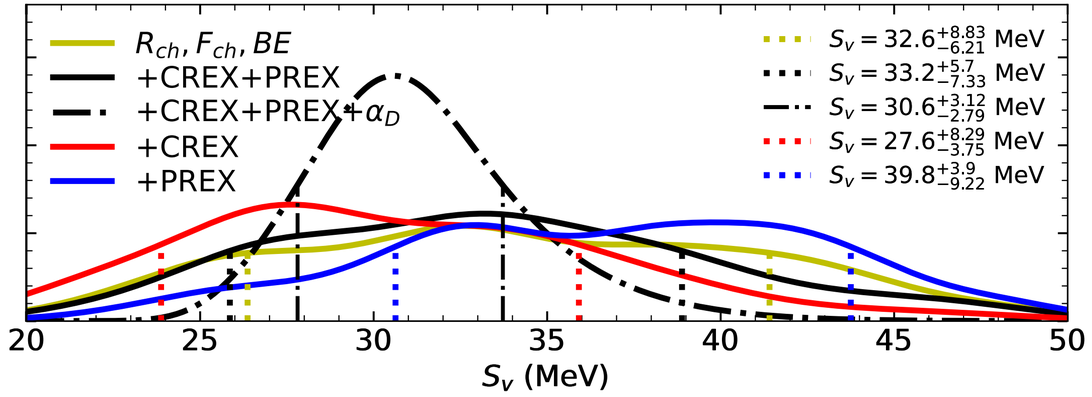

Skyrme EDF

Z. Zhang et. al. 2022

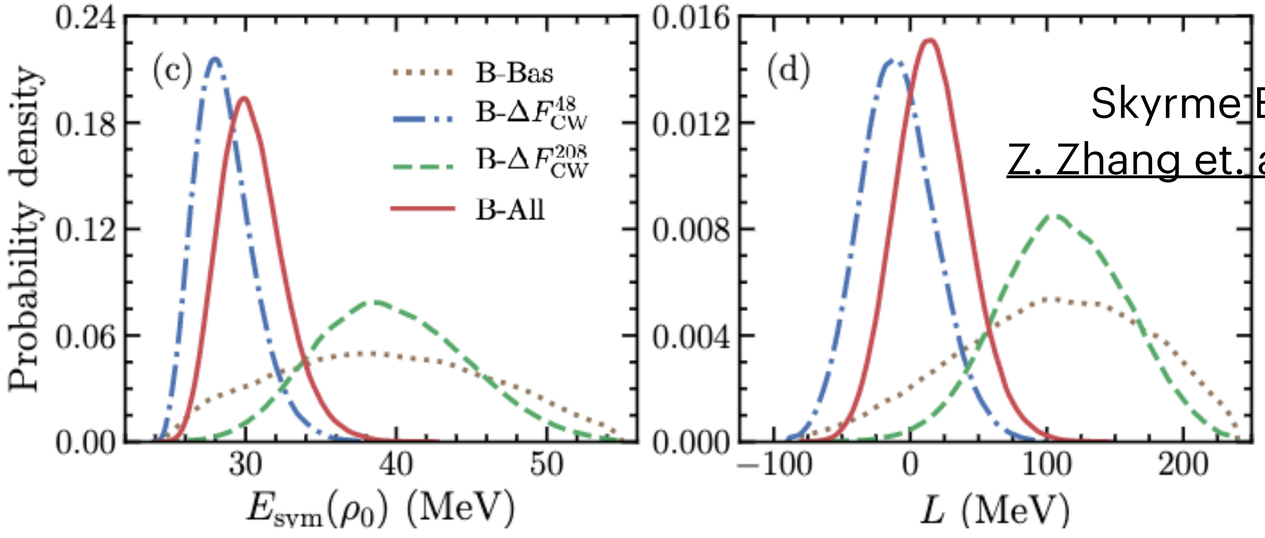

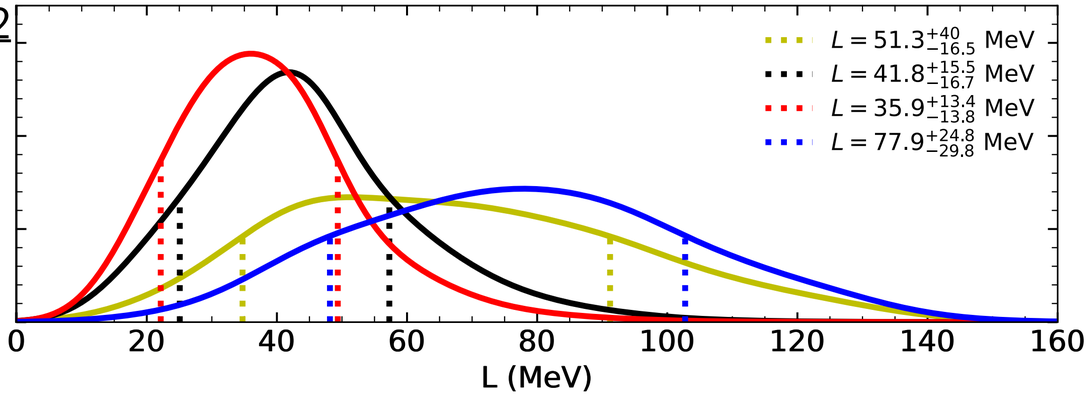

Skyrme Bayesian Analysis

Posterior of Sv and L

- The weak form factor of PREX+CREX:
  $S_V = 30.5^{+5.47}_{-3.78}\text{MeV}, L = 64^{+20}_{-32.2}\text{MeV}$
- Dipole polarizability of ^{208}Pb:
  $L = \left[6.11 \pm 0.316\right] S_v - \left[146 \pm 1\right]\ \text{MeV}$
  $S_V = 34.1^{+3.93}_{-3.84}\ \text{MeV}$

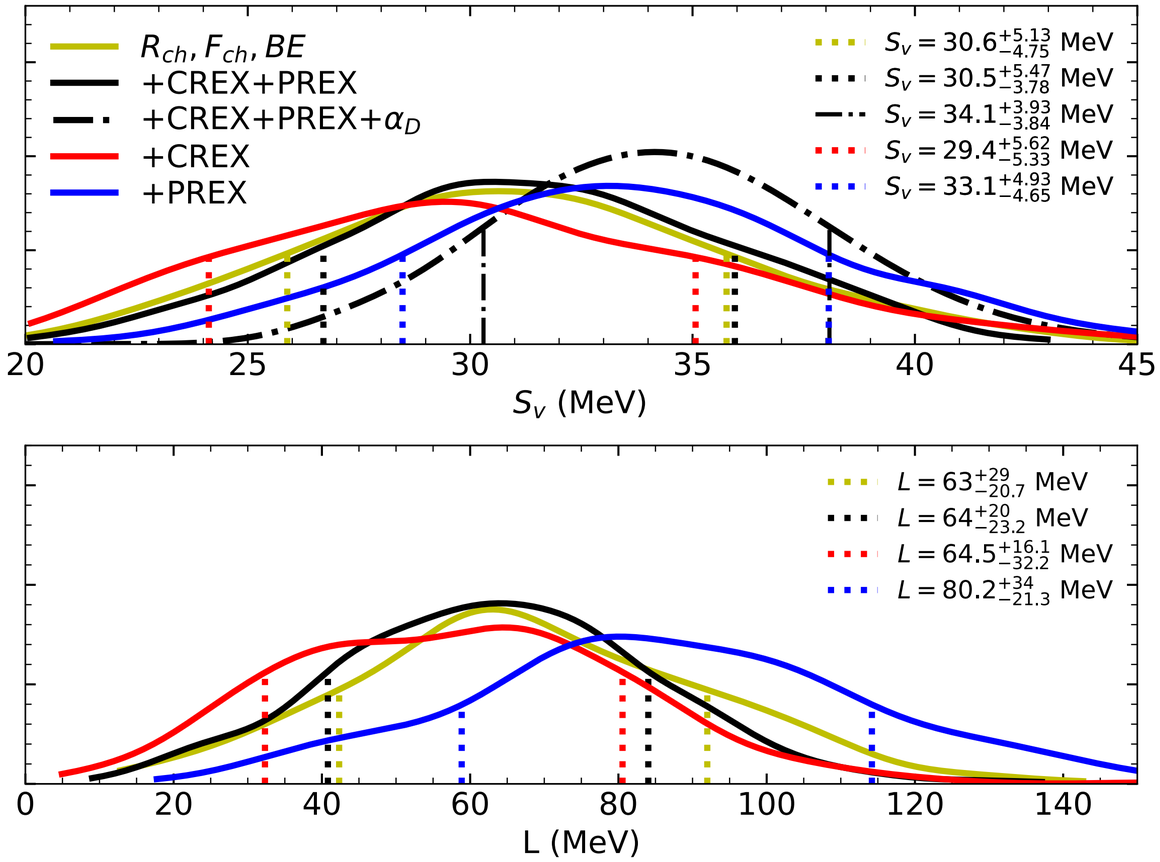

RMF vs Skyrme

due to Rch+Fch+BE constraints

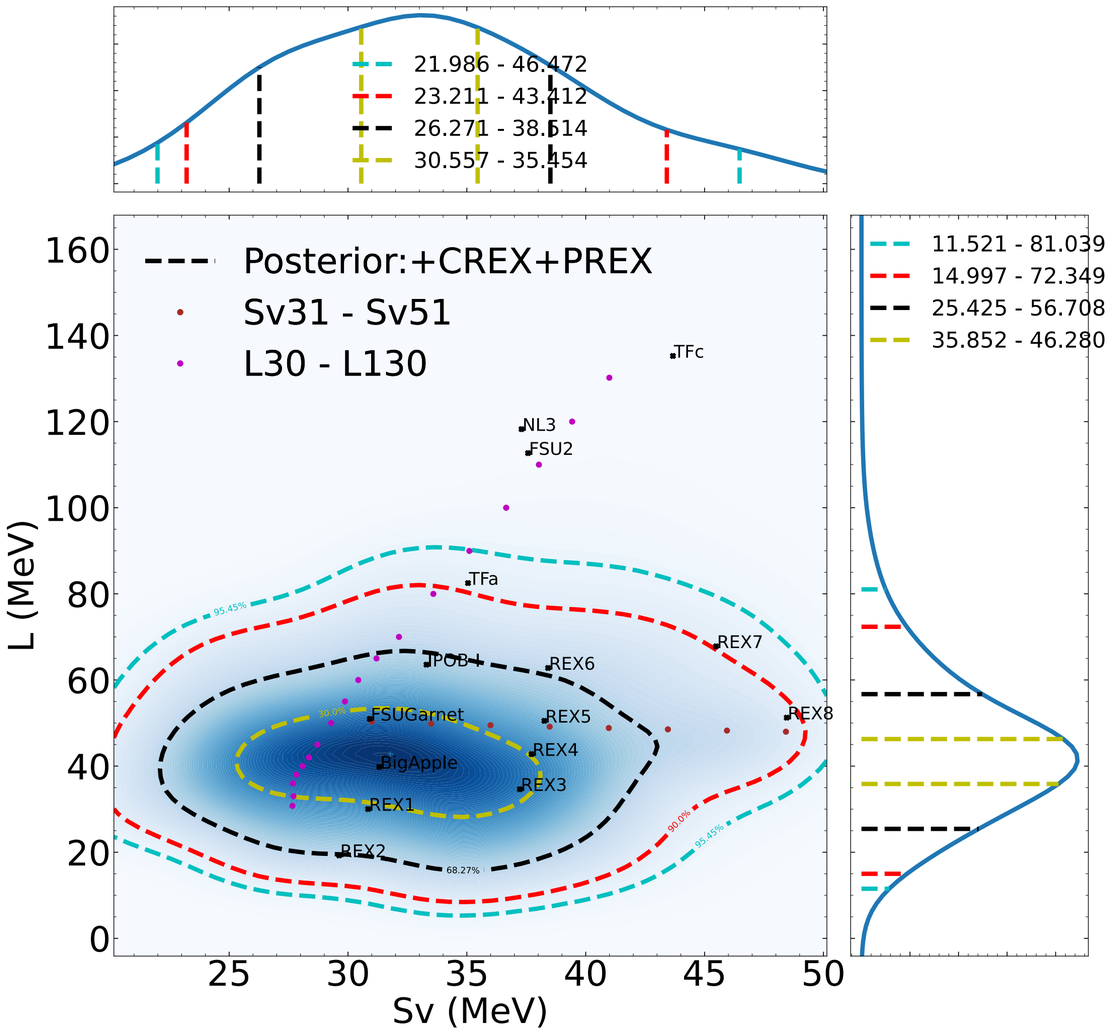

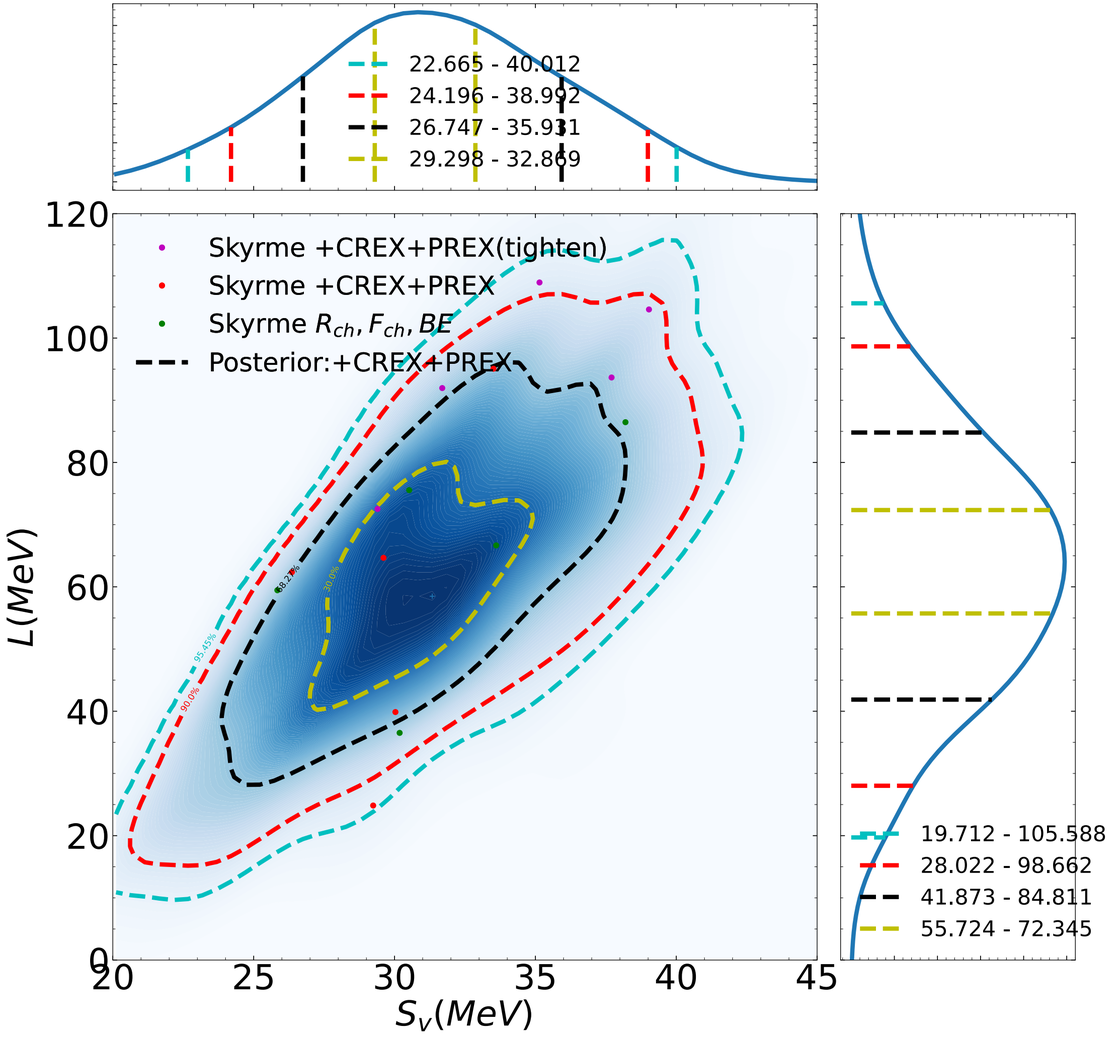

RMF vs Skyrme

due to Rch+Fch+BE constraints

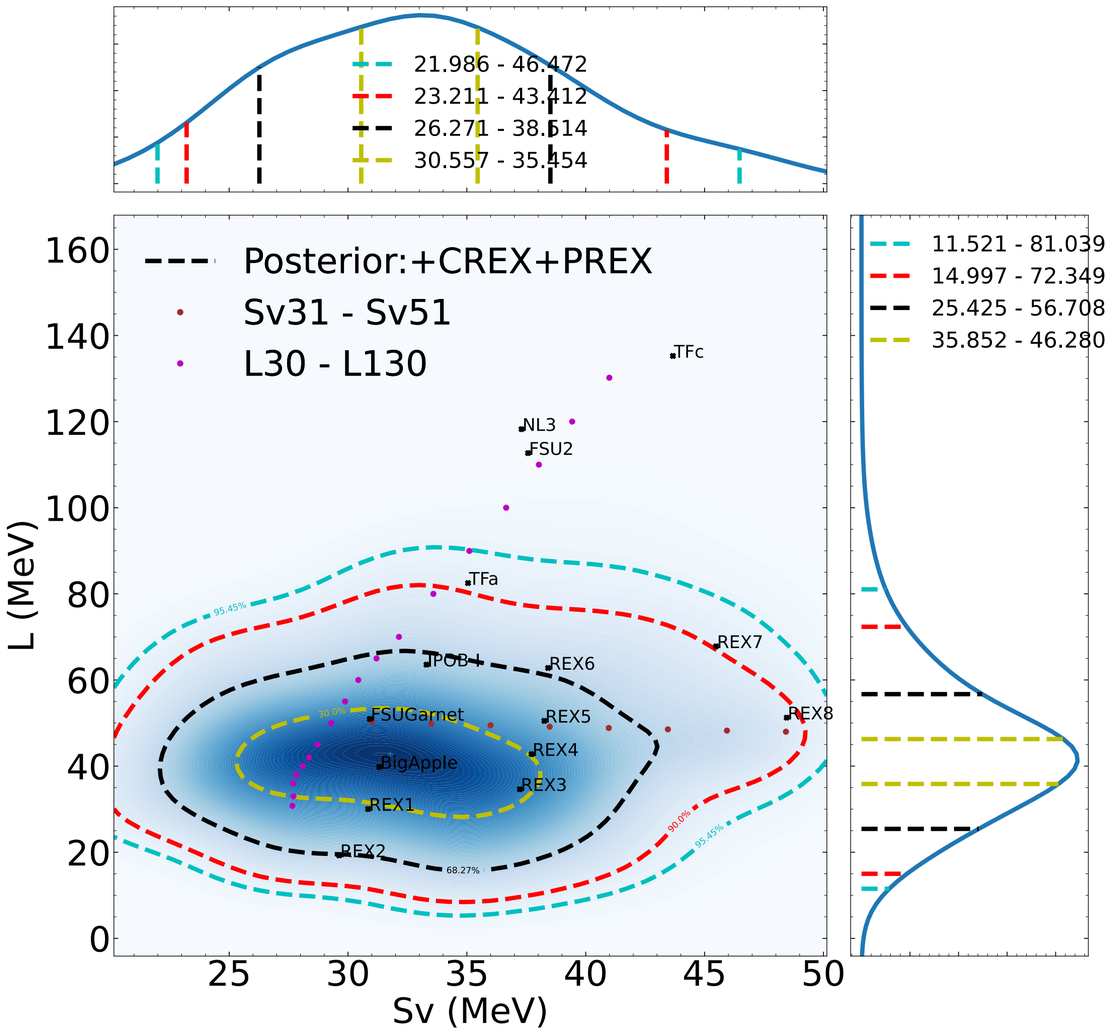

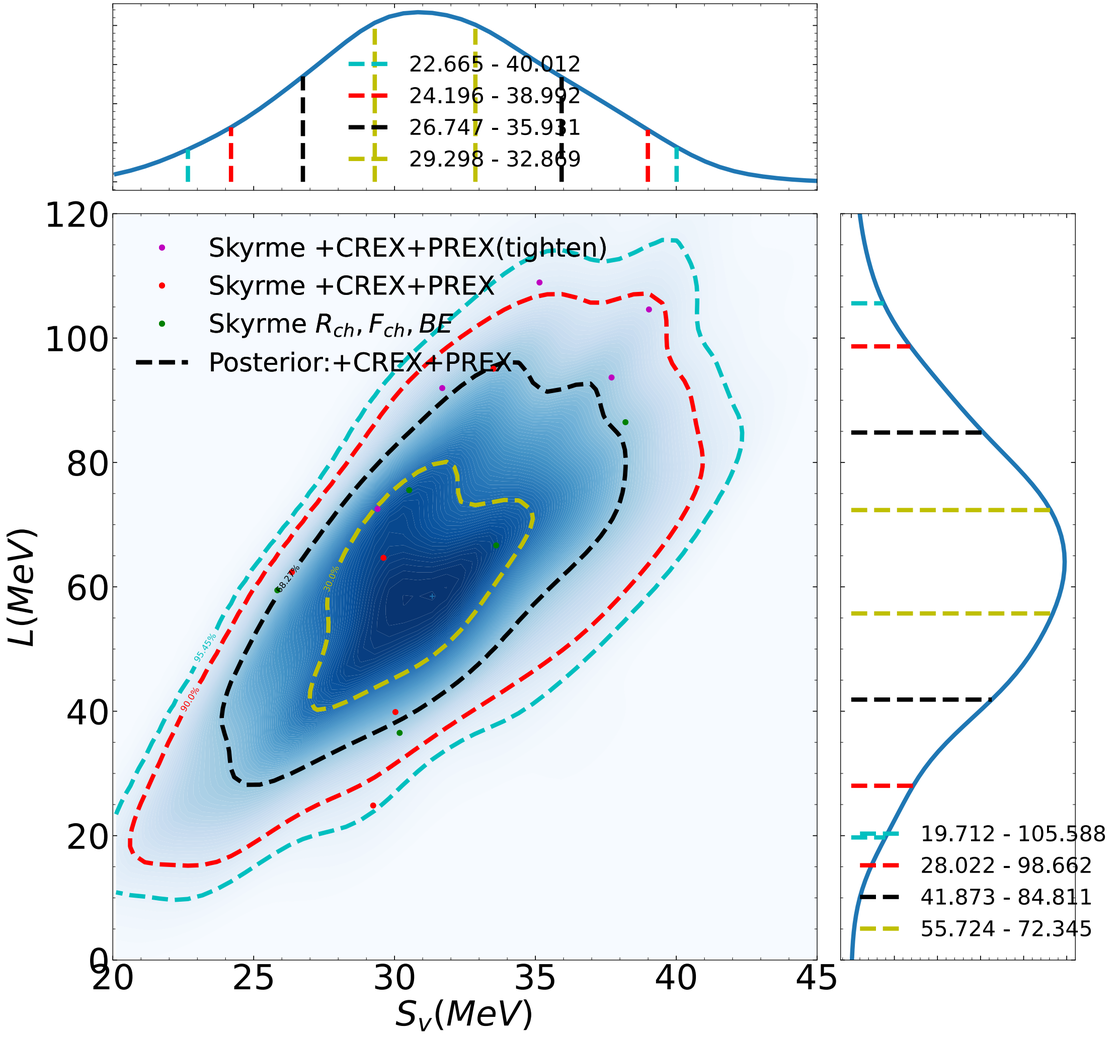

Compared with Astro

- Likelihood in uniform L

$$P(\mathcal{M} \mid \mathcal{O}_{M_{max}}) = \exp\left[-\frac{(M_{max} - M^{\mathcal{O}}_{max})^2}{2\sigma_{M_{max}}}\right]$$

$$P(\mathcal{M} \mid \mathcal{O}) = \int dM \exp\left[-\frac{(\beta_{\mathcal{O}} - \beta(M \mid \mathcal{M}))^2}{2\sigma^2_{\beta_{\mathcal{O}}}} - \frac{(M_{\mathcal{O}} - M)^2}{2\sigma^2_{M_{\mathcal{O}}}}\right]$$

$$P(\mathcal{M} \mid \mathcal{O}_{GW170817}) = \Theta(\Lambda^{\mathcal{O}}_{1.4} - \Lambda_{1.4})$$

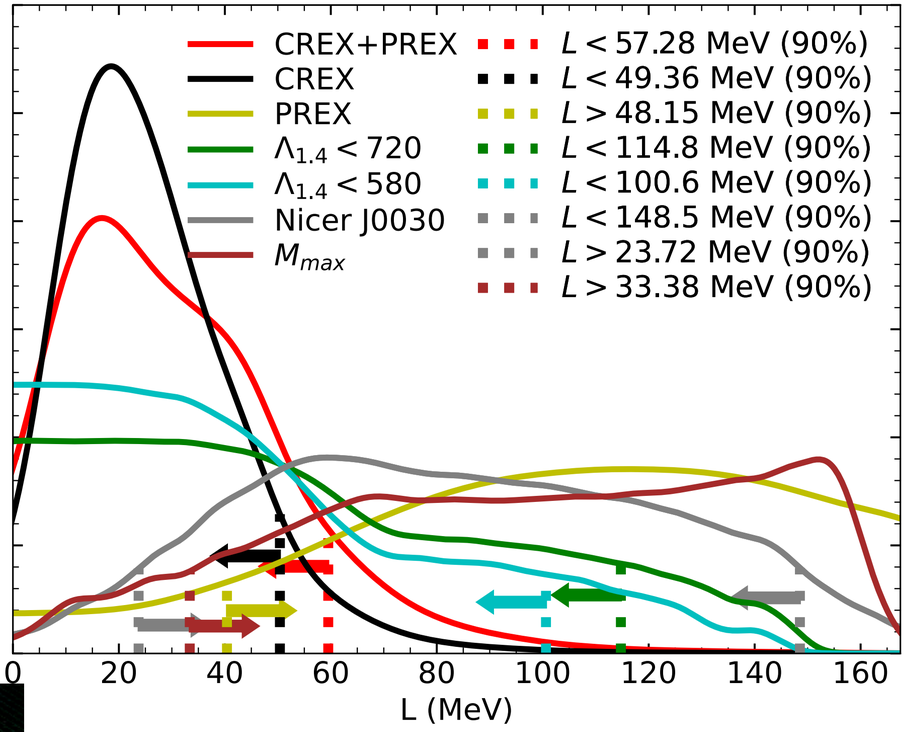

Remove

	value	σ_i
R_{ch}^{48Ca}	3.48	0.060
R_{ch}^{90Zr}	4.27	0.0854
R_{ch}^{208Pb}	5.5	0.11
BE^{48Ca}	6[illegible]	0.1734
BE^{90Zr}	8.71	0.1742
BE^{208Pb}	7.87	0.1574
F_{ch}^{48Ca}	0.1581	0.001
F_{ch}^{208Pb}	0.409	0.001
F_W^{48Ca}	0.1304	0.00557
F_W^{208Pb}	0.368	0.013
M_{max}	2.2	0.1
β_{J0030}	0.159	0.011
$\Lambda_{1.4}$	<720	

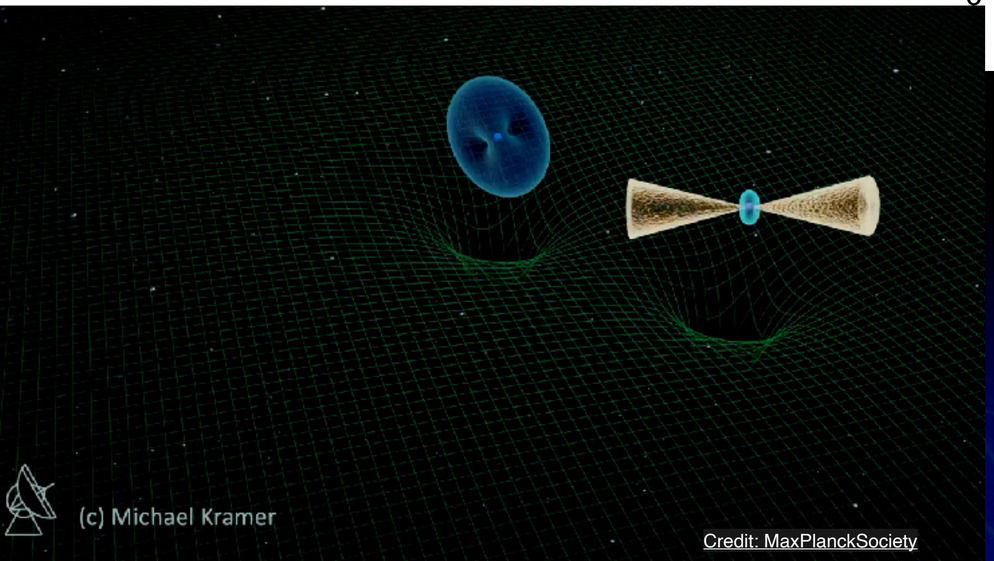

Credit: MaxPlanckSociety

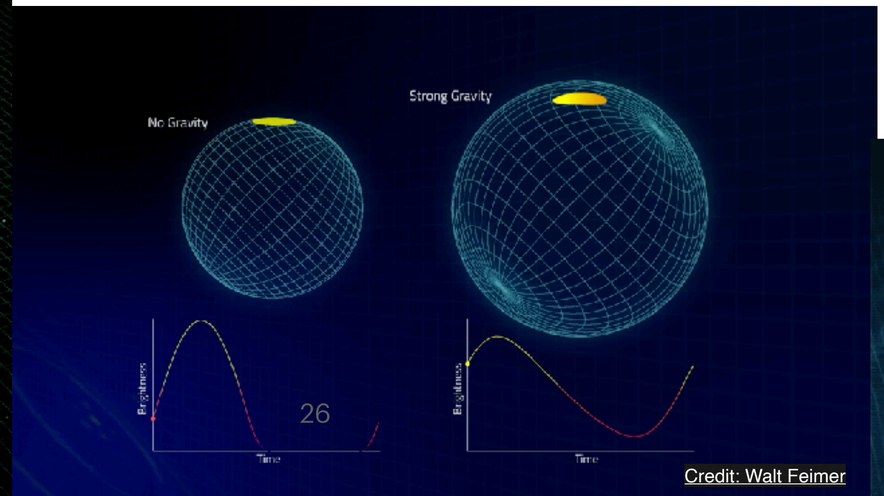

Credit: Walt Feimer

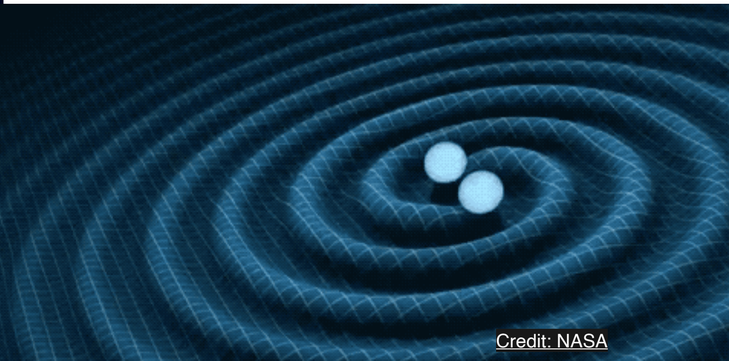

Credit: NASA

Impact on Equation of State(EOS)

- PREX is sensitive to EOS at 0.1 fm^{-3}.
- CREX is sensitive to EOS around saturation.
- PREX+CREX modulates posterior consistent UG and χEFT
- Astronomical constraints are relatively weak at low density.

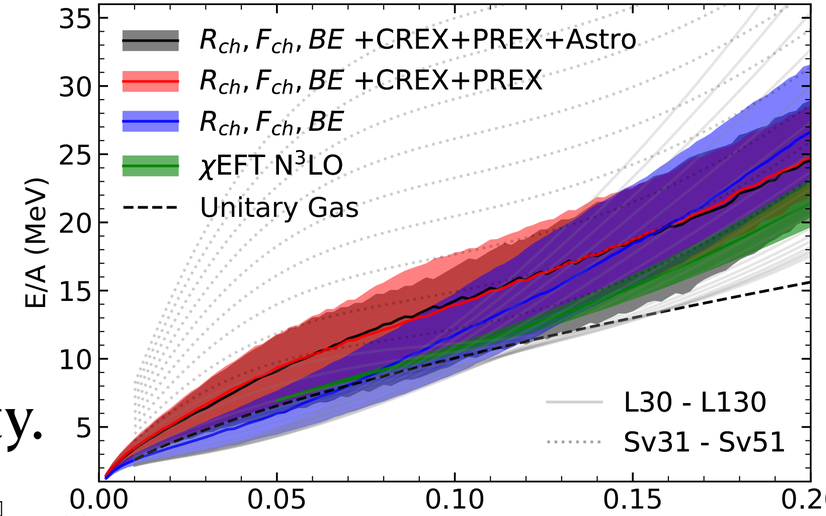

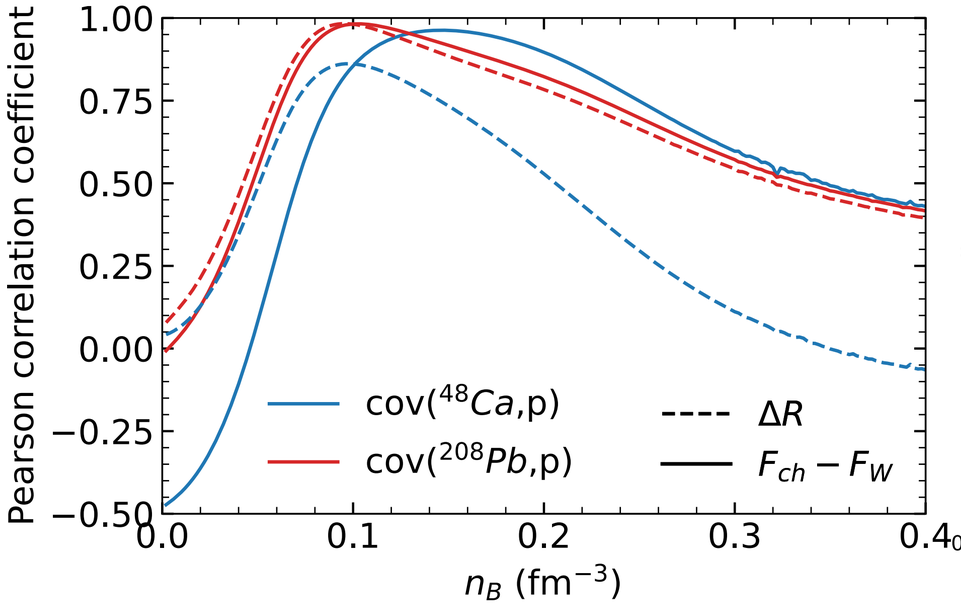

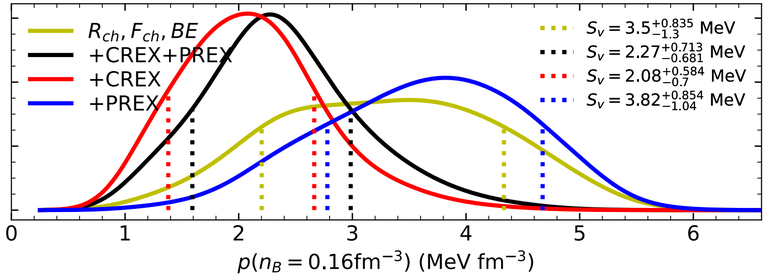

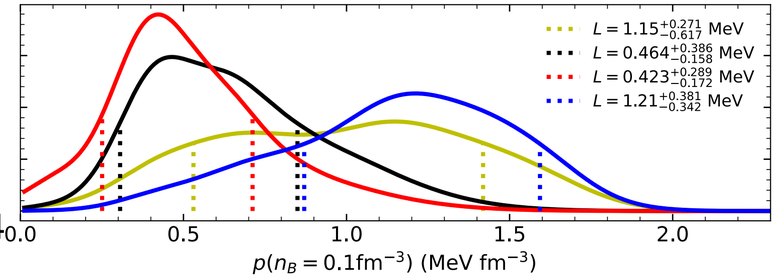

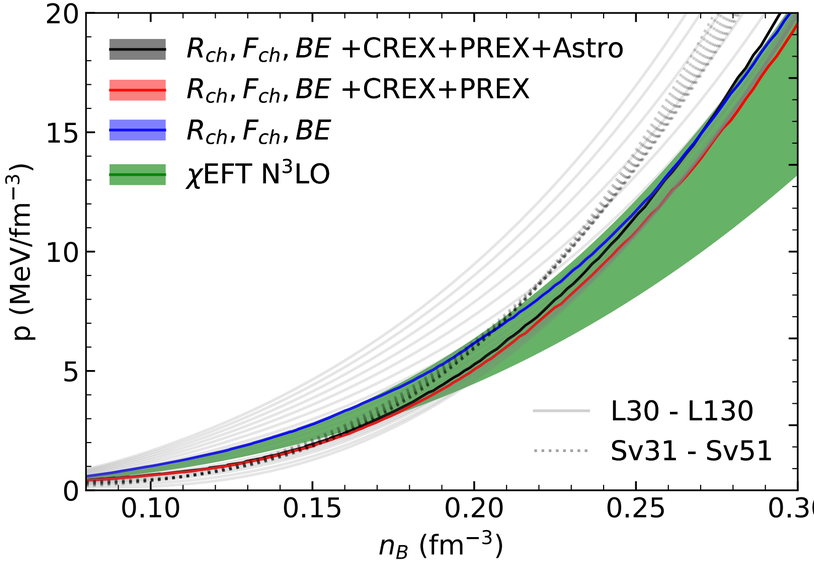

Direct Urca Process

- Direct Urca Process:

$$p + e \rightarrow n + \nu$$
$$\bar{\nu} + p + e \leftarrow n$$

- Kinetic condition:

$$p_F^e + p_F^p > p_F^n$$
$$n_p/n_n \gtrsim 0.14$$

- Modified Urca process with superfluidity explains majority cooling data.
- PREX+CREX is consistent with the small probability of a direct Urca process.

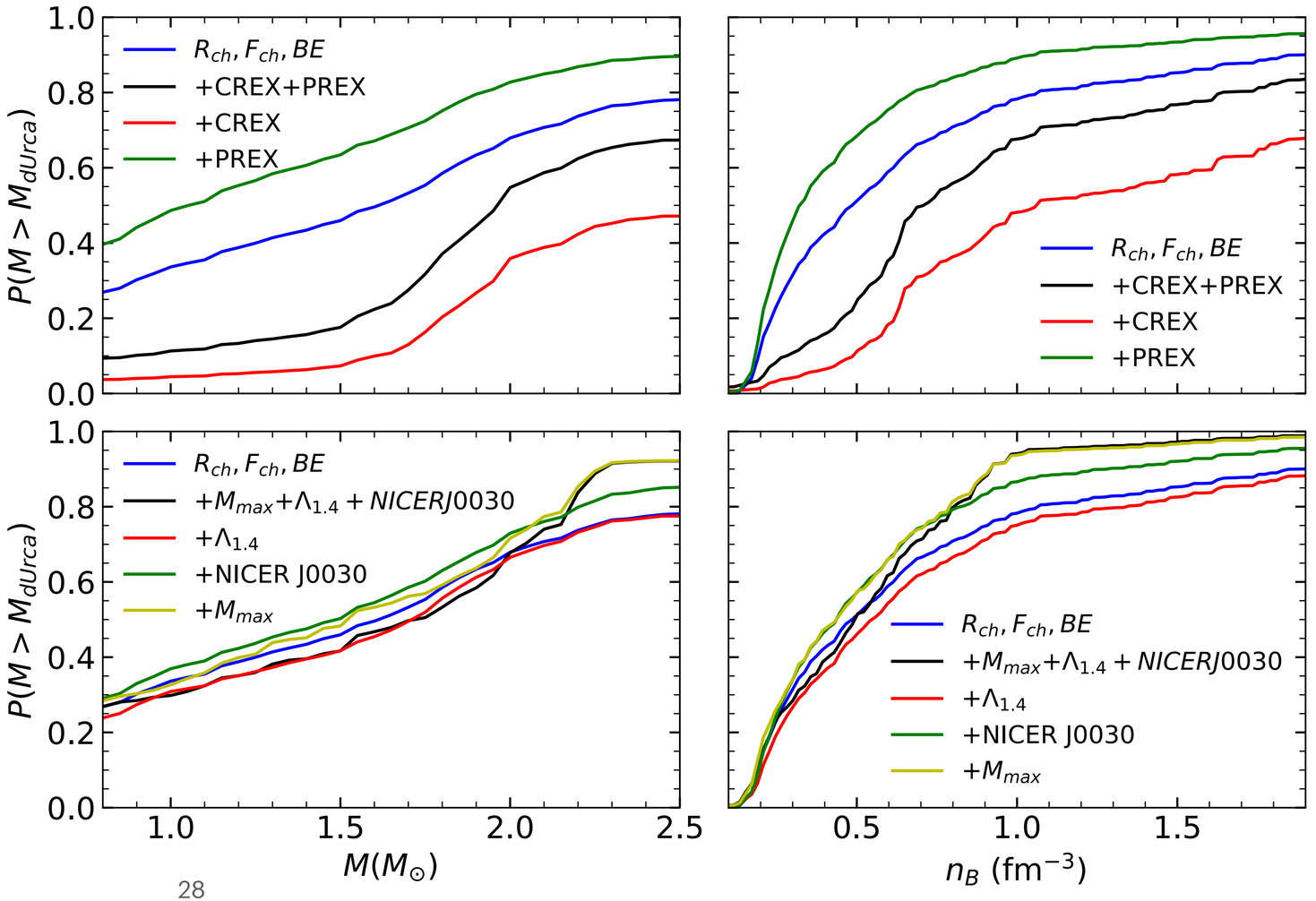

Conclusion

- There's 1.5 to 2 sigma tension between PREX + CREX and the model.
- The mild tension helps constrain density dependence of symmetry energy
- CREX indeed provides more information than PREX.
- PREX + CREX is consistent with ab-initio calculation, dipole polarizability, and other experiments regarding symmetry energy.
- Astronomical observation has very limited constraints on EOS below saturation.
- Small probability of a direct Urca process is supported by PREX + CREX.
- Looking forward to MREX confirming PREX.

Backup Slides

Posterior (Rch+Fch+BE) vs Posterior (+PREX+CREX)

RMF

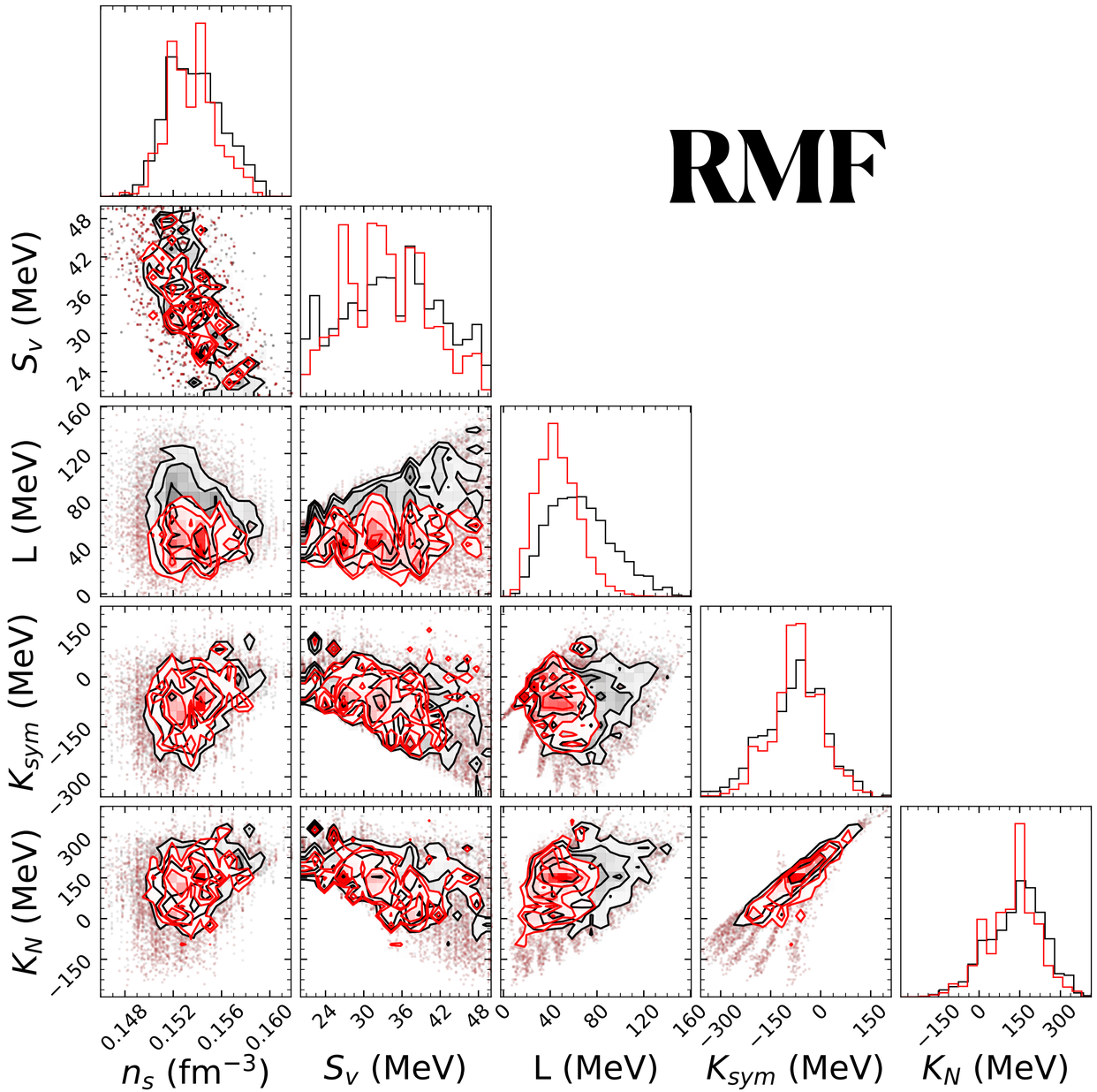

Skyrme

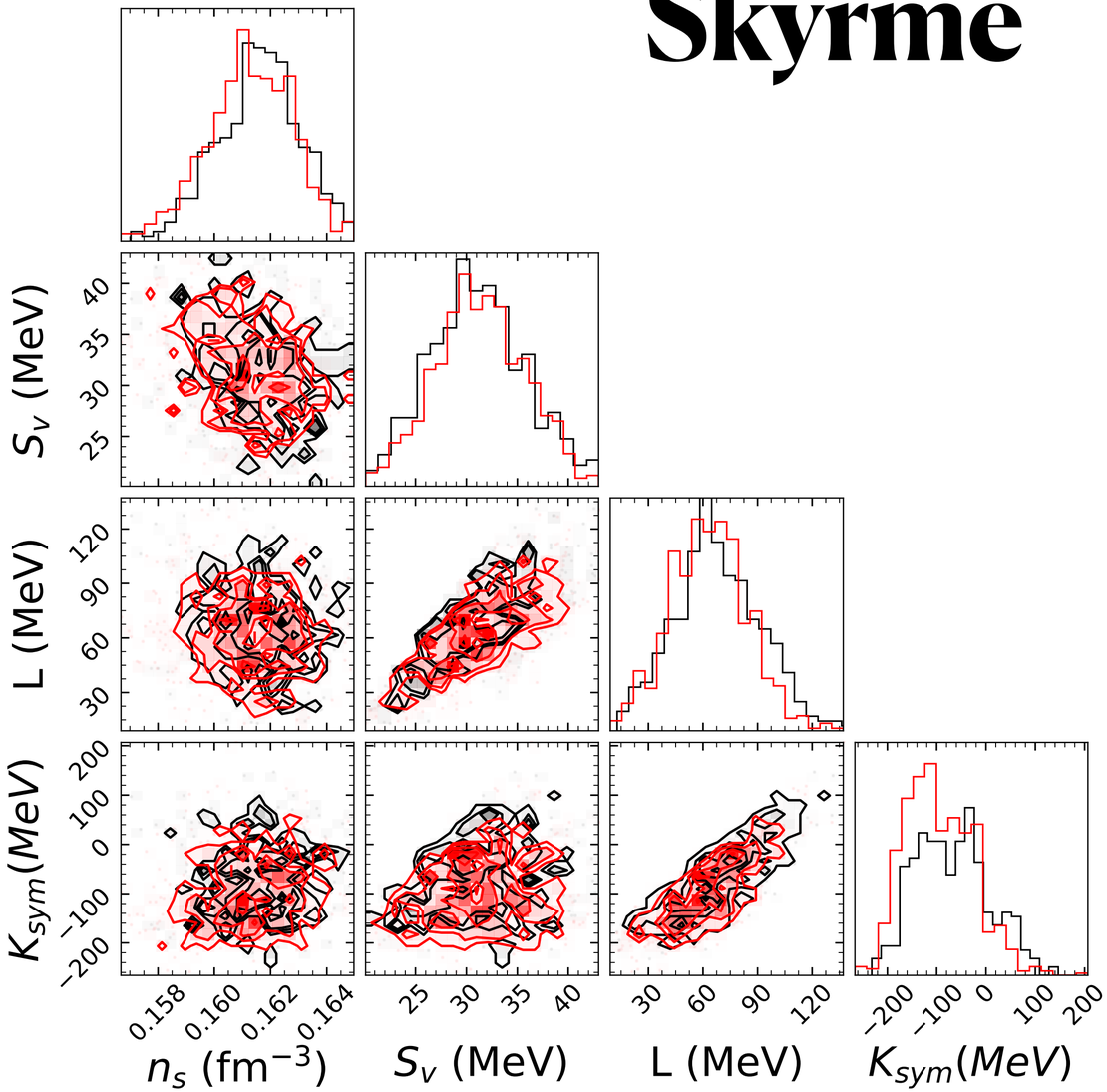

Posterior (Rch+Fch+BE) vs Posterior (+PREX+CREX)

RMF

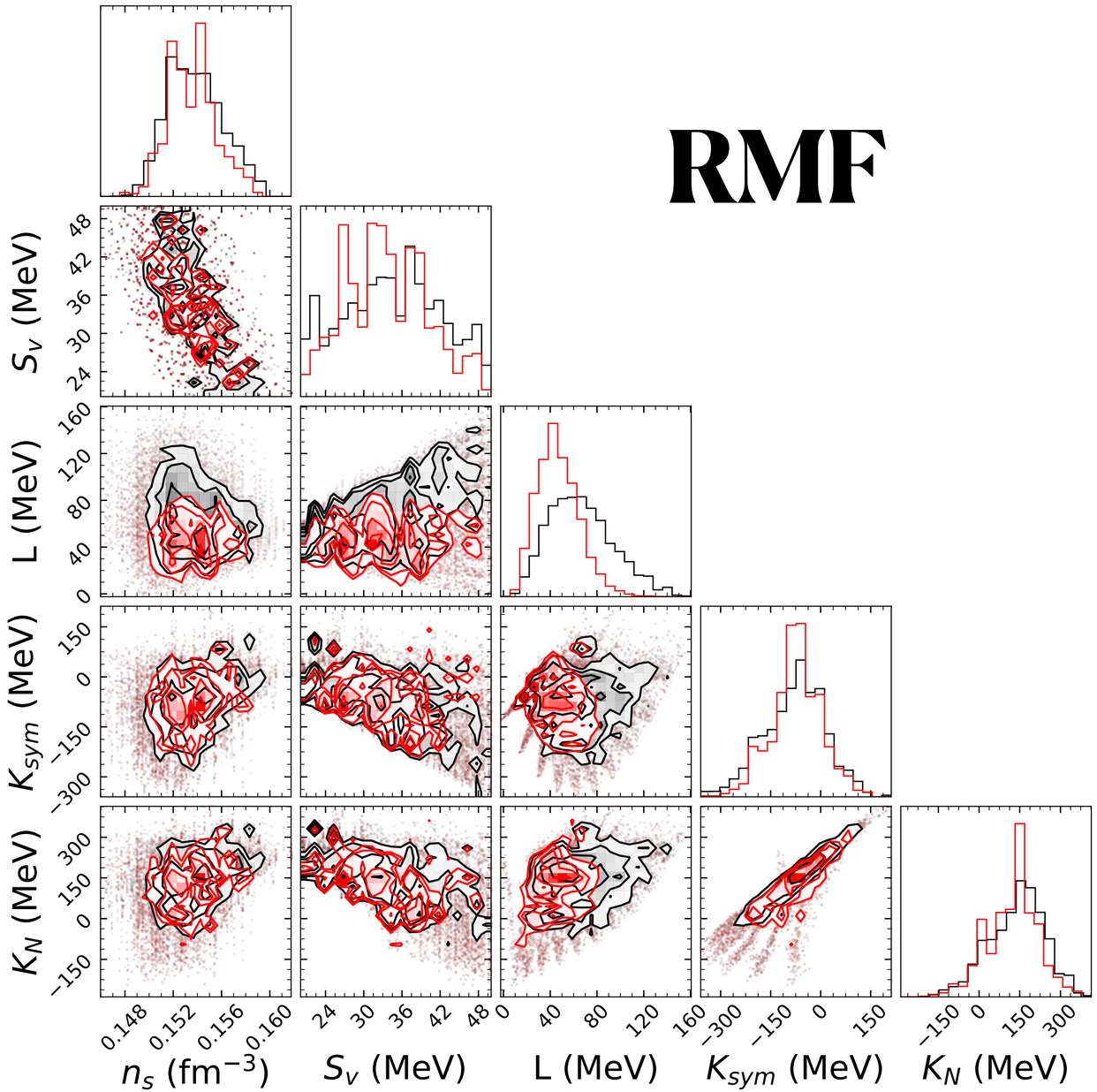

Skyrme

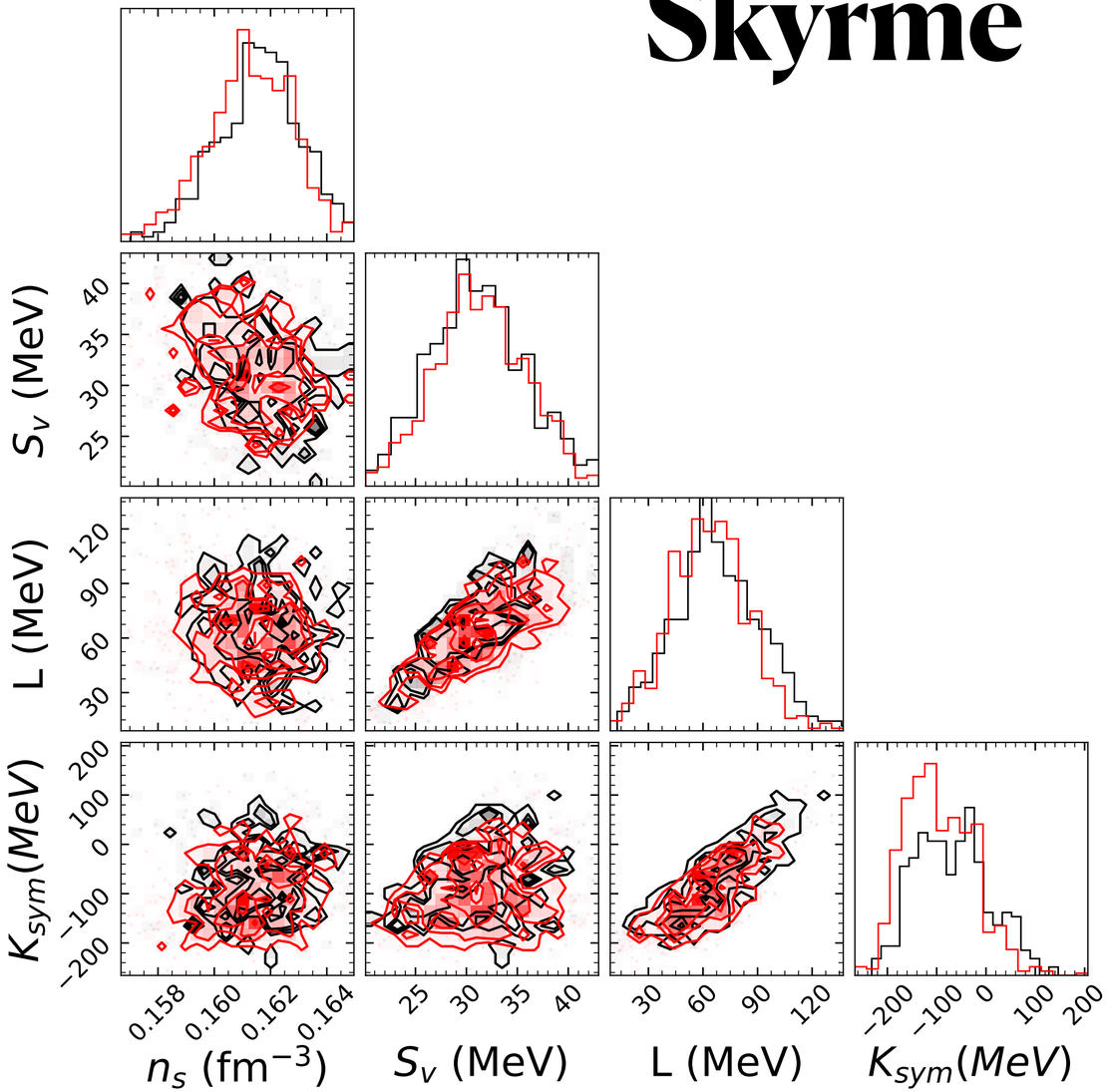

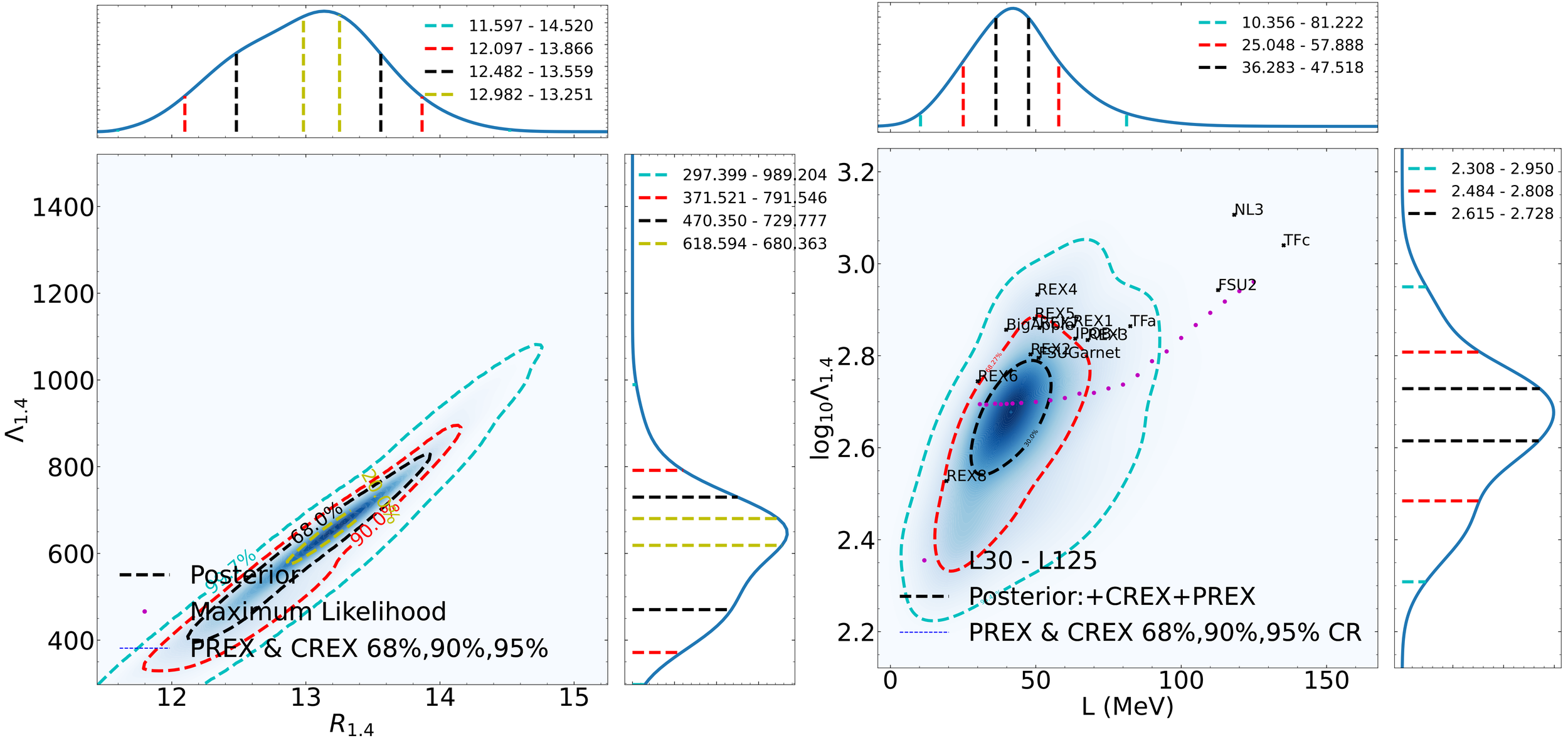
11.597 - 14.520
12.097 - 13.866
12.482 - 13.559
12.982 - 13.251
297.399 - 989.204
371.521 - 791.546
470.350 - 729.777
618.594 - 680.363
10.356 - 81.222
25.048 - 57.888
36.283 - 47.518
2.308 - 2.950
2.484 - 2.808
2.615 - 2.728
Posterior
Maximum Likelihood
PREX & CREX 68%,90%,95%
68.0%
90.0%
95.7%
68.27%
90.0%
30.0%
$\Lambda_{1.4}$
$R_{1.4}$
$\log_{10}\Lambda_{1.4}$
L (MeV)
L30 - L125
Posterior:+CREX+PREX
PREX & CREX 68%,90%,95% CR
NL3
TFc
FSU2
REX4
REX5
REX7
REX1
TFa
BigApple
IPP
JPR
REX3
REX2
FSUGarnet
REX6
REX8

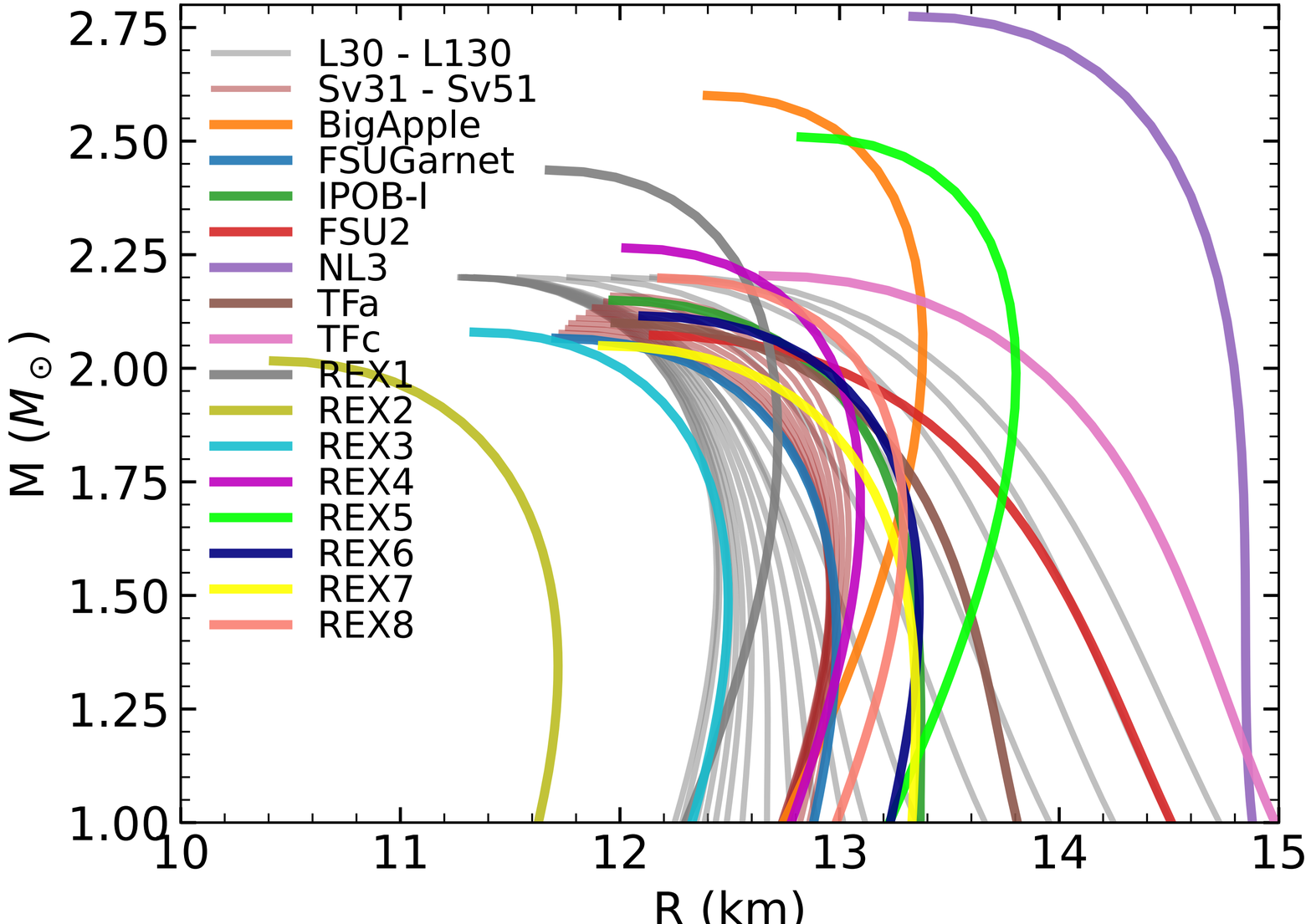
L30 - L130
Sv31 - Sv51
BigApple
FSUGarnet
IPOB-I
FSU2
NL3
TFa
TFc
REX1
REX2
REX3
REX4
REX5
REX6
REX7
REX8
M ($M_\odot$)
R (km)
2.75
2.50
2.25
2.00
1.75
1.50
1.25
1.00
10
11
12
13
14
15

TABLE V. Finite nuclei properties of ^{48}Ca, ^{90}Zr and ^{208}Pb with RMF models in Table III.

model	$R_{ch}^{^{48}Ca}$	$R_{ch}^{^{90}Zr}$	$R_{ch}^{^{208}Pb}$	BE$^{^{48}Ca}$	BE$^{^{90}Zr}$	BE$^{^{208}Pb}$	$F_{ch}^{^{48}Ca}$	$F_{ch}^{^{208}Pb}$	$F_{W}^{^{48}Ca}$	$F_{W}^{^{208}Pb}$	$\Delta R^{^{48}Ca}$	$\Delta R^{^{208}Pb}$
30	3.471	4.243	5.501	8.671	8.706	7.868	0.1579	0.4086	0.1261	0.3943	0.1527	0.1138
33	3.472	4.243	5.5	8.679	8.702	7.869	0.1578	0.4087	0.1244	0.3926	0.169	0.125
36	3.473	4.245	5.501	8.677	8.693	7.875	0.1579	0.4087	0.1228	0.3909	0.1761	0.1357
38	3.474	4.246	5.501	8.677	8.692	7.878	0.1579	0.4087	0.1218	0.3897	0.1815	0.1432
40	3.474	4.246	5.5	8.675	8.69	7.878	0.1579	0.4088	0.121	0.3887	0.1862	0.1504
42	3.474	4.247	5.5	8.675	8.691	7.88	0.1579	0.4088	0.1202	0.3877	0.1903	0.157
45	3.475	4.247	5.5	8.674	8.69	7.88	0.1579	0.4089	0.1192	0.3864	0.1958	0.1656
50	3.475	4.248	5.5	8.673	8.69	7.88	0.1579	0.4089	0.1179	0.3845	0.2034	0.1778
55	3.475	4.248	5.499	8.681	8.699	7.888	0.158	0.409	0.1168	0.3829	0.2097	0.1882
60	3.477	4.249	5.501	8.667	8.686	7.873	0.1578	0.4088	0.1157	0.3813	0.2157	0.1974
65	3.476	4.248	5.5	8.677	8.698	7.876	0.1579	0.4089	0.1149	0.38	0.2206	0.2065
70	3.477	4.248	5.5	8.677	8.704	7.869	0.1577	0.409	0.1141	0.3786	0.2281	0.216
80	3.478	4.248	5.5	8.667	8.705	7.861	0.1576	0.409	0.1127	0.3763	0.2385	0.2315
90	3.479	4.25	5.502	8.654	8.704	7.853	0.1576	0.4088	0.1116	0.3738	0.2427	0.2467
100	3.478	4.251	5.502	8.66	8.723	7.866	0.1579	0.4089	0.1108	0.3718	0.246	0.2612
110	3.477	4.253	5.503	8.653	8.727	7.867	0.1582	0.4087	0.11	0.3695	0.2469	0.2749
120	3.477	4.255	5.505	8.647	8.732	7.87	0.1584	0.4084	0.1093	0.3673	0.2493	0.2883
130	3.473	4.255	5.504	8.67	8.771	7.905	0.1591	0.4086	0.109	0.3656	0.2446	0.3016
Sv31	3.472	4.259	5.514	8.645	8.721	7.909	0.1602	0.4072	0.1257	0.3866	0.1647	0.1565
Sv335	3.471	4.258	5.513	8.646	8.746	7.865	0.1599	0.4073	0.1258	0.3853	0.1696	0.1684
Sv36	3.47	4.257	5.512	8.654	8.778	7.827	0.1598	0.4074	0.126	0.384	0.1746	0.1804
Sv385	3.47	4.256	5.512	8.66	8.807	7.788	0.1596	0.4074	0.1261	0.3826	0.1797	0.1927
Sv41	3.47	4.254	5.512	8.665	8.837	7.75	0.1595	0.4073	0.1261	0.3812	0.185	0.2055
Sv435	3.469	4.253	5.512	8.672	8.868	7.713	0.1594	0.4073	0.1262	0.3797	0.1904	0.219
Sv46	3.468	4.25	5.512	8.682	8.902	7.679	0.1594	0.4072	0.1263	0.3782	0.1958	0.2334
Sv485	3.468	4.248	5.512	8.689	8.934	7.644	0.1594	0.4072	0.1264	0.3766	0.2016	0.2493
Sv51	3.468	4.245	5.513	8.693	8.964	7.609	0.1593	0.4071	0.1263	0.3748	0.2077	0.2671
BigApple	3.503	4.277	5.52	8.532	8.676	7.878	0.1523	0.4062	0.1187	0.3865	0.1703	0.1514
FSUGarnet	3.477	4.265	5.517	8.609	8.694	7.903	0.1591	0.4067	0.1238	0.3853	0.1691	0.1621
IPOB-I	3.494	4.289	5.545	8.637	8.69	7.868	0.1548	0.4024	0.1132	0.3719	0.2022	0.2212
FSU2	3.475	4.268	5.517	8.616	8.685	7.881	0.1594	0.4067	0.1101	0.3656	0.2351	0.2887
NL3	3.496	4.288	5.533	8.64	8.698	7.89	0.1536	0.4041	0.1055	0.3639	0.2288	0.2821
TFa	3.485	4.278	5.527	8.622	8.689	7.882	0.1564	0.405	0.1112	0.3696	0.2174	0.2521
TFc	3.486	4.28	5.526	8.619	8.746	7.879	0.1565	0.4053	0.1057	0.3583	0.2535	0.3329
REX1	3.484	4.254	5.502	8.561	8.668	7.791	0.1553	0.4086	0.1235	0.3917	0.1649	0.1337
REX2	3.479	4.231	5.478	8.589	8.687	7.803	0.1563	0.412	0.126	0.3979	0.1992	0.1148
REX3	3.468	4.245	5.494	8.681	8.818	7.782	0.1573	0.4095	0.1235	0.3863	0.1829	0.1798
REX4	3.466	4.253	5.506	8.711	8.802	7.753	0.1583	0.4078	0.1234	0.3823	0.184	0.1957
REX5	3.463	4.252	5.517	8.716	8.777	7.712	0.1599	0.4062	0.1241	0.3782	0.1839	0.214
REX6	3.45	4.194	5.525	8.676	8.819	7.719	0.1626	0.4058	0.131	0.3766	0.176	0.2244
REX7	3.411	4.206	5.508	8.864	8.884	7.478	0.1604	0.4072	0.1285	0.3705	0.2082	0.2849
REX8	3.437	4.205	5.51	8.703	8.916	7.512	0.1588	0.4071	0.1301	0.3747	0.1906	0.2652
noREX	3.457	4.215	5.482	8.764	8.727	7.791	0.1579	0.41	0.1114	0.3901	0.2139	0.1412
noREX	3.462	4.224	5.484	8.744	8.657	7.778	0.1582	0.41	0.1126	0.3925	0.1975	0.1258
noREX	3.474	4.238	5.493	8.719	8.644	7.851	0.157	0.4089	0.1106	0.3943	0.1926	0.1061
noREX	3.468	4.232	5.488	8.714	8.635	7.787	0.1575	0.4095	0.1115	0.3937	0.1939	0.1139
noREX	3.459	4.221	5.485	8.789	8.76	7.839	0.1578	0.4097	0.1093	0.3882	0.2203	0.1518
withREX	3.449	4.204	5.482	8.871	8.795	7.775	0.1584	0.4097	0.115	0.3904	0.2078	0.1389
withREX	3.452	4.207	5.477	8.854	8.767	7.802	0.1581	0.4106	0.1175	0.3952	0.1897	0.1147
withREX	3.461	4.218	5.486	8.849	8.78	7.809	0.1568	0.4093	0.1146	0.3922	0.1942	0.1245
withREX	3.459	4.22	5.488	8.891	8.8	7.847	0.1575	0.409	0.114	0.3932	0.189	0.1146
withREX	3.452	4.207	5.484	8.878	8.822	7.779	0.1568	0.4092	0.116	0.3929	0.1986	0.1203
extremeREX	3.421	4.177	5.468	9.144	9.087	7.639	0.1595	0.4108	0.1192	0.3832	0.227	0.2021
extremeREX	3.453	4.217	5.471	9.118	8.983	7.734	0.1561	0.4112	0.1194	0.384	0.1813	0.1967
extremeREX	3.439	4.203	5.478	9.308	9.174	7.781	0.1578	0.4099	0.119	0.3825	0.1926	0.197
extremeREX	3.438	4.194	5.468	9.207	9.134	7.764	0.1565	0.411	0.1217	0.3886	0.1861	0.1657
extremeREX	3.441	4.204	5.472	9.23	9.097	7.78	0.1571	0.4106	0.1196	0.3851	0.1855	0.1841

TABLE VI. The data and adopted errors σ_i of E_B.

model	n_s	BE	K	M^*	S_V	L	M_{max}	$R_{1.4}$	$\Lambda_{1.4}$	$\log\mathcal{L}_B$	$\log\mathcal{L}_G$	$\log\mathcal{L}_P$	$\log\mathcal{L}_{BGP}$
30	0.1555	-16.04	230.1	640.2	27.66	30.77	2.2	12.42	495	0	0	0	0
33	0.1552	-16.02	229.9	642.3	27.71	33	2.2	12.44	494	0.01728	-0.2817	0.2548	-0.009641
36	0.155	-16.01	229.5	642.7	27.69	36	2.2	12.48	496.4	0.02705	-0.6258	0.5025	-0.09627
38	0.155	-16.01	228.7	643.5	27.82	38	2.2	12.5	494.9	0.03393	-0.8879	0.6559	-0.198
40	0.1549	-16.02	228.9	643.6	28.09	40	2.2	12.53	495.8	0.05865	-1.134	0.7892	-0.2861
42	0.1548	-16.03	229	643.7	28.36	42	2.2	12.56	496.8	0.07054	-1.372	0.9067	-0.3951
45	0.1547	-16.04	229.1	644.2	28.71	45	2.2	12.6	498.1	0.08156	-1.712	1.053	-0.5778
50	0.1546	-16.05	229.2	645.1	29.29	50	2.2	12.66	500.7	0.08813	-2.237	1.248	-0.9012
55	0.1545	-16.07	229.5	645.9	29.87	55.01	2.2	12.72	504.7	0.1012	-2.678	1.39	-1.186
60	0.1544	-16.06	229.5	647	30.43	59.99	2.2	12.79	510.6	0.0569	-3.186	1.526	-1.603
65	0.1542	-16.08	231.3	647.4	31.2	65	2.2	12.87	521.9	0.08276	-3.548	1.627	-1.838
70	0.1542	-16.11	231.6	650.7	32.14	70	2.2	12.92	523.9	0.05157	-3.989	1.718	-2.22
80	0.1544	-16.15	229.5	650.3	33.59	79.99	2.2	13.06	546	0.0008136	-4.768	1.847	-2.92
90	0.1541	-16.18	229.6	636.2	35.11	89.96	2.2	13.34	613.8	-0.005327	-5.422	1.95	-3.478
100	0.1539	-16.24	229.9	622.6	36.65	100	2.2	13.6	689.6	0.1044	-5.9	2.009	-3.787
110	0.1535	-16.28	230.6	607.2	38.03	110	2.2	13.89	782.1	0.06874	-6.378	2.044	-4.265
120	0.153	-16.32	231.2	594.7	39.43	120	2.2	14.13	871.8	-0.07659	-6.903	2.05	-4.93
130	0.1529	-16.42	232.2	585.6	40.99	130.2	2.2	14.34	950.5	-0.4792	-7.075	2.034	-5.52
Sv31	0.1533	-16.22	230.1	540.9	31	50.3	2.068	12.98	625.5	-3.623	-0.06018	1.024	-2.66
Sv335	0.1531	-16.25	228.8	536	33.5	49.86	2.078	12.96	623.8	-2.96	-0.03957	1.163	-1.836
Sv36	0.1528	-16.28	227.4	531.1	35.99	49.49	2.088	12.95	623.4	-2.708	-0.01316	1.292	-1.429
Sv385	0.1525	-16.31	226	526.4	38.48	49.15	2.099	12.94	624.7	-2.649	-0.0003713	1.418	-1.231
Sv41	0.1522	-16.35	224.6	521.8	40.97	48.85	2.11	12.94	627.3	-2.785	0.006699	1.536	-1.242
Sv435	0.1519	-16.38	223.2	517.3	43.46	48.54	2.122	12.94	631.1	-3.127	0.01524	1.645	-1.466
Sv46	0.1516	-16.41	221.8	512.8	45.94	48.25	2.134	12.95	637	-3.654	0.03263	1.743	-1.878
Sv485	0.1514	-16.44	220.5	508.4	48.42	47.99	2.147	12.97	643.5	-4.263	0.0375	1.833	-2.393
Sv51	0.1511	-16.48	219.1	504.1	50.9	47.75	2.16	12.99	650.8	-4.946	0.03136	1.913	-3.001
BigApple	0.1546	-16.34	227	572.8	31.32	39.8	2.6	13.1	718.4	-20.88	-1.903	1.043	-21.74
FSUGarnet	0.1532	-16.23	229.6	543	30.92	50.96	2.066	12.99	624.1	-3.094	-0.3951	1.169	-2.319
IPOB-I	0.1495	-16.1	222.6	557.2	33.3	63.56	2.15	13.36	687.2	-27.57	-4.441	2.006	-30
FSU2	0.1504	-16.26	237.7	557	37.57	112.7	2.072	14.14	876.4	-3.339	-6.314	2.035	-7.618
NL3	0.1483	-16.24	271.6	558.7	37.3	118.2	2.775	14.85	1278	-21.78	-9.696	2.002	-29.47
TFa	0.1494	-16.23	245	563.4	35.05	82.5	2.1	13.63	731.6	-9.371	-5.667	2.043	-13
TFc	0.1479	-16.46	260.5	535.2	43.67	135.2	2.204	14.66	1097	-8.17	-9.498	1.771	-15.9
REX1	0.1558	-16.17	224.6	618.2	30.84	30.02	2.436	12.58	555.1	-4.226	-0.4741	0.3952	-4.304
REX2	0.1582	-16.23	230.8	696.8	29.63	19.25	2.016	11.71	337	-6.304	-0.01278	-0.5927	-6.91
REX3	0.1531	-16.33	240	600.3	37.23	34.64	2.08	12.49	503.9	-0.6687	-0.4631	1.06	-0.07224
REX4	0.1512	-16.17	237.4	560.5	37.72	42.77	2.265	13.02	660.4	-1.102	-0.5002	1.445	-0.1572
REX5	0.1492	-16	234.9	522.2	38.26	50.5	2.509	13.56	856.8	-5.979	-0.3481	1.743	-4.584
REX6	0.1508	-15.93	225.3	481.2	38.42	62.79	2.115	13.36	731.6	-16.33	0.2914	1.832	-14.21
REX7	0.1467	-15.68	242.6	508.1	45.48	67.81	2.05	13.33	682.6	-9.193	0.2395	2.032	-6.921
REX8	0.1483	-16.13	245.3	501.2	48.45	51.25	2.198	13.23	725.8	-5.679	0.2966	1.919	-3.464
noREX	0.1631	-15.66	240.4	N/A	25.84	59.45	2.125	12.53	N/A	-0.9013	-5.513	0.6121	-5.802
noREX	0.1623	-15.53	237.5	N/A	24.34	49.03	2.096	12.19	N/A	-0.8896	-4.788	0.2791	-5.399
noREX	0.1625	-15.61	236.3	N/A	22.39	38.18	2.002	11.68	N/A	-0.6997	-6.021	0.006654	-6.714
noREX	0.1622	-15.54	235.9	N/A	23.74	40.19	2.02	11.74	N/A	-0.4993	-5.475	0.09515	-5.879
noREX	0.1615	-15.76	248.5	N/A	26.76	61.56	2.162	12.68	N/A	-0.6555	-6.884	0.8484	-6.691
withREX	0.1637	-15.52	227.8	N/A	26.36	62.36	2.096	12.56	N/A	-1.559	-3.508	0.5643	-4.503
withREX	0.1642	-15.51	226.3	N/A	24.52	45.57	2.04	11.87	N/A	-2.262	-2.394	-0.1301	-4.786
withREX	0.1626	-15.58	233.7	N/A	25.58	49.01	2.084	12.11	N/A	-1.616	-3.738	0.3252	-5.029
withREX	0.1616	-15.54	235.1	N/A	24.51	41.55	1.984	11.69	N/A	-1.23	-4.012	0.1775	-5.065
withREX	0.1631	-15.55	229.4	N/A	26.28	45.35	2.041	11.82	N/A	-2.134	-3.064	0.2122	-4.986
extremeREX	0.1612	-15.54	226.7	N/A	39.52	79.68	2.051	12.48	N/A	-10.59	-1.733	1.367	-10.96
extremeREX	0.1584	-15.51	228	N/A	37.02	64.06	1.965	11.98	N/A	-9.48	-1.644	1.296	-9.829
extremeREX	0.1575	-15.53	227.8	N/A	38.98	66.22	0	0	N/A	-11.22	-1.78	1.43	-11.57
extremeREX	0.16	-15.6	229.2	N/A	36.43	46.89	0	0	N/A	-11.86	-0.9294	0.7909	-11.99
extremeREX	0.1582	-15.5	227.6	N/A	36.7	55.6	0	0	N/A	-9.894	-1.583	1.182	-10.29

TABLE III. σ meson mass and 7 coupling constant of RMF models.

model	m_σ	g_σ^2	g_ω^2	g_ρ^2	κ (MeV)	λ	$\Lambda_{\sigma\rho}$	ζ
L30	500.1	81.751	119.91	179.42	7.4845	-0.024318	0.092903	0.0053833
L33	500.19	81.449	119.09	155.34	7.5974	-0.024669	0.088229	0.0051654
L36	499.05	81.099	119.06	134.04	7.6224	-0.024778	0.082677	0.0051286
L38	497.92	80.631	118.67	123.49	7.7144	-0.02521	0.077907	0.0050035
L40	497.25	80.444	118.7	116.35	7.7136	-0.0252	0.072255	0.0049666
L42	496.68	80.284	118.71	110.61	7.7187	-0.025212	0.067042	0.0049309
L45	495.82	79.952	118.52	103.47	7.7534	-0.025341	0.060248	0.0048287
L50	494.55	79.428	118.14	94.974	7.8177	-0.025582	0.050398	0.0046414
L55	493.46	78.953	117.74	89.225	7.884	-0.025828	0.041994	0.0044482
L60	492.47	78.473	117.3	85.127	7.9535	-0.026085	0.034784	0.0042427
L65	492.57	78.448	117.23	83.739	7.9125	-0.025701	0.028314	0.004143
L70	490.69	77.198	115.48	84.144	8.1749	-0.026608	0.023158	0.0035813
L80	487.77	76.438	115.45	83.248	8.2992	-0.027554	0.014898	0.0033988
L90	490.59	80.397	123.08	84.162	7.2805	-0.023961	0.0088188	0.0053127
L100	492.59	84.128	130.56	85.557	6.441	-0.020639	0.0047621	0.0072955
L110	494.81	88.735	139.89	86.286	5.5534	-0.016629	0.0018613	0.01001
L120	495.33	92.428	148.26	87.32	4.895	-0.013096	-0.00024765	0.012987
L130	494.5	95.062	155.21	89.154	4.4078	-0.0097899	-0.0018036	0.016403
Sv31	499.2	111.95	189.02	208.74	3.2339	-0.0035059	0.04398	0.023522
Sv335	498.73	113.66	192.52	244.61	3.2429	-0.0039255	0.03556	0.02303
Sv36	498.34	115.41	195.97	280.53	3.2564	-0.0043455	0.029612	0.022536
Sv385	497.74	117.03	199.34	316.77	3.2733	-0.0047616	0.025206	0.022038
Sv41	497.01	118.58	202.64	353.14	3.2929	-0.0051763	0.021818	0.021535
Sv435	496.29	120.08	205.84	390	3.3149	-0.0055817	0.019142	0.021037
Sv46	495.54	121.59	209.06	427.55	3.3385	-0.0059843	0.016977	0.020537
Sv485	494.59	122.95	212.14	464.71	3.364	-0.0063865	0.015191	0.020027
Sv51	493.46	124.15	215.1	501.45	3.391	-0.0067861	0.013695	0.019511
BigApple	492.73	93.507	151.68	200.56	5.2033	-0.021739	0.047471	0.0007
FSUGarnet	496.94	110.35	187.69	192.93	3.2602	-0.003551	0.043377	0.0235
IPOB-I	500.51	108.06	178.13	123.75	3.6924	-0.0077096	0.024354	0.01742
FSU2	497.48	108.09	183.79	80.466	3.0029	-0.000533	0.000823	0.0256
NL3	508.19	104.39	165.59	79.6	3.8599	-0.01591	0	0
TFa	502.2	106.5	176.18	97.356	3.1824	-0.00347	0.01267	0.02
TFc	496.8	113.96	198.05	103.4	2.6079	-0.001864	0	0.02
REX1	494.46	84.289	128.98	217.51	6.9521	-0.027204	0.063364	0.00038602
REX2	466.33	60.46	90.129	217.45	12.833	-0.03388	0.12543	0.0039813
REX3	507.67	95.517	146.25	261.94	4.6353	-0.0097502	0.035249	0.015813
REX4	515.37	109.47	168.82	253.14	3.8892	-0.011267	0.027072	0.011055
REX5	517.44	120.8	188.96	246.9	3.5499	-0.013254	0.021693	0.006214
REX6	484.61	135.08	247.32	306.58	3.18	-0.003575	0.021449	0.025196
REX7	524.67	146.98	235.72	294.61	2.4094	0.0015445	0.0134	0.027682
REX8	510.64	133.55	221.21	441.4	2.8455	-0.004774	0.013882	0.018458

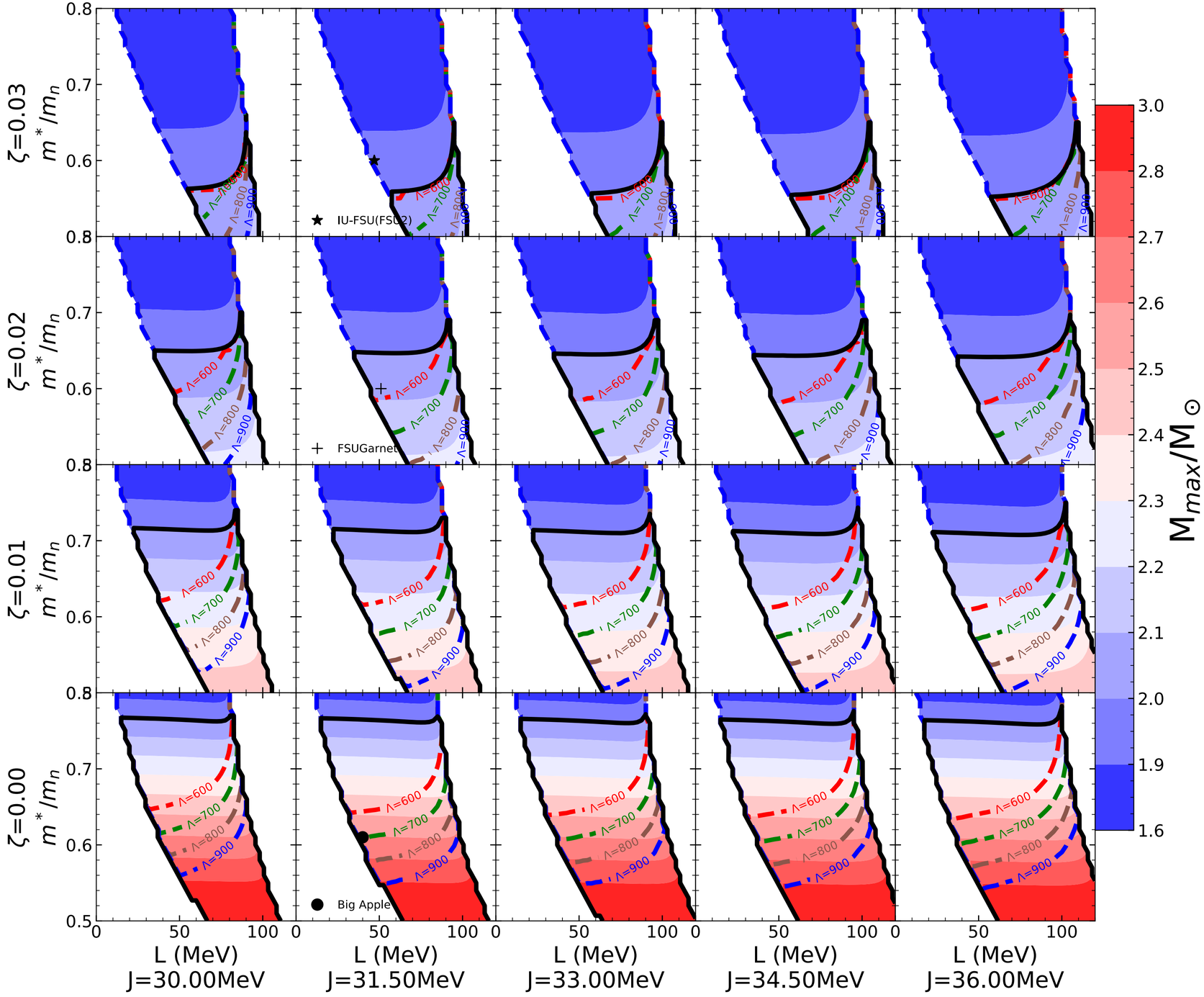
ζ=0.03
ζ=0.02
ζ=0.01
ζ=0.00
m*/mn
0.8
0.7
0.6
0.5
Λ=600
Λ=700
Λ=800
Λ=900
IU-FSU(FSU2)
FSUGarnet
Big Apple
0
50
100
L (MeV)
J=30.00MeV
J=31.50MeV
J=33.00MeV
J=34.50MeV
J=36.00MeV
Mmax/M⊙
3.0
2.8
2.7
2.6
2.5
2.4
2.3
2.2
2.1
2.0
1.9
1.6

Why electron-weak probe?

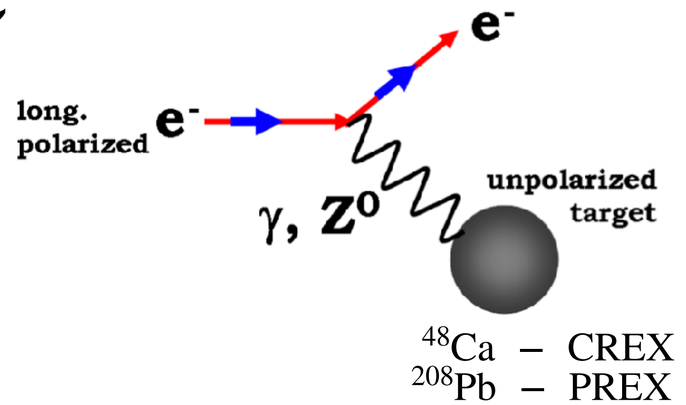

^{48}Ca – CREX
^{208}Pb – PREX

- $\mathscr{L} = \ldots + \frac{g_W}{\cos(\Theta_W)} J_Z^\mu Z_\mu - \frac{M_Z^2}{2} Z^\mu Z_\mu + \ldots$ $\quad G_F = \frac{g_W^2}{4\sqrt{2} M_W^2}$
  $\sin^2(\Theta_W) = 0.223$
- The only source of parity violation:
  $J_Z^\mu = -\frac{1}{2}\bar{\psi}_L \gamma^\mu \psi_L - \sin^2(\Theta)\bar{\psi}\gamma^\mu\psi = -\frac{1}{4}\bar{\psi}\left[1 - 4\sin^2(\Theta_W) - \gamma^5\right]\psi$
- Approximately zero-range, since $M_Z \approx 500\ \mathrm{fm}^{-1}$:
  $\Phi_W(r) = \int \frac{\rho_W(r') e^{-M_Z|r-r'|}}{4\pi|r-r'|} dr'^3 \approx \frac{\rho_W(r')}{M_Z^2}$
- Weak compared with Coulomb interaction: $\Phi_W << \Phi_E$
- $Q_p = 1 - 4\sin^2(\Theta_W)$ $\quad << \quad$ $Q_n = -1$
  (0.0721 with correction) (–0.9878 with radiative correction)

Sv-L Posterior with RMF

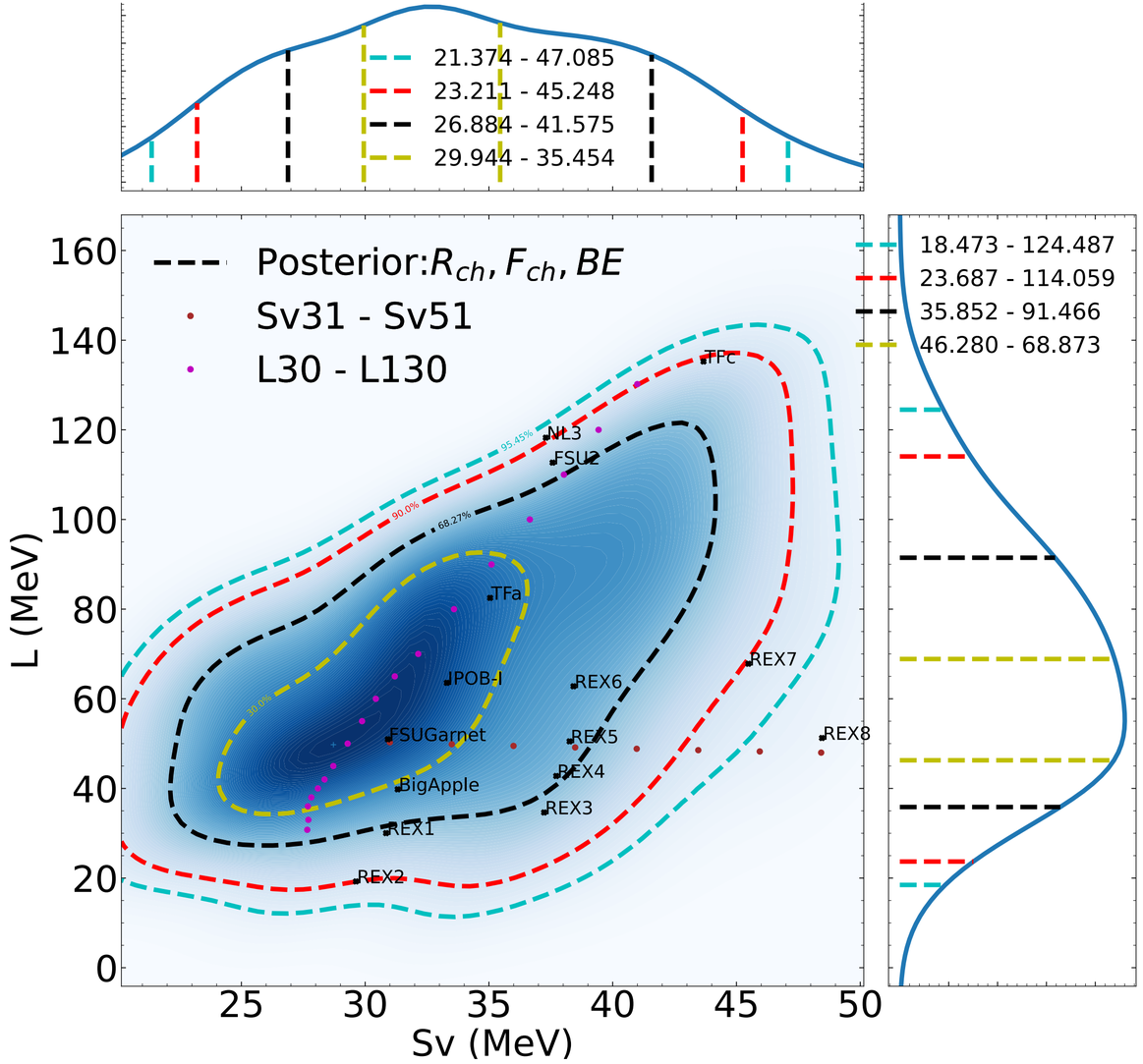

Flowchart of Applying PREX and CREX Data

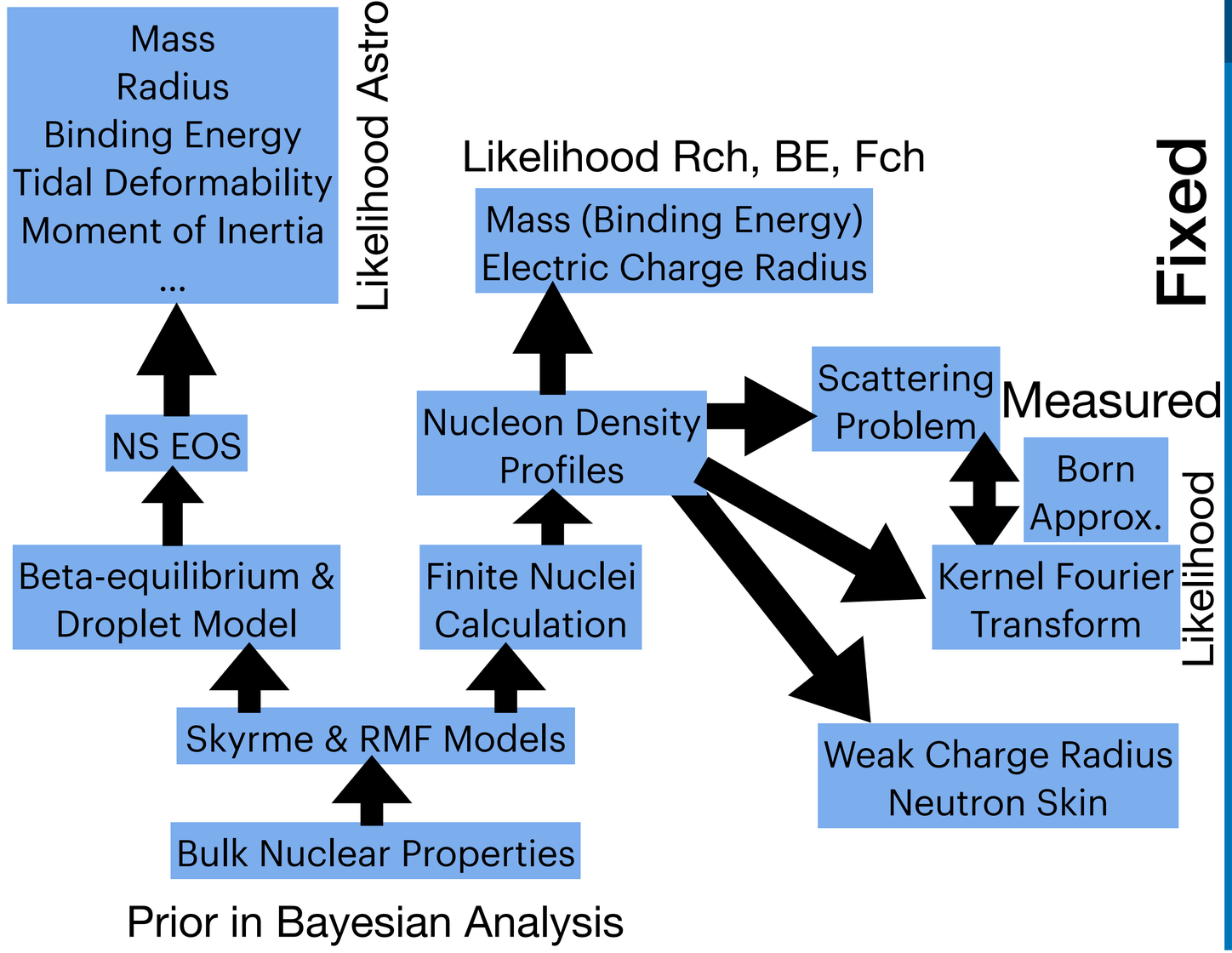

	CREX	PREX
(N,Z)	(28,20) Ca	(126,82) Pb
q (fm-1)	0.8733	0.3977
Fch, Rch(fm)	0.1581, 3.481	0.409, 5.503
Apv	2668±106(stat) ±40(syst)	550±16(stat) ±8(syst)
Fw	0.1304±0.0052(stat) ±0.002(syst)	0.368±0.013(exp) ±0.001(theo)
Fch-Fw	0.0277±0.0052(stat) ±0.002(syst)	0.041±0.013(exp) ±0.001(theo)
Rw	3.64±0.026(exp) ±0.023(theo)	5.8±0.075(tot)
Rw-Rch	0.159±0.026(exp) ±0.023(theo)	0.297±0.075(tot)
Rn-Rp	0.121±0.026(exp) ±0.024(theo)	0.283±0.071(tot)
	CREX 2022	PREX I 2012 PREX II 2021

Pearson Correlation

Skyrme Result

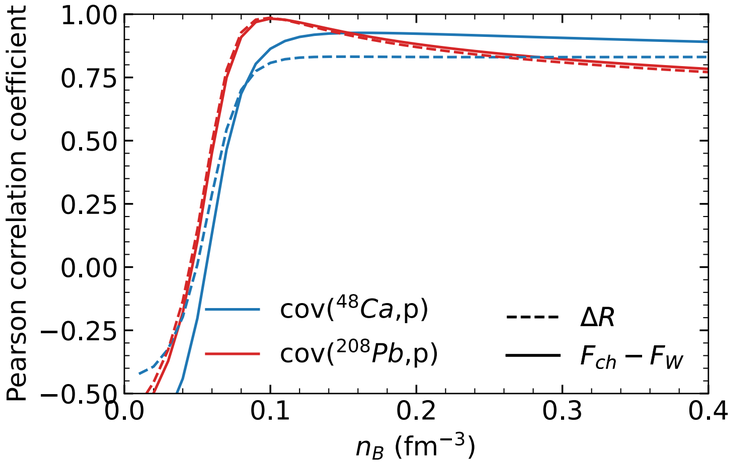

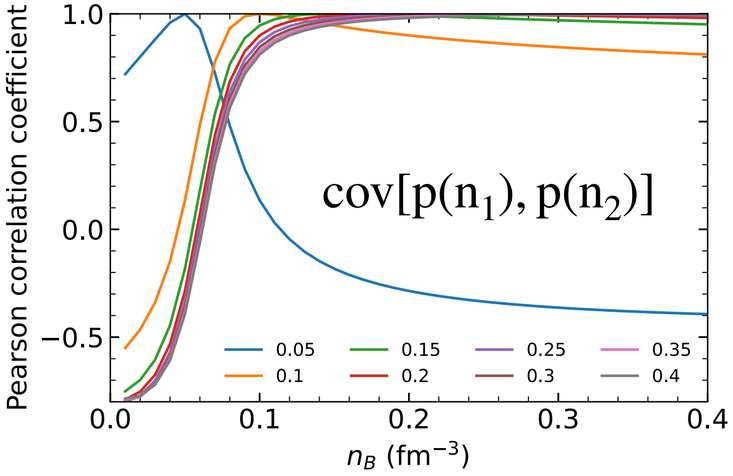

RMF Result

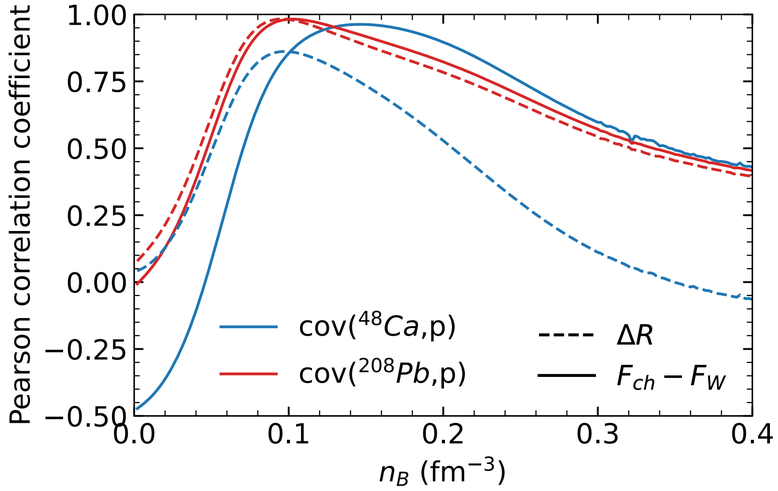

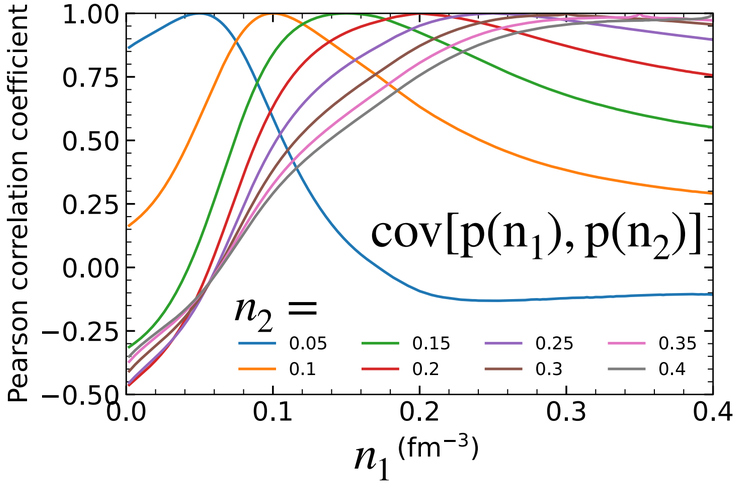

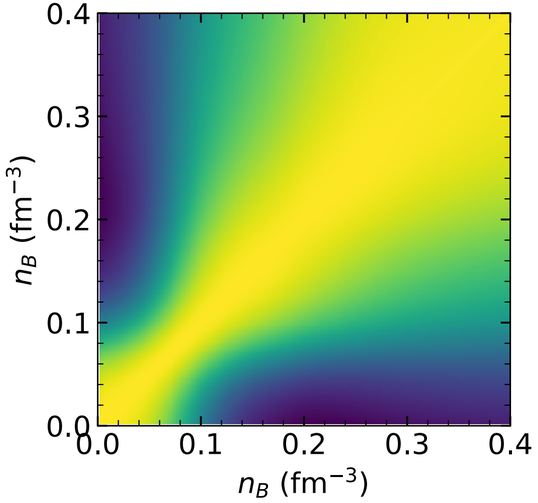

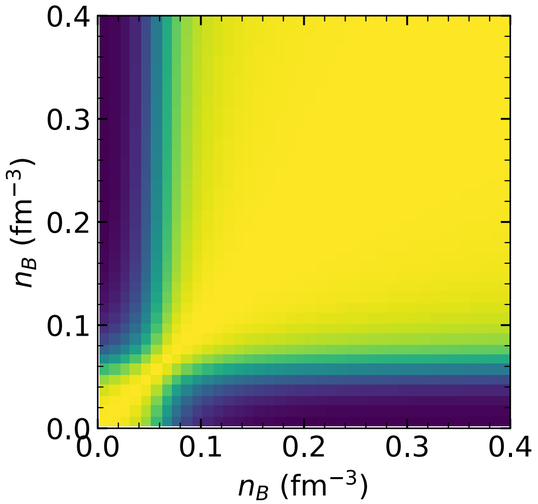

Finite nuclei with MFT

- Nucleon densities of ${}^{A}_{Z}X$:
  (1) Guess the initial 4 density profiles.
  (2) Solve Klein-Gorden Eq for 4 mesons fields.
  (3) Construct local 4 single-particle potentials.
  (4) Solve Dirac Eq for lowest Z (N) proton (neutron) levels.
  (5) Compute ground state 4 density profiles.
  (6) Repeat (2) To (5) until converge.

	value	σ_i
$R_{ch}^{^{48}Ca}$	3.48	0.0696
$R_{ch}^{^{90}Zr}$	4.27	0.0854
$R_{ch}^{^{208}Pb}$	5.5	0.11
$\mathrm{BE}^{^{48}Ca}$	8.67	0.1734
$\mathrm{BE}^{^{90}Zr}$	8.71	0.1742
$\mathrm{BE}^{^{208}Pb}$	7.87	0.1574
$F_{ch}^{^{48}Ca}$	0.1581	0.001
$F_{ch}^{^{208}Pb}$	0.409	0.001

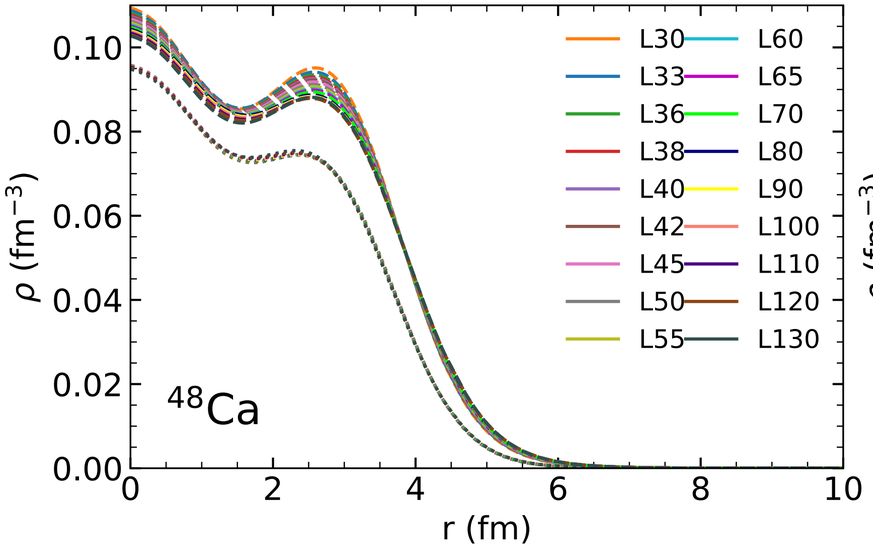

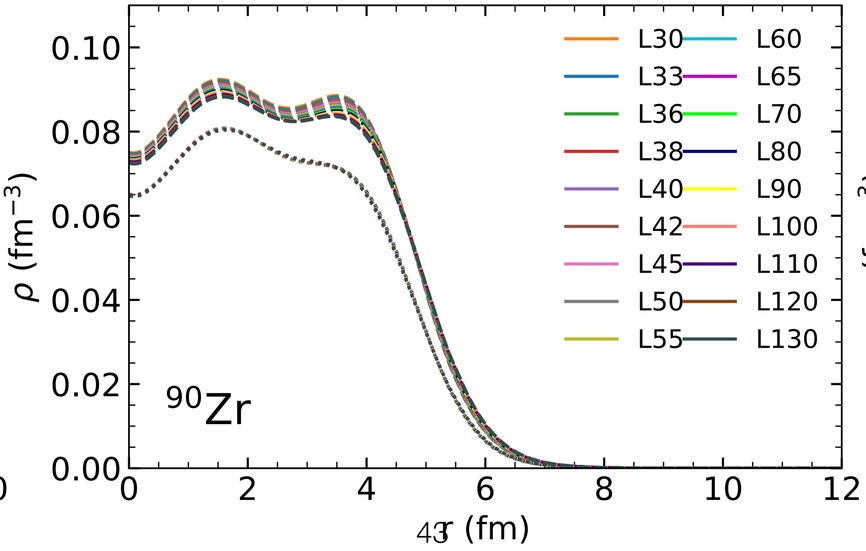

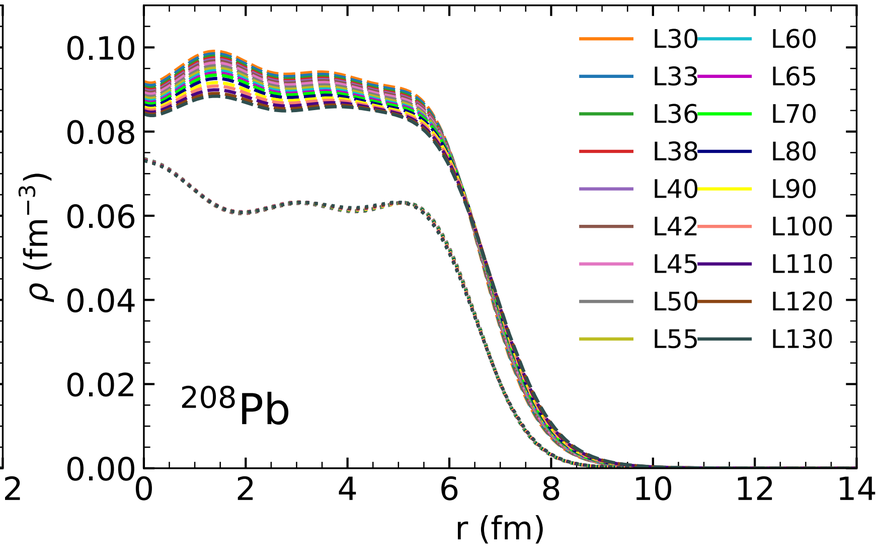

	Scalar	Vector
Isoscalar	σ	$\gamma^\mu \omega_\mu$
Isovector	$\vec{\tau}\,\vec{\delta}$	$\gamma^\mu \vec{\tau}\,\vec{\rho}_\mu$

FSU-type RMF model

$$\mathscr{L} = \mathscr{L}_0 + \bar{\psi}\left(g_\sigma \sigma - g_\omega \gamma^\mu \omega_\mu - \frac{g_\rho}{2}\gamma^\mu \boldsymbol{\tau}\boldsymbol{\rho}_\mu \right)\psi - \frac{\kappa}{3!}(g_\sigma\sigma)^3 - \frac{\lambda}{4!}(g_\sigma\sigma)^4 + \frac{\zeta}{4!}(g_\omega^2 \omega^\mu \omega_\mu)^2 + \Lambda_{\omega\rho}(g_\rho^2 \boldsymbol{\rho}^\mu \boldsymbol{\rho}_\mu)(g_\omega^2 \omega^\mu \omega_\mu)$$

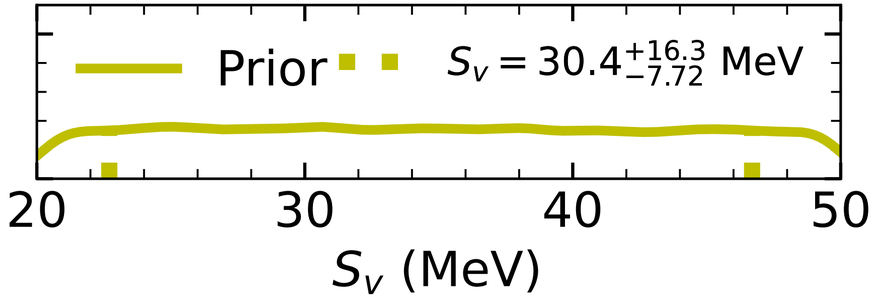

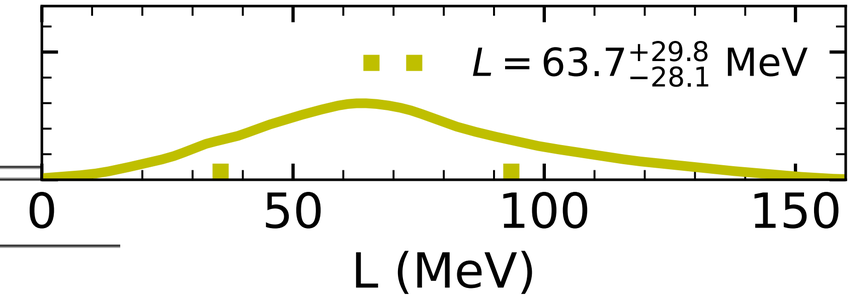

	NL3	FSU	FSU2
m_σ	508.194	491.5	497.479
m_ω	782.501	782.5	782.5
m_ρ	763	763	763
g_σ^2	104.3871	112.1996	108.0943
g_ω^2	165.5854	204.5469	183.7893
g_ρ^2	79.6	138.4701	80.4656
κ	3.8599	1.4203	3.0029
λ	-0.015905	0.023762	-0.000533
ζ	0	0.06	0.0256
Λ	0	0.03	0.000823

	prior
m_σ (MeV)	[450,550]
m_ω (MeV)	782.5
m_ρ (MeV)	763
n_s (MeV)	[0.14,0.165]
BE (MeV)	[-15.5,-16.5]
M^* (MeV)	[0.5,0.8]$\times$ 939
K (MeV)	[210,250]
S_V (MeV)	[20,50]
L (MeV)	$[L_{min}, L(\Lambda = 0)]$
ζ_ω	[0,0.03]

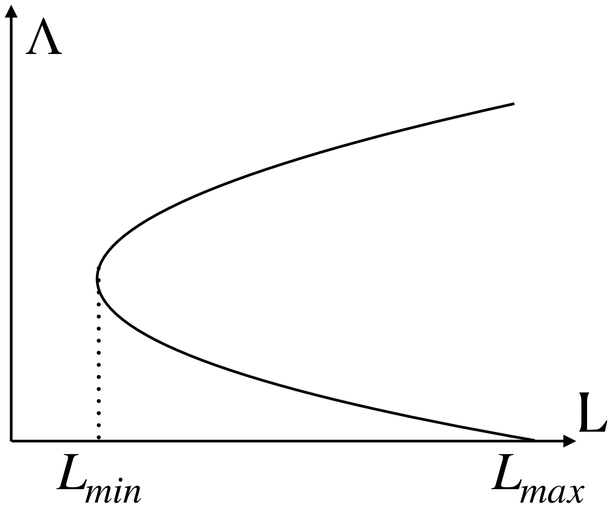

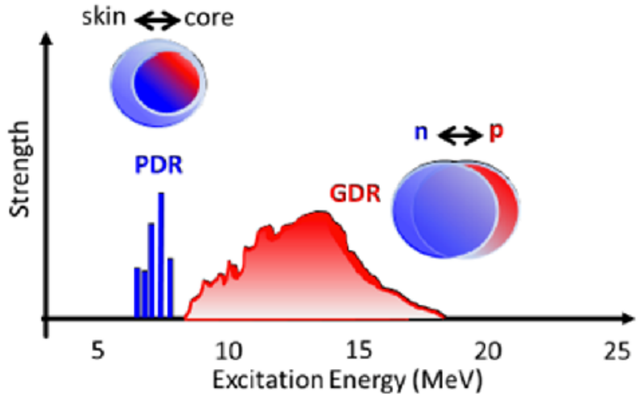

Dipole Polarizability

E.M. interaction probe: photo-absorption

- Strength function of Dipole operator D:

$$S(\omega) = \sum_{k>0} \left| < k|D|0 > \right|^2 \delta(\omega - \omega_k) \propto \frac{\sigma_{abs}(\omega)}{\omega}$$

- Moments of strength function:

$$m_n = \int_0^\infty S(\omega)\omega^n d\omega \qquad m_1 \approx 15\frac{NZ}{A}\text{fm}^2\text{MeV}$$

- Common Observable:

Centroid energy $E_0 = \frac{m_1}{m_0}, E_{-1} = \sqrt{\frac{m_1}{m_{-1}}}$

Polarizability $\alpha_D = \frac{8\pi e^2}{9} m_{-1}$, in terms of photo-absorption, $\alpha_D = \frac{\hbar c}{2\pi^2 e^2} \int \frac{\sigma_{abs}}{\omega^2} d\omega$

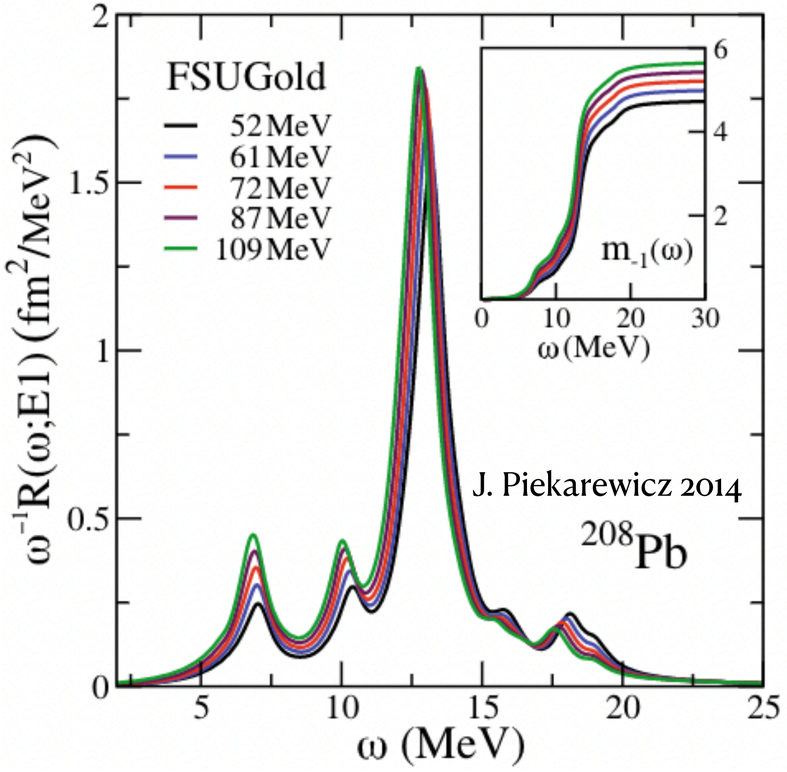

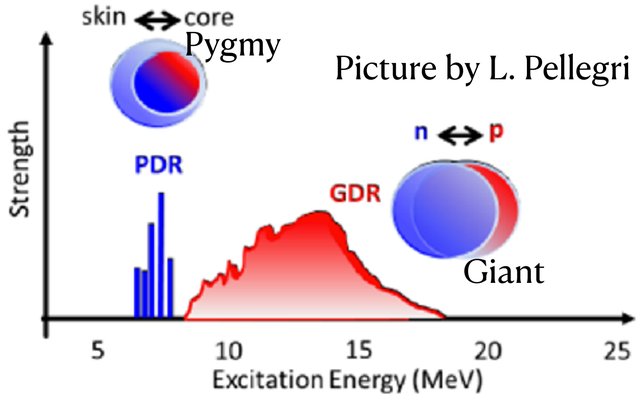

Dipole Polarizability

- Photon excitation works below neutron ionization.
- Proton Coulomb excitation at RCNP, Osaka
- $\alpha_D S_V$ is a better observable than α_D

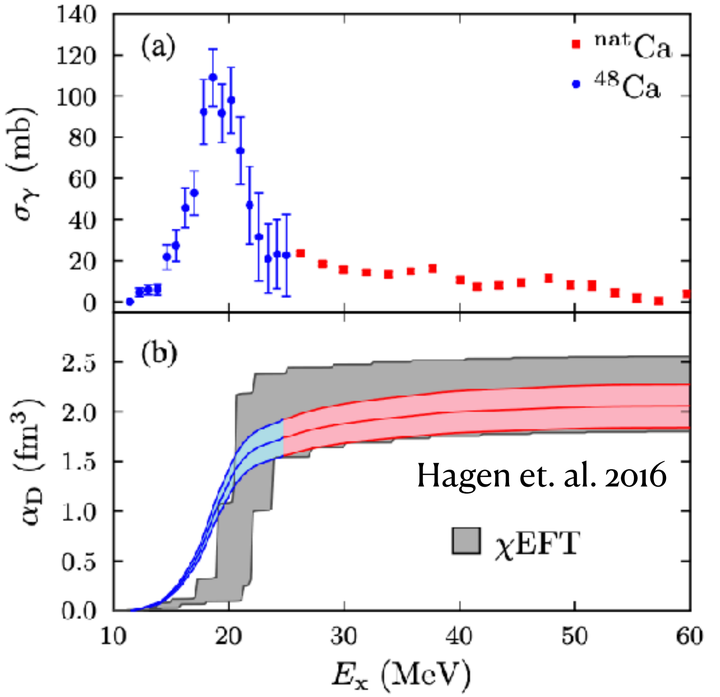

Electric Dipole Polarizability of 48Ca

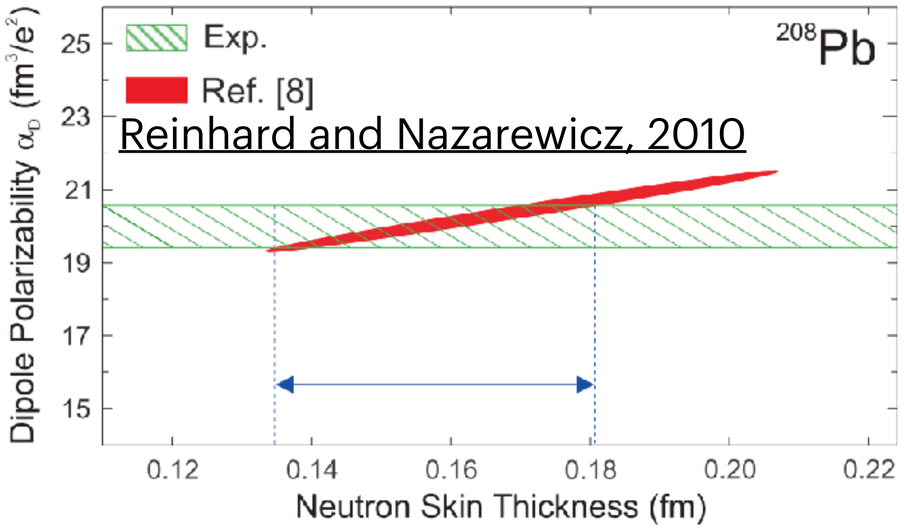

Reinhard and Nazarewicz, 2010

Complete Electric Dipole Response and the Neutron Skin in 208Pb

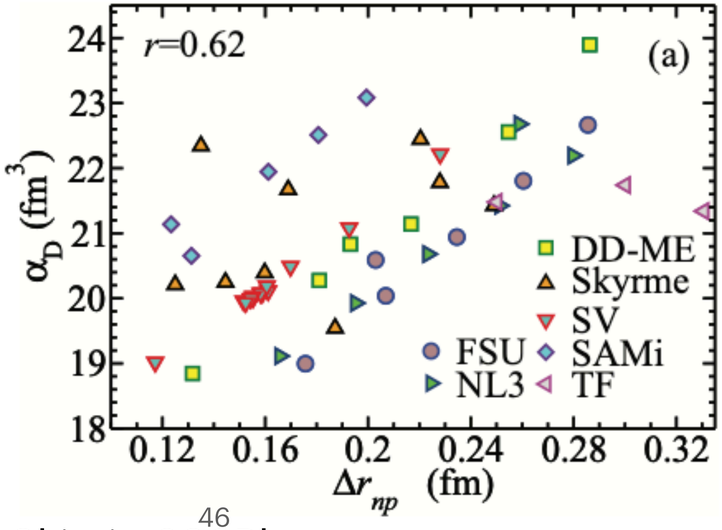

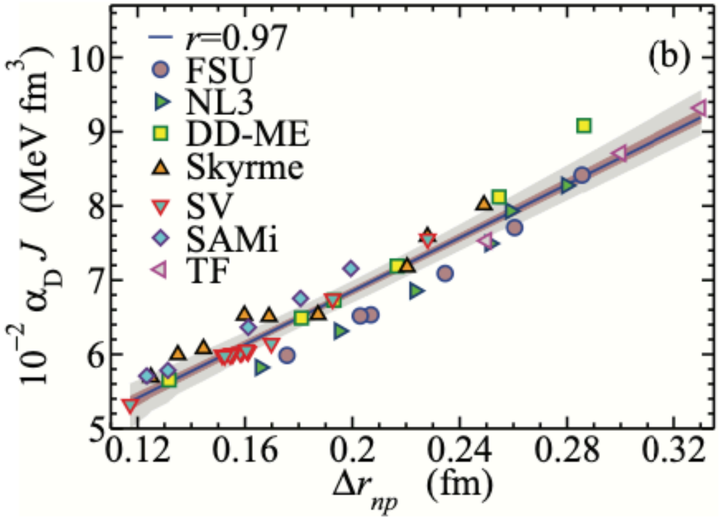

Moca-Maza et. al. 2013

Electric Charge Distribution

Well measured!!!

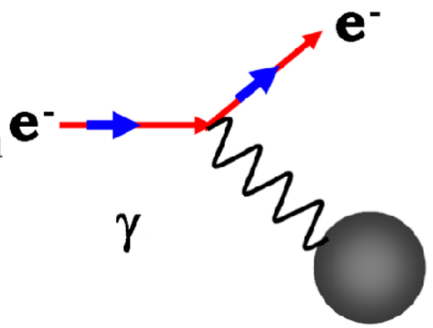

$$\frac{d\sigma}{d\Omega} = \left[\frac{d\sigma}{d\Omega}\right]_{Mott} |F(\mathbf{q})|^2 \qquad F(q) = \frac{\int j_0(qr)\rho(r)d^3r}{\int \rho(r)d^3r}$$

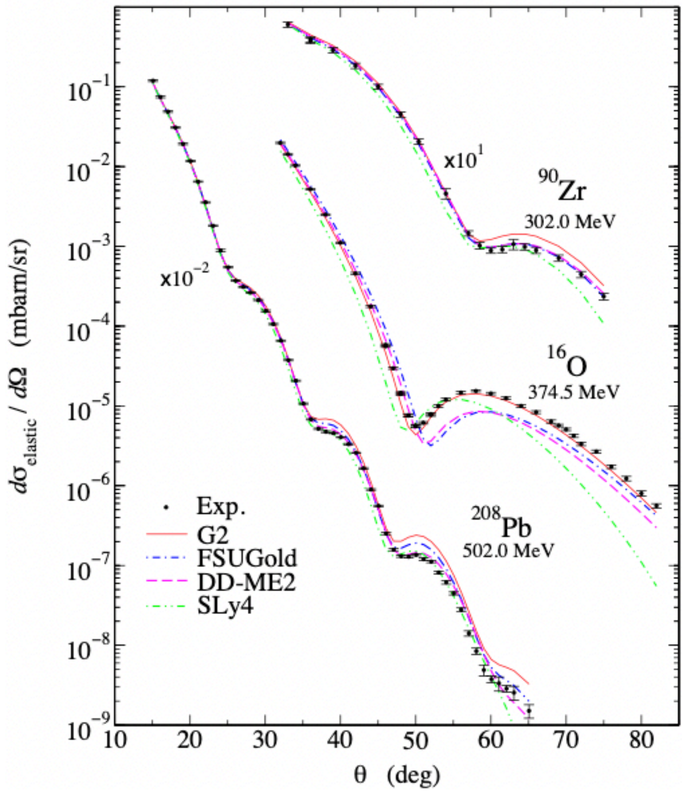

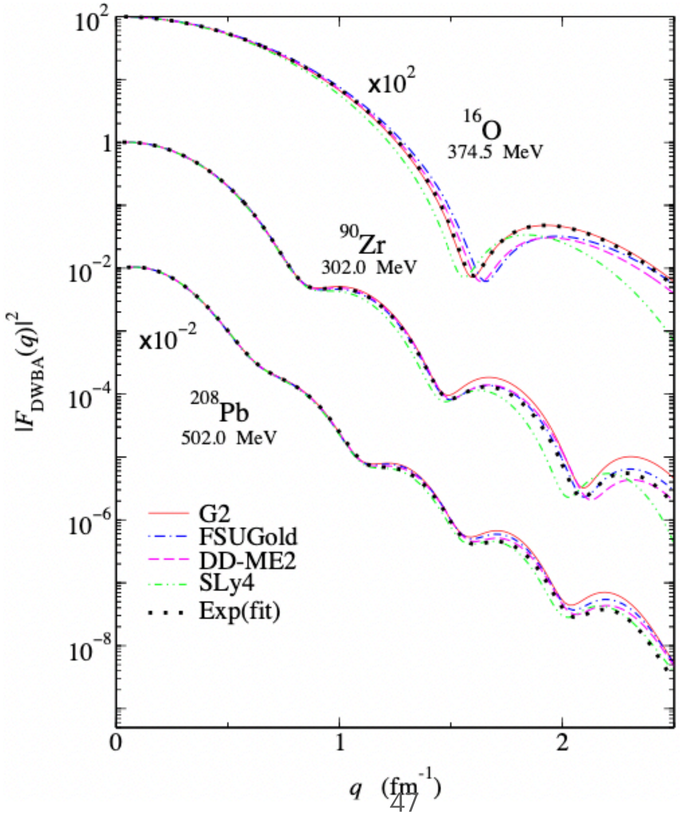

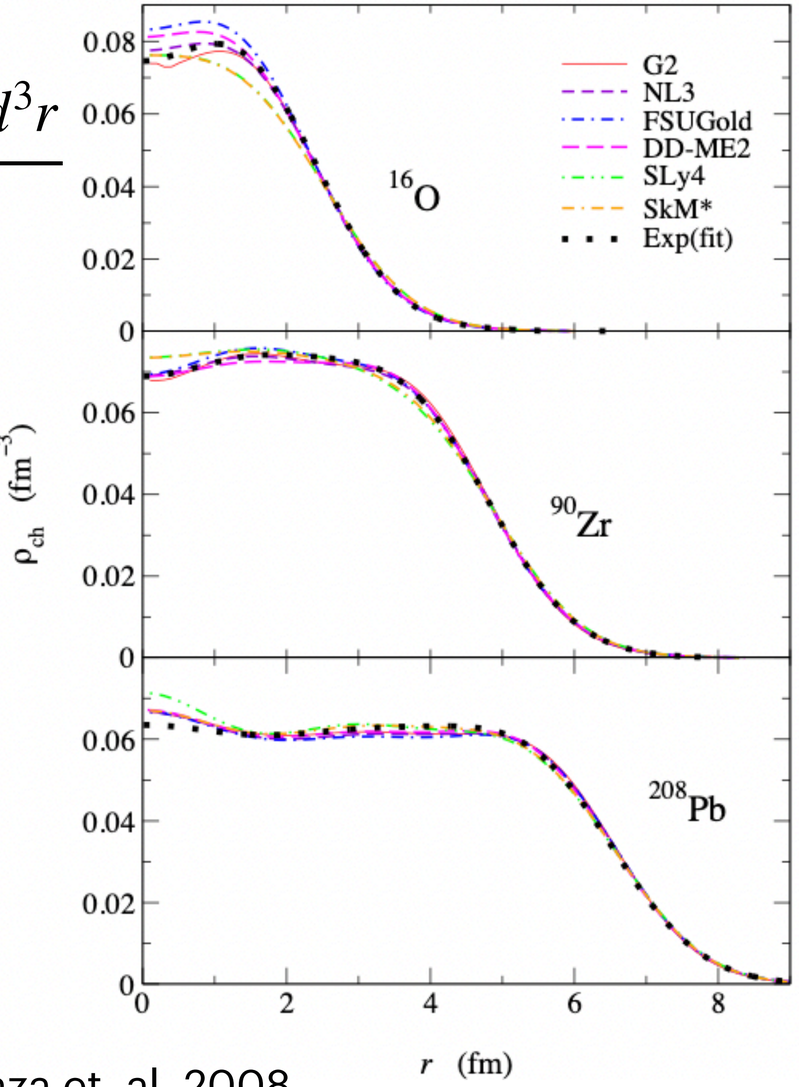

Moca-Maza et. al. 2008

Weak Charge Distribution

Extremely hard!!!

Jefferson Lab
Krishna Kumar 2018
Tao Ye 2021
Robert Radloff 2022

- $$F(\mathbf{q}) = \frac{1}{Q}\int e^{i\mathbf{q}\cdot\mathbf{r}}\rho(\mathbf{r})d^3r$$
$$= \frac{1}{Q}\int\left(1 + i\mathbf{q}\cdot\mathbf{r} - \frac{1}{2}(\mathbf{q}\cdot\mathbf{r})^2 + \ldots\right)\rho(\mathbf{r})d^3r$$
$$= 1 - \frac{1}{6}q^2 < r^2 > + \ldots \quad \text{(spherical symmetry)}$$

$$\lim_{q<<\sqrt{<r^2>}} < r^2 > = \frac{6[1 - F(q)]}{q^2}$$

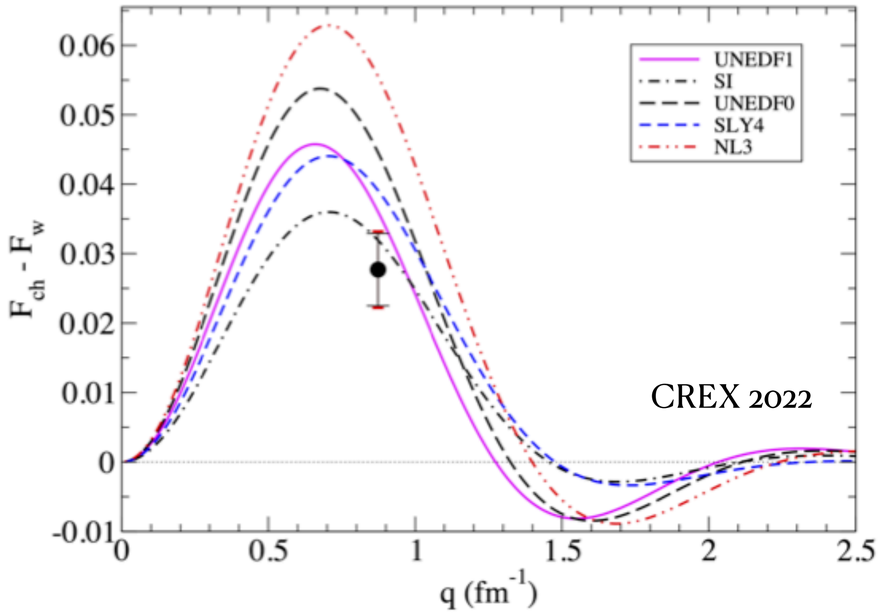

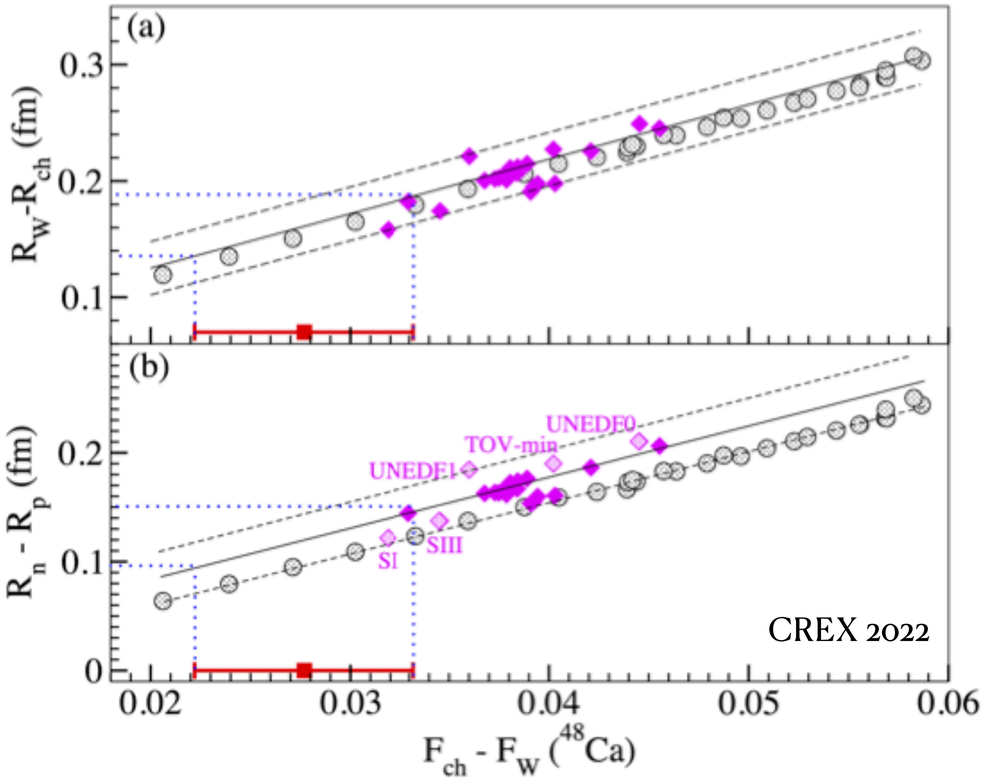

$$p + e \rightarrow n + \nu$$
$$\bar{\nu} + p + e \leftarrow n$$

Direct Urca Process

$$p_F^e + p_F^p > p_F^n$$
$$n_p/n_n \gtrsim 0.14$$

- Modified Urca process with superfluidity explains most cooling data.
- PREX+CREX is consistent with the absence of evidence for the direct Urca process.

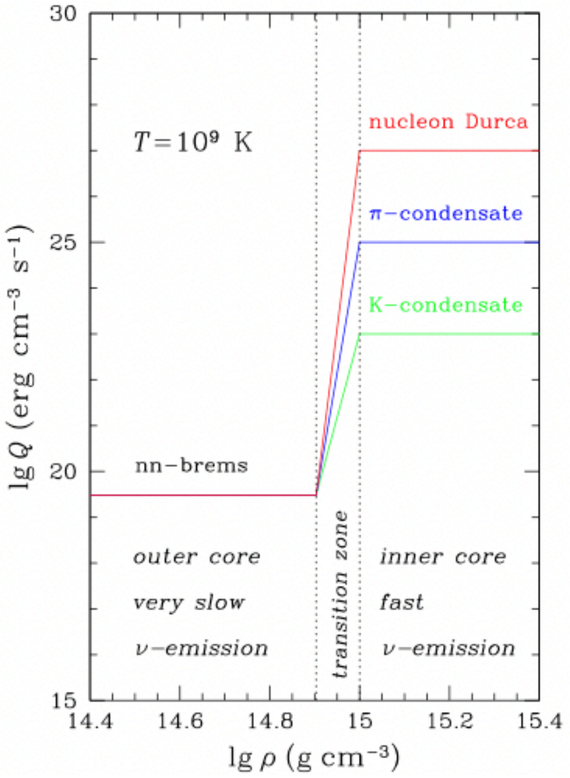

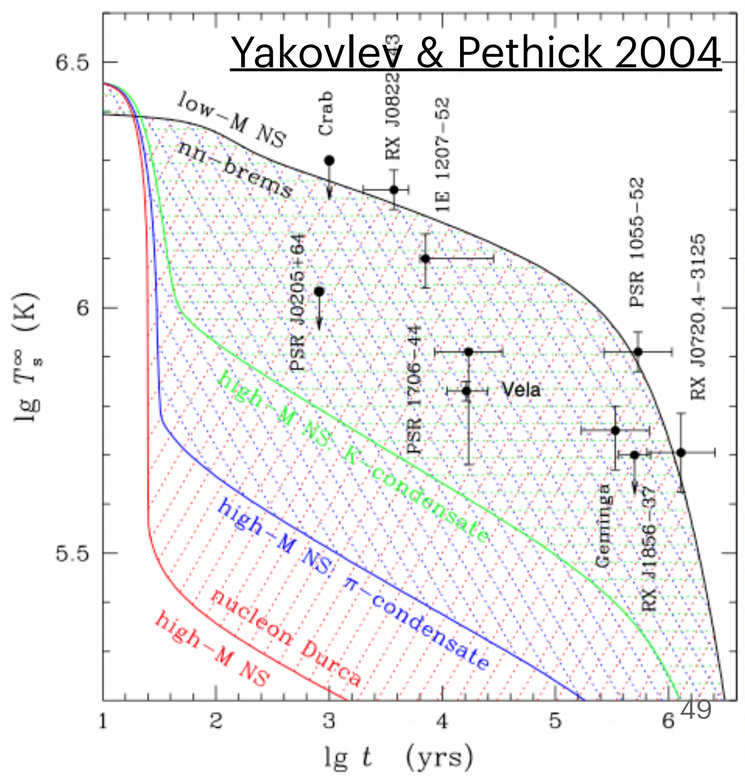

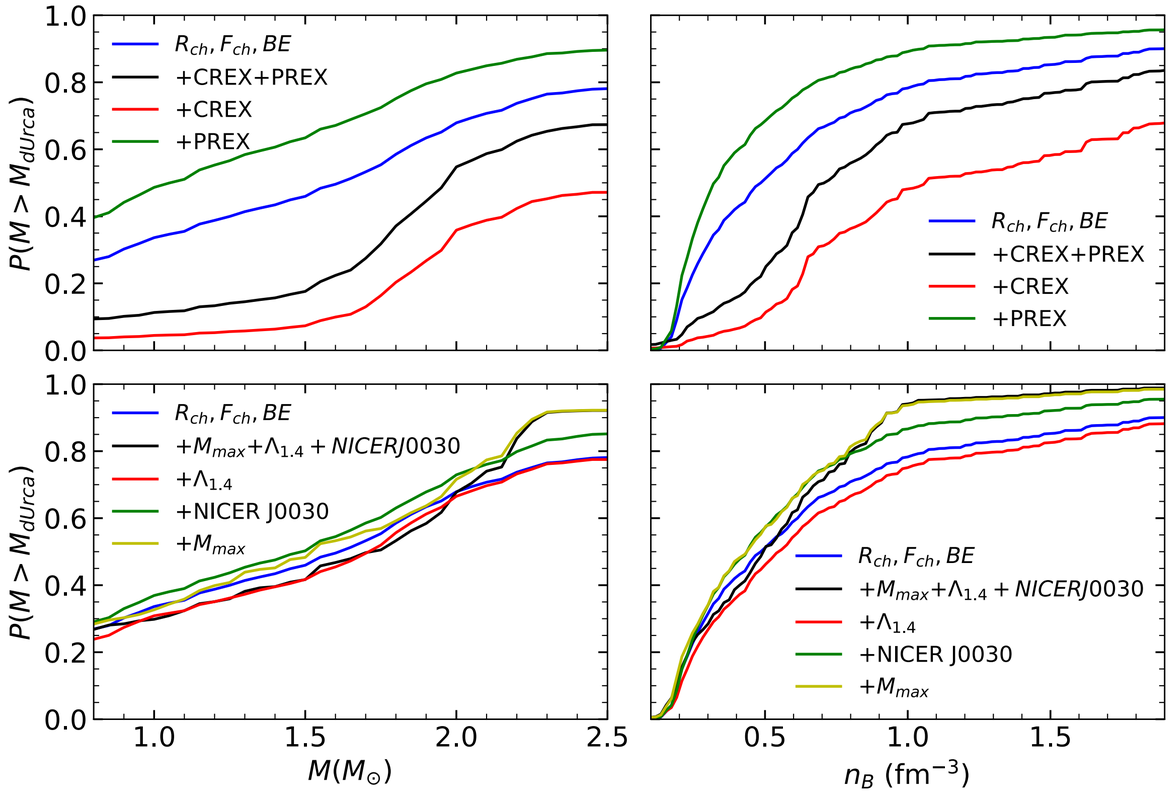

QED and Weak interaction

- Lagrange involving electron:

  $\mathscr{L} = \mathbf{i}\bar{\psi}\gamma^{\mu}\partial_{\mu}\psi - m\bar{\psi}\psi + eJ^{\mu}A_{\mu} + \frac{g_W}{\cos(\Theta_W)}J_Z^{\mu}Z_{\mu} - \frac{M_Z^2}{2}Z^{\mu}Z_{\mu} + \ldots$

  $J^{\mu} = (\rho_E, \mathbf{j}) = \bar{\psi}\gamma^{\mu}\psi$ is electron 4-current,

  and $J_Z^{\mu} = -\frac{1}{2}\bar{\psi}_L\gamma^{\mu}\psi_L - \sin^2(\Theta)\bar{\psi}\gamma^{\mu}\psi = -\frac{1}{4}\bar{\psi}\left[1 - 4\sin^2(\Theta_W) - \gamma^5\right]\psi$

  Weak mixing angle: $\cos(\Theta_W) = \frac{M_W}{M_Z} = 0.882$

  $M_W = 80.4\,\text{GeV},\ \ M_Z = 91.2\,\text{GeV},\ \ \sin^2(\Theta_W) = 0.223$

- Z boson propagator: $\frac{g_{\mu\nu}}{M_Z^2 - q^2}$

- 4-Fermi effective interaction at zero momentum : $G_F = \frac{g_W^2}{4\sqrt{2}M_W^2}$

Maxwell Equations of E.M. and Weak fields

- Lagrange involving photon and Z boson:

$$\mathscr{L} = \left[-\frac{1}{4}F^{\mu\nu}F_{\mu\nu} + eJ^{\mu}A_{\mu}\right] + \left[-\frac{1}{4}Z^{\mu\nu}Z_{\mu\nu} + \frac{g_W}{\cos(\Theta_W)}J_Z^{\mu}Z_{\mu} - \frac{1}{2}M_Z^2Z^{\mu}Z_{\mu}\right]$$

where $F_{\mu\nu} = \partial^{\mu}A_{\nu} - \partial^{\nu}A_{\mu}, Z_{\mu\nu} = \partial^{\mu}Z_{\nu} - \partial^{\nu}Z_{\mu}$

$A_{\mu} = (\Phi, \mathbf{A}), Z_{\mu} = (\Phi_Z, \mathbf{Z})$ are gauge boson fields,

and $J^{\mu} = (\rho_E, \mathbf{j}) = \bar{\psi}\gamma^{\mu}\psi$ is E.M. 4-current of an electron.

- E.M. field follows Maxwell Equations: $\nabla^2\Phi - \frac{\partial^2\Phi}{\partial_t^2} = \rho_E +$ ($M^2\Phi$ for massive Z boson)

Static electric potential: $\Phi(r) = \int \frac{\rho_E(r')}{4\pi|r-r'|}dr'^3$

Static Z-boson potential: $\Phi_Z(r) = \int \frac{\rho_Z(r')e^{-M_Z|r-r'|}}{4\pi|r-r'|}dr'^3 \approx \rho_Z(r')\int \frac{e^{-M_Z|r-r'|}}{4\pi|r-r'|}dr'^3 = \frac{\rho_Z(r')}{M_Z^2}$

Weak interaction is approximately zero-range, since $M_Z \approx 500\ \text{fm}^{-1}$

Dirac equation in E.M. and weak field

V-A theory

- Lagrange involving electron:

$$\mathscr{L} = \mathbf{i}\bar{\psi}\gamma^{\mu}\partial_{\mu}\psi - m\bar{\psi}\psi + eJ^{\mu}A_{\mu} + \frac{g_W}{\cos(\Theta_W)}J_Z^{\mu}Z_{\mu} - \frac{M_Z^2}{2}Z^{\mu}Z_{\mu} + \dots$$

- Electron weak 4-current:

$$J_Z^{\mu} = -\frac{1}{2}\bar{\psi}_L\gamma^{\mu}\psi_L + \sin^2(\Theta)\bar{\psi}\gamma^{\mu}\psi = -\frac{1}{4}\bar{\psi}\gamma^{\mu}\left[1 - 4\sin^2(\Theta_W) - \gamma^5\right]\psi \approx \frac{1}{4}\bar{\psi}\gamma^{\mu}\gamma^5\psi$$

- Dirac equation: $\left[\alpha\mathbf{p} + \beta m + \hat{V}(r)\right]\Psi = E\psi$

  where $\hat{V}(r) = V(r) + \gamma_5 A(r)$, $V(r) = \int d^3\mathbf{r}'\frac{\rho_p(\mathbf{r})}{|\mathbf{r}' - \mathbf{r}|}$, $A(r) = \frac{G_F}{2^{3/2}}\rho_W(r)$

- In the massless limit(Weyl basis): $\left[\alpha\mathbf{p} + V_{L,R}(r)\right]\Psi_{L,R} = E\psi_{L,R}$, where $V_{L,R}(r) = V(r) \pm A(r)$

Parity violating asymmetry A_{PV}

The observable in PREX and CREX

- Parity violating asymmetry: $A_{PV} = \dfrac{\sigma_R - \sigma_L}{\sigma_R + \sigma_L}$

  where σ_R, σ_L are cross-section of the scattering problem:

  $\left[\alpha \mathbf{p} + V_{L,R}(r)\right] \Psi_{L,R} = E\psi_{L,R}$, where $V_{L,R}(r) = V(r) \pm A(r)$,

  $V(r) = \int d^3\mathbf{r}' \dfrac{\rho_p(\mathbf{r})}{|\,\mathbf{r}' - \mathbf{r}\,|}, \;\; A(r) = \dfrac{G_F}{2^{3/2}} \rho_W(r)$

  which is called “Coulomb distortion” in this context:
  Coulomb distortion stands for repeated electromagnetic interactions with the nucleus remaining in its ground state. This is of order $Z\alpha/\pi$, 20 % for 208Pb.

Form Factor

- Point charge Coulomb (Mott) scattering: $\left[\frac{d\sigma}{d\Omega}\right]_{Mott} = \frac{Z^2e^4(1-\beta^2\sin^2\frac{\theta}{2})}{64\pi^2\varepsilon_0^2p^2\beta^2\sin^2\frac{\theta}{2}}$

- Extended Coulomb scattering: $-\frac{Ze^2}{r} \longrightarrow e^2\int\frac{\rho(r')d^3r'}{|r-r'|}$

$$\frac{d\sigma}{d\Omega} = \left[\frac{d\sigma}{d\Omega}\right]_{Mott} |F(\mathbf{q})|^2$$

$$F(\mathbf{q}) = \frac{1}{Q}\int e^{i\mathbf{q}\cdot\mathbf{r}}\rho(\mathbf{r})d^3r = \frac{1}{Q}\int\left(1 + i\mathbf{q}\cdot\mathbf{r} - \frac{1}{2}(\mathbf{q}\cdot\mathbf{r})^2 + \ldots\right)\rho(\mathbf{r})d^3r$$

$$= 1 - \frac{1}{6}q^2 < r^2 > + \ldots \qquad \text{assuming spherical symmetry}$$

- At small q, $\lim_{q<<\sqrt{<r^2>}} < r^2 > = \frac{6[1-F(q)]}{q^2}$

Born approximation

- Axial weak potential, $A(r) = \dfrac{G_F}{2^{3/2}}\rho_W(r)$
- Scattering amplitude:
  $$\int < \psi_{in} \,|\, A(r) \,|\, \psi_{out} > d^3r = \frac{G_F}{2^{3/2}} \int e^{i\mathbf{q}\cdot\mathbf{r}} \rho_W(\mathbf{r}) d^3r = \frac{G_F Q_W}{2^{3/2} q^2} F_W(q)$$
- $$A_{PV} = \frac{\sigma_R - \sigma_L}{\sigma_R + \sigma_L} \approx \frac{G_F q^2 \,|\, Q_W \,|}{4\sqrt{2}\pi\alpha Z} \frac{F_W(q)}{F_E(q)} \propto \frac{(F_E + F_W)^2 - (F_E - F_W)^2}{(F_E + F_W)^2 + (F_E - F_W)^2}$$
  where $F(q) = \dfrac{\int j_0(qr)\rho(r)d^3r}{\int \rho(r) d^3r}$, and $j_0(qr) = \dfrac{\sin(qr)}{qr}$ is spherical Bessel function

Weak Charge of Nuclei

- Weak charge: $Q_W = 2T_3 - 4Q_E \sin^2(\Theta_W)$
  where weak isospin $T_3 = -\frac{1}{2}$ for $e^-, u^{+\frac{2}{3}}, n$, and $T_3 = \frac{1}{2}$ for $\nu, d^{-\frac{1}{3}}, p^+$
  Neutron weak charge: $Q_n = -1$ (–0.9878 with radiative correction)
  Proton weak charge $Q_p = 1 - 4\sin^2(\Theta_W)$ (0.0721 with radiative correction)
- Neutron form factor: $G_n^W = Q_n G_p^E + Q_p G_n^E + Q_n G_s^E$
  Proton form factor: $G_p^W = Q_p G_p^E + Q_n G_n^E + Q_n G_s^E$
- Weak charge distribution: $\rho_W(r) = \int d^3r' \left[G_n^W(r - r')\rho_n(r) + G_p^W(r - r')\rho_p(r) \right]$
- Electric charge distribution: $\rho_E(r) = \int d^3r' \left[G_n^E(r - r')\rho_n(r) + G_p^E(r - r')\rho_p(r) \right]$
  Additional complicity: many-body correction, center-of-mass correction, the magnetic contribution from spin-orbital current(SHF) or tensor density (RMF)

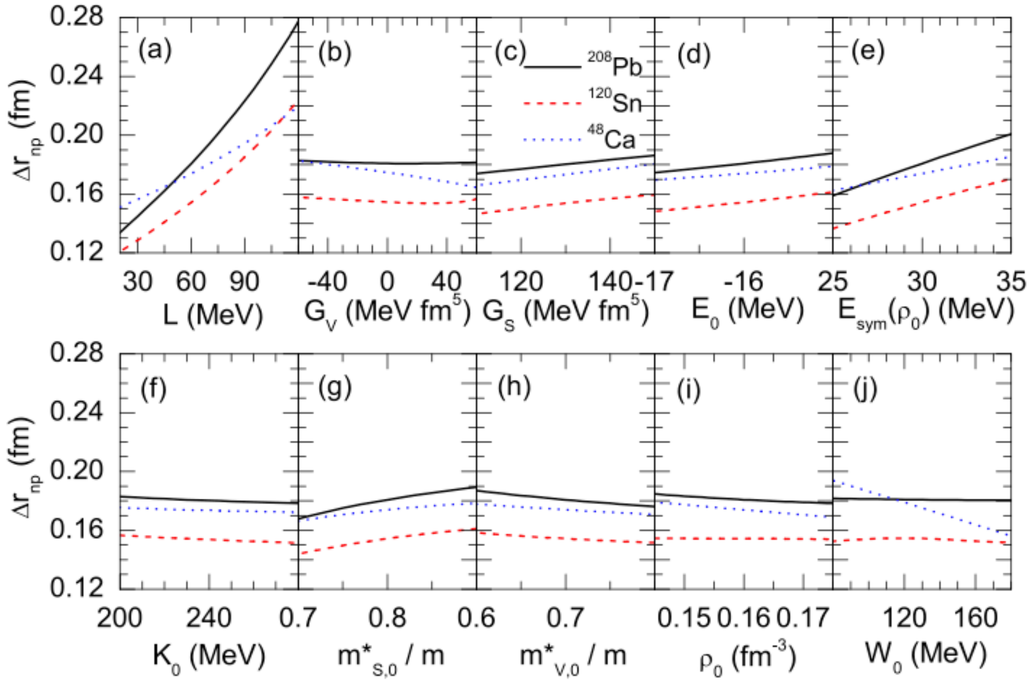

FIG. 3: (Color online) The neutron skin thickness Δr_{np} of ^{208}Pb, ^{120}Sn and ^{48}Ca from SHF with MSL0 by varying individually L (a), G_V (b), G_S (c), $E_0(\rho_0)$ (d), $E_{\rm sym}(\rho_0)$ (e), K_0 (f), $m^*_{s,0}$ (g), $m^*_{v,0}$ (h), ρ_0 (i), and W_0 (j).

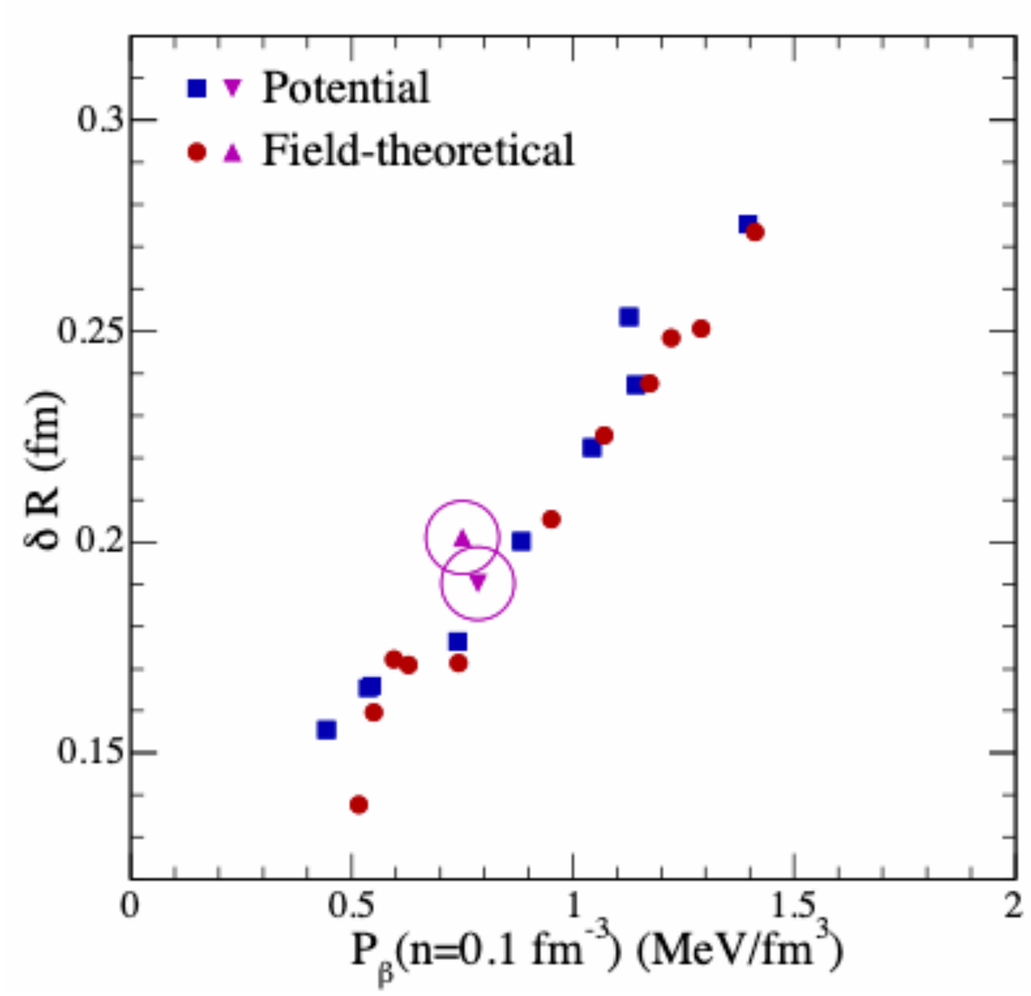

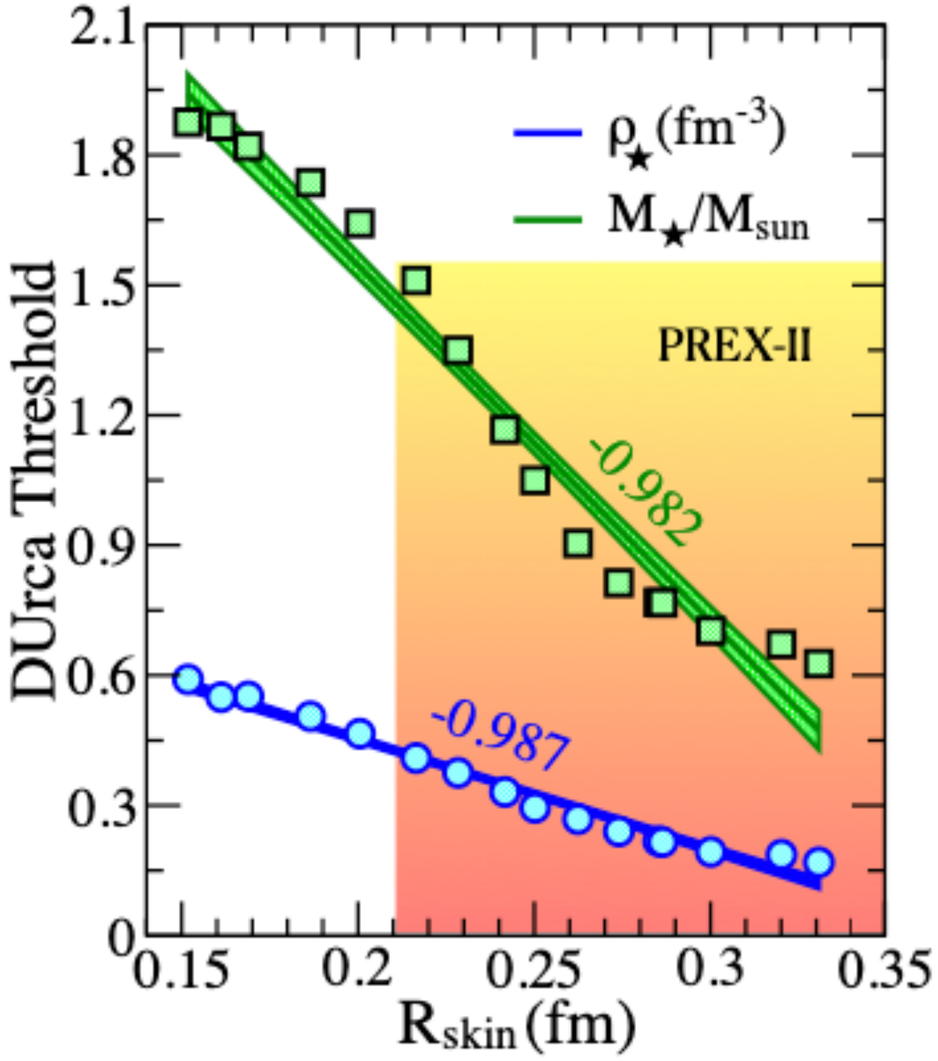
DUrca Threshold
R_{skin} (fm)
$\rho_\star$ (fm^{-3})
$M_\star/M_{sun}$
PREX-II
-0.982
-0.987

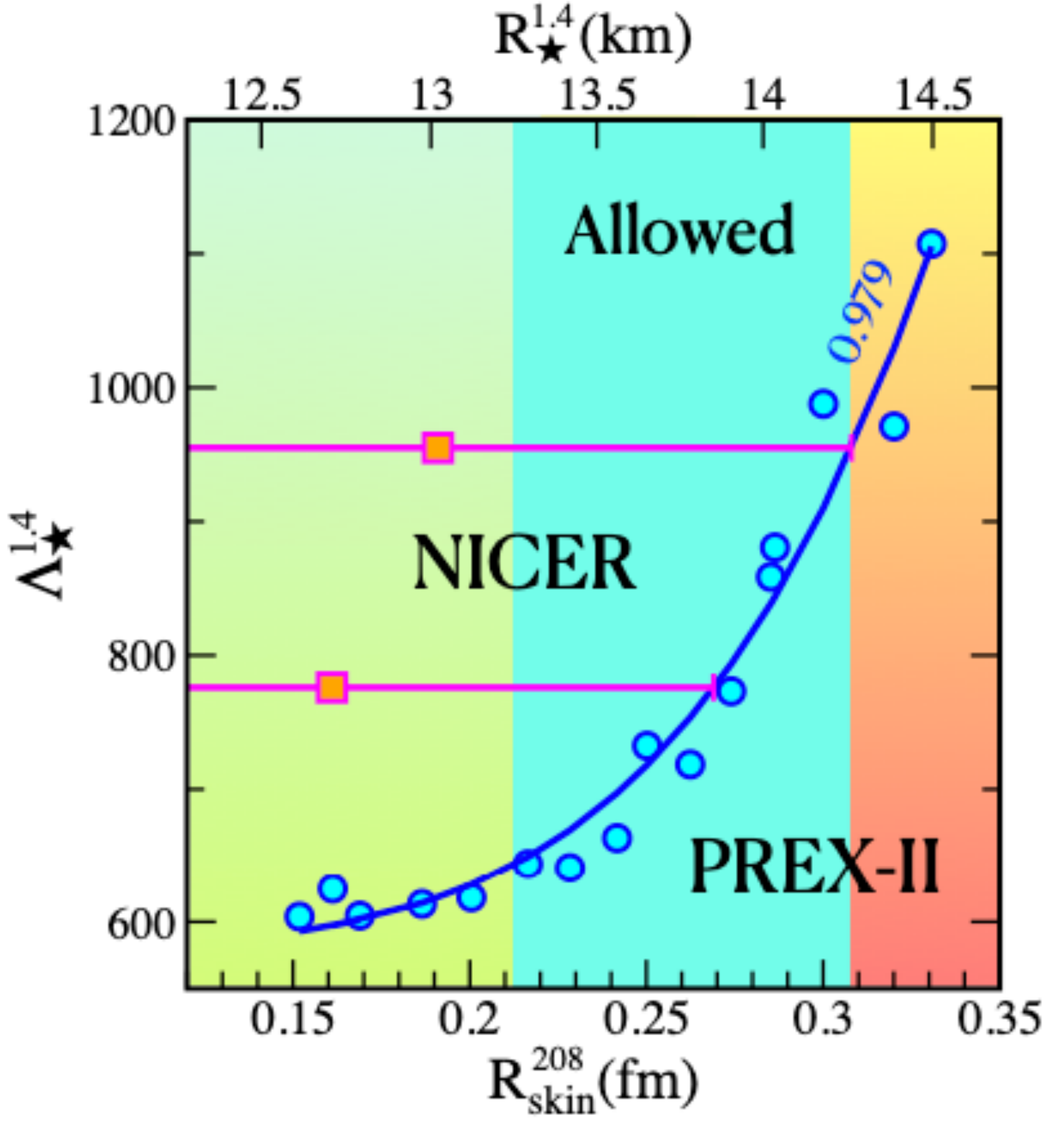
$R^{1.4}_\star$ (km)
$\Lambda^{1.4}_\star$
R^{208}_{skin} (fm)
Allowed
NICER
PREX-II
0.979